

# **Light Water Reactor Sustainability Program**

## **Plant-Level Scenario-Based Risk Analysis for Enhanced Resilient PWR – SBO and LBLOCA**



**September 2018**

U.S. Department of Energy

Office of Nuclear Energy

**DISCLAIMER**

This information was prepared as an account of work sponsored by an agency of the U.S. Government. Neither the U.S. Government nor any agency thereof, nor any of their employees, makes any warranty, expressed or implied, or assumes any legal liability or responsibility for the accuracy, completeness, or usefulness, of any information, apparatus, product, or process disclosed, or represents that its use would not infringe privately owned rights. References herein to any specific commercial product, process, or service by trade name, trade mark, manufacturer, or otherwise, does not necessarily constitute or imply its endorsement, recommendation, or favoring by the U.S. Government or any agency thereof. The views and opinions of authors expressed herein do not necessarily state or reflect those of the U.S. Government or any agency thereof.

# **Plant-Level Scenario-Based Risk Analysis for Enhanced Resilient PWR – SBO and LBLOCA**

**Zhegang Ma  
Carlo Parisi  
Hongbin Zhang  
Diego Mandelli  
Cole Blakely  
Jianguo Yu  
Robert Youngblood  
Nolan Anderson**

**September 2018**

**Prepared for the  
U.S. Department of Energy  
Office of Nuclear Energy**





## EXECUTIVE SUMMARY

This report documents the activities performed by Idaho National Laboratory (INL) during the fiscal year (FY) 2018 for the DOE Light Water Reactor Sustainability (LWRS) Program, Risk-Informed System Analysis (RISA) Pathway, Enhanced Resilient Plant (ERP) Systems research. The purpose of the RISA Pathway research and development is to support plant owner-operator decisions with the aim to improve the economics, reliability, and maintain the high levels of safety of current nuclear power plants over periods of extended plant operations. The concept of ERP refers to the combinations of Accident Tolerant Fuel (ATF), optimal use of Diverse and Flexible Coping Strategy (FLEX), enhancements to plant components and systems, and the incorporation of augmented or new passive cooling systems, as well as improved fuel cycle efficiency. The objective of the ERP research effort is to use the RISA methods and toolkit in industry applications, including methods development and early demonstration of technologies, in order to enhance existing reactors safety features (both active and passive) and to substantially reduce operating costs through risk-informed approaches to plant design modifications to the plant and their characterization.

There are two main focus areas in FY 2018 for the ERP R&D efforts. One is to evaluate the risk impact brought by the ATF designs and FLEX in the selected accident scenarios. The other is to investigate various approaches to accomplish the ERP research objective, i.e., use RISA methods and toolkit to enhance existing reactors safety features and reduce plant operating costs.

In this report, two accident scenarios, Station Blackout (SBO) and Large Break Loss-of-Coolant-Accident (LBLOCA), were selected to evaluate the risk impact brought by the FeCrAl and Cr-coated ATF designs and FLEX. A generic SAPHIRE probabilistic risk assessment (PRA) model for a typical pressurized water reactor (PWR) was used to identify and group accident scenarios to be analyzed by RELAP5-3D system thermal-hydraulic code and RAVEN risk-analysis code. The FeCrAl and Cr-coated fuel cladding models were developed and incorporated into the generic RELAP5-3D PWR model. The thermal hydraulic analyses for the selected accident scenarios were performed to estimate the differences in the timing when the peak cladding temperature (PCT) reaches the corresponding clad melting temperature and the timing when 0.5 kilogram hydrogen were produced due to the accident between the ATF designs and the conventional fuel cladding design. The timing differences were factored into the SAPHIRE PRA model to yield a new core damage frequency (CDF) due to the ATF design and FLEX, which was compared to the base case CDF to provide the risk benefits brought by the supposed plant changes.

For SBO, the RELAP5-3D simulations estimate only marginal increase of the coping time with FeCrAl and Cr-coated in most SBO scenarios, from about several minutes in short term SBO to about twenty minutes in long term SBO with a battery life of 4 hours. The maximum increase of the coping time is 1 hour in long term SBO with a battery life of 8 hours for FeCrAl. The timing to core damage is dictated by the timing of the core uncover, the decay power level and the oxidation kinetics. FeCrAl is showing here some slight advantage on Cr-coated.

With only marginal increase of the time to core damage with the FeCrAl and Cr-coated designs, the risk benefit on behalf of the CDF as the risk metrics would be very small. A simplified approach using a multiplication factor is developed in this report to

estimate the risk impact of the ATF design with the small increase of the coping time, which show that the marginal coping time increase would lead to about 4% and 2% CDF reductions for the FeCrAl and Cr-coated designs, respectively. However, this should not be misinterpreted as that ATF brings no risk benefits. Actually the hydrogen production with ATF is one or two order of magnitude lower than the Zircaloy clad. And the timing to release significant hydrogen production (0.5 Kg) with ATF is about 0.5 hour to 1.5 hours later than that with Zircaloy.

Coupled calculations of RELAP5-3D and RAVEN were conducted for evaluating the effects of aleatory uncertainties on the SBO accident. RAVEN was used to perturb selected parameters of RELAP5-3D input deck and to derive Limit Surfaces (LS) for different cases. The LS calculations provided a qualitative and quantitative assessment of the change of CDF and they highlighted the slight improvements derived from the ATF introduction for the PWR SBO accident.

For LBLOCA, a dynamic PRA analysis was performed for LBLOCA by employing RELAP5-3D and RAVEN with the scope of identifying the safety impact of ATF from a PRA perspective. We were able to identify few accident sequences where ATF was able to withstand the loss of cooling without reaching code damage condition.

An investigation of other analysis approaches for the ERP was performed for the project. For example, risk-informed plant enhancement analysis uses a risk informed approach to analyze potential design changes that could enhance the plant operation safety with minimum economy burdens due to the changes. SBO model was used as a case study for the analysis.

Risk-informed sensitivity analysis used one at a time methods to obtain a qualitative understanding of the relations between coping time increases and various fuel cladding material properties. The selected inputs include thermal conductivity and volumetric heat capacity for both fuel and cladding, as well as the cladding side oxidation parameters of activation energy, rate, and heat release. The analysis concludes that it seems like that no meaningful increases in coping time during a station blackout could be achieved through improvements in thermal conductivity or volumetric heat capacity of clad or fuel, and no significant gains could be acquired through improvements in cladding oxidation. Other figures of merit, such as the total core hydrogen production, are likely more significantly affected by ATF designs.

Fuel performance analysis using the BISON fuel performance code was conducted for SBO scenario. It is suggested that the evolution of the full-length fuel rod behavior is mainly determined in terms of cladding or coolant temperatures. Though the clad melting temperature may be a direct indicator of the failure of fuel rods, our results from BISON modeling and simulations strongly suggest that it is probably more realistic to use cladding failure criterion due to the cladding burst to determine the coping time. In the future, it is desirable to carry out more extensive investigations of thermo-mechanical behavior of fuel rod under accident scenarios, including the effect of high burnup with different fuel rod designs, and cladding failure due to the cladding burst.

# CONTENTS

EXECUTIVE SUMMARY .....	iii
ACRONYMS .....	xi
1. INTRODUCTION .....	1
2. ENHANCED RESILIENT PLANT SYSTEMS ANALYSIS .....	3
2.1 ERP Analysis Process .....	3
2.2 Classical Risk Analysis .....	5
2.3 Advanced Risk Analysis .....	6
2.4 Risk-Informed Sensitivity Analysis .....	6
2.5 Fuel Performance Analysis .....	6
2.6 FY 2018 Work .....	6
3. ERP ANALYSIS TOOLS .....	8
3.1 SAPHIRE .....	8
3.2 RELAP5-3D .....	8
3.2.1 The INL Generic PWR Model .....	9
3.2.2 Model Qualification .....	12
3.2.3 Metal-Water Reactor Model in RELAP5-3D .....	14
3.3 RAVEN .....	17
3.4 BISON .....	19
4. SBO SCENARIO ANALYSIS .....	21
4.1 Generic PWR SBO PRA Model .....	21
4.2 RELAP5-3D Analysis .....	27
4.2.1 SBO Control Logic .....	27
4.2.2 Creep Model .....	28
4.2.3 Clad Oxidation Kinetics and Fuel Geometry .....	28
4.2.4 Sample RELAP5-3D results for LT-SBO sequence .....	29
4.3 SBO Analysis Results .....	36
4.3.1 RELAP5-3D Results .....	36
4.3.3 Risk Impact Evaluation .....	41
4.4 Limit Surface Search Results .....	43
4.4.1 Background .....	43
4.4.2 Two-dimensional Limit Surface Search .....	44
4.4.3 Three-dimensional Limit Surfaces Search .....	46
5. LBLOCA SCENARIO ANALYSIS .....	50
5.1 RELAP5-3D Model .....	50
5.2 LBLOCA Analysis .....	51
5.3 Results .....	53
6. RISK-INFORMED PLANT ENHANCEMENT ANALYSIS .....	58

7.	RISK-INFORMED SENSITIVITY ANALYSIS FOR ATF .....	63
8.	FUEL PERFORMANCE ANALYSIS .....	71
9.	RESILIENCE ANALYSIS FOR LONG-TERM SBO SCENARIOS .....	74
9.1	Overview of This Section .....	74
9.2	Comparison of Success Strategies .....	74
9.2.1	The SOARCA Analysis for Long-Term SBO .....	74
9.2.2	NEI Guidance for Long-Term SBO .....	77
9.3	Comparison .....	78
9.3.1	Prevention Worth .....	78
9.3.2	Comparison .....	79
9.4	Summary .....	82
10.	SUMMARY AND FUTURE WORK .....	84
11.	REFERENCES .....	86
	APPENDIX A - SBO EVENT TREE MODEL .....	A-1
	APPENDIX B - RELAP5-3D SBO RESULTS .....	B-1

## FIGURES

Figure 2-1.	Enhanced Resilient Plant Engineering Analysis. ....	4
Figure 3-1.	SAPHIRE 8 Graphic User Interface.....	8
Figure 3-2.	RELAP5-3D Role in LOOP and SBO Calculations. ....	9
Figure 3-3.	RELAP5-3D RPV Model (left) and MCC & SG Models (right).....	11
Figure 3-4.	RELAP5-3D Core Model.....	12
Figure 3-5.	Logic Path for the Metal-Water Reaction Model Coding. ....	15
Figure 3-6.	Relationship between Simulator Physics Code ( <i>H</i> ) and Control Logic ( <i>C</i> ).....	18
Figure 3-7.	Scheme of RAVEN Statistical Framework Components.....	19
Figure 4-1.	SBO Model Event Tree Logic.....	22
Figure 4-2.	Generic PWR SBO Main Event Tree.....	23
Figure 4-3.	LT_SBO 1.0 Zry – TD-AFW Mass Flow. ....	30
Figure 4-4.	LT_SBO 1.0 Zry – MCP Seal Leakage Mass Flow. ....	31
Figure 4-5.	LT_SBO 1.0 Zry – Primary and Secondary Sides Pressures. ....	31
Figure 4-6.	LT_SBO 1.0 Zry –Accumulators Mass Flow. ....	31
Figure 4-7.	LT_SBO 1.0 Zry – SG Levels.....	32
Figure 4-8.	LT_SBO 1.0 – RPV Water Level for Zry, Cr-Coated, FeCrAl Clads.....	32
Figure 4-9.	LT_SBO 1.0 – PCT for Zry, Cr-Coated, FeCrAl Clads.....	32

Figure 4-10. LT_SBO 1.3 Zry – TD-AFW Mass Flow. ....	33
Figure 4-11. LT_SBO 1.3 Zry – MCP Seal Leakage Mass Flow. ....	34
Figure 4-12. LT_SBO 1.3 Zry – Primary and Secondary Sides Pressures. ....	34
Figure 4-13. LT_SBO 1.3 Zry –Accumulators Mass Flow. ....	34
Figure 4-14. LT_SBO 1.3 Zry – SG Levels.....	35
Figure 4-15. LT_SBO 1.3 – RPV Water Level for Zry, Cr-Coated, FeCrAl Clads.....	35
Figure 4-16. LT_SBO 1.3 – PCT for Zry, Cr-Coated, FeCrAl Clads.....	35
Figure 4-17. Limit Surface Search workflow in RAVEN.....	43
Figure 4-18. 2D Limit Surface – Case 1. ....	45
Figure 4-19. 2D Limit Surface – Case 2. ....	46
Figure 4-20. 3D Limit Surface – Case 1. ....	47
Figure 4-21. 2D projections of 3D Limit Surface – Case 1. ....	47
Figure 4-22. 3D Limit Surface – Case 2. ....	48
Figure 4-23. 2D projections of 3D Limit Surface – Case 2. ....	48
Figure 5-1. PWR Scheme. ....	50
Figure 5-2. LBLOCA Event Tree. ....	52
Figure 5-3. Expanded LBLOCA Event-Tree Structure. ....	52
Figure 5-4. Scheme of the Classical and Dynamic PRA Integration for the LBLOCA Test Case.....	53
Figure 5-5. Outcome of the Simulations associated to Each Branch of the Expanded LBLOCA Event-Tree for the Three Considered Fuel Types. ....	54
Figure 7-1. Relap5-3D Coolant Primary Coolant Loop.....	63
Figure 7-2. Coping Time versus Fuel Thermal Conductivity. ....	64
Figure 7-3. Coping Time versus Fuel Volumetric Heat Capacity. ....	65
Figure 7-4. Coping Time versus Clad Thermal Conductivity.....	66
Figure 7-5. Coping Time versus Clad Volumetric Heat Capacity. ....	67
Figure 7-6. Coping Time versus Clad Oxidation Activation Energy.....	68
Figure 7-7. Coping Time versus Clad Oxidation Rate.....	69
Figure 7-8. Coping Time versus Clad Oxidation Heat Release. ....	69
Figure 8-1. Evolution of the Full-Length Fuel Rod Behavior of a 3-loop Operation (~4.5 years) during Normal Reactor Operation of UO <sub>2</sub> Fuel with FeCrAl and Zircaloy-4 Claddings. ....	72
Figure 8-2. Evolution of the Full-Length Fuel Rod Behavior from Normal Reactor Operation to SBO after the First-Loop Operation (~1.5 years) during Normal Reactor Operation of UO <sub>2</sub> fuel with FeCrAl and Zircaloy-4 Claddings for a 17x17 design.....	73
Figure 9-1. The SOARCA Report Success Path(s), Viewed in Reliability Block Diagram Format. ....	76

Figure 9-2. A notional description of the NEI Table D-1 guidance, viewed in Reliability Block Diagram format. The dark shading under  $R_{Leak Rate}$  corresponds to items that are not discussed in the NEI report, but are shown here for comparison purposes ..... 78

## TABLES

Table 3-1. Failure Criteria for Different Fuel Clads .....	9
Table 3-2. Relevant Design Parameters of the IGPWR .....	10
Table 3-3. RELAP5-3D Steady State Values .....	13
Table 4-1. Overview of LOOP/SBO Event Trees Quantification Results .....	21
Table 4-2. Grid-Related SBO Sequence Results .....	24
Table 4-3. PRA SBO Sequences to RELAP5-3D Scenarios .....	25
Table 4-4. Grid-Related SBO Sequence Results .....	27
Table 4-5. RELAP5-3D Control Logic for SBO .....	27
Table 4-6. RELAP5-3D Parameters for the Fuel Clads .....	29
Table 4-7. Sequence of Events for LT-SBO-1.0, Zry clad. ....	30
Table 4-8. Sequence of Events for LT-SBO-1.3, Zry clad. ....	33
Table 4-9. RELAP5-3D Results for SBO Scenarios without AC Power Recovery – Zry vs. FeCrAl – Clad Performance .....	37
Table 4-10. RELAP5-3D Results for SBO Scenarios without AC Power Recovery – Zry vs. FeCrAl – H <sub>2</sub> Production .....	38
Table 4-11. RELAP5-3D Results for SBO Scenarios without AC Power Recovery – Zry vs. Cr-coated – Clad Performance .....	39
Table 4-12. RELAP5-3D Results for SBO Scenarios without AC Power Recovery – Zry vs. Cr-coated – H <sub>2</sub> Production .....	40
Table 4-13. Failure Probabilities for Operator to Recover AC Power .....	41
Table 4-14. Estimated Coping Time Factor .....	42
Table 4-15. CDF Estimation for FeCrAl .....	42
Table 4-16. CDF Estimation for Cr-Coated .....	42
Table 4-17. Parameters for the 2D Limit Surface Search – Case 1 .....	44
Table 4-18. LS Integral for SBO-3.0. Case 1 .....	45
Table 4-19. Parameters for the 2D Limit Surface Search – Case 2 .....	45
Table 4-20. Parameters for the 2D Limit Surface Search – Case 2 .....	46
Table 4-21. Parameters for the 3D Limit Surface Search – SBO-3.0 – Case 1 .....	47
Table 4-22. Parameters for the 3D Limit Surface Search – SBO-3.0 – Case 2 .....	48
Table 4-23. LS Integral for SBO-3.0. 3D Case .....	49

Table 5-1. Time to Reach CD Condition for Branches 2, 3 and 5 of the Expanded Event-Tree of Figure 5-5 .....	55
Table 5-2. Time to Reach CD Conditions for Branches 6, 8 and 9 of the Expanded Event-Tree of Figure 5-5. ....	56
Table 5-3. Time to Reach CD Conditions for Branches 10, 11 and 12 of the Expanded Event-Tree of Figure 5-5. ....	57
Table 6-1. Risk Significant Grid-Related PWR SBO Sequences .....	59
Table 6-2. Sequence Cut Set and Importance Measure Review for Potential Plant Enhancement .....	60
Table 6-3. Preliminary List of Potential Plant Enhancements .....	61
Table 7-1. Multiplicative Factors of Material Properties for Sensitivity Analysis of Coping Time.....	64
Table 7-2. Approximate Material Properties for Traditional and ATF Fuel.....	66
Table 7-3. Approximate Material Properties for Traditional and ATF Fuel.....	67
Table 9-1. SPAR-H for a Conservatively-Assessed “Action” .....	80
Table 9-2. SPAR-H for a Less Conservatively Assessed “Action” .....	81
Table 9-3. Methods for Reduction of RCP Seal Leakage .....	83
Table 9-4. Different Strategies for RCS Makeup.....	83





## ACRONYMS

ACC	accumulator system
AFW	auxiliary feedwater
ATF	accident tolerant fuel
BEPU	best estimate plus uncertainty
BWR	boiling water reactor
CD	core damage
CDF	core damage frequency
CS	containment spray
DEGB	double-ended guillotine break
DG	diesel generator
DOE	Department of Energy
DPRA	dynamic probabilistic risk assessment
ECCS	emergency core cooling system
EDG	emergency diesel generator
EPRI	Electric Power Research Institute
ERP	enhanced resilient plant
ERPS	enhanced resilient plant systems
EPS	emergency power system
FAB	feed and bleed
FLEX	diverse and flexible coping strategy
FY	fiscal year
HPI	high pressure injection
IGPWR	INL Generic PWR
IE	initiating event
INL	Idaho National Laboratory
LERF	large early release frequency
LBLOCA	large break loss of coolant accident
LOFW	loss of feedwater
LOOP	loss of offsite power
LOSC	loss of seal cooling
LPI	low pressure injection

LPR	low pressure recirculation
LS	limit surface
LWR	light water reactor
LWRS	light water reactor sustainability
MSPI	mitigating systems performance index
NEI	Nuclear Energy Institute
NOED	notices of enforcement discretion
NPP	nuclear power plant
NRC	Nuclear Regulatory Commission
NUREG	nuclear regulatory report
OAT	one at a time
OPR	offsite power recovery
PCT	peak clad temperature
PORV	pilot-operated relief valve
PRA	probabilistic risk assessment
PRZ	pressurizer
PSA	probabilistic safety assessment
PWR	pressurized water reactor
RA	risk assessment
RAVEN	Risk Analysis and Virtual Control Environment
RCS	reactor cooling system
RCP	reactor coolant pump
R&D	research and development
RELAP5-3D	Reactor Excursion and Leak Analysis Program 5 – 3D
RISA	risk-informed system analysis
RISMC	Risk Informed Safety Margin Characterization
ROM	reduced order model
RPV	reactor pressure vessel
RWST	reactor water storage tank
SA	severe accident
SBO	station blackout
SDP	significance determination process
SG	steam generator
SGTR	steam generator rupture
SOARCA	state-of-the-art reactor consequence analyses

SSC	structure, system, and component
SV	safety valve
TDAFP	turbine driven auxiliary feedwater pump
TDAFW	turbine driven auxiliary feedwater
TH	thermal-hydraulic
U.S.	United States
UTS	ultimate tensile strength



# Plant-Level Scenario-Based Risk Analysis for Enhanced Resilient PWR – SBO and LBLOCA

## 1. INTRODUCTION

This report documents the activities performed by Idaho National Laboratory (INL) during fiscal year (FY) 2018 for the U.S. Department of Energy (DOE) Light Water Reactor Sustainability (LWRS) Program, Risk-Informed Systems Analysis (RISA) Pathway, Enhanced Resilient Plant (ERP) Systems research (INL, 2018). The LWRS Program is a research and development (R&D) program that provides technical foundations for the continued operation of the nation's nuclear power plants, develops methods that support safe and economical long-term management and operation of existing nuclear power plants, and investigate new technologies to address enhanced nuclear power plant performance, economics, and safety. With the continuing economic challenges faced by nuclear power plants, the LWRS Program has redirected some of its R&D efforts to consider how to leverage the results from other ongoing R&D activities to improve the economic performance of LWRs in current and future energy markets. The RISA pathway is one of the primary technical areas of R&D under the LWRS Program to support decision-making related to economics, reliability, and safety by providing integrated plant system analysis and solutions through collaborative demonstrations to enhance economic competitiveness of operating nuclear power plants. The purpose of the RISA Pathway research and development is to support plant owner-operator decisions with the aims to improve the economics and reliability, and to maintain the high levels of safety of current nuclear power plants over periods of extended plant operations. The goals of the RISA Pathway are:

- To demonstrate risk-assessment methods coupled to safety margin quantification that can be used by decision-makers as a part of their margin recovery strategies;
- To apply the “RISA toolkit” to enable more accurate representation of safety margins for the long-term benefit of nuclear assets.

The objective of the ERP research effort is to use the RISA methods and toolkit in industry applications, including methods development and early demonstration of technologies, in order to enhance existing reactors safety features (both active and passive) and to substantially reduce operating costs through risk-informed approaches.

There are two main focus areas in FY 2018 for the ERP R&D efforts. One is to evaluate the risk impact brought by the ATF designs and FLEX in the selected accident scenarios. The other is to investigate various approaches to accomplish the ERP research objective, i.e., use RISA methods and toolkit to enhance existing reactors safety features and reduce plant operating costs.

One of the research efforts under the RISA pathway is to support the DOE and industry initiatives including the Accident Tolerant Fuel (ATF) and the Diverse and Flexible Coping Strategy (FLEX), in order to improve the safety and economic performance of the current fleet nuclear power plants. The ATF, combined with the optimal use of FLEX, the enhancements to plant components and systems, the incorporation of augmented or new passive cooling systems, and the improved fuel cycle efficiency are called ERP Systems. The desired attributes of ATF include: (1) improved fuel properties, for example, enhanced retention of fission products and enhanced fuel thermo-physical properties; (2) improved fuel cladding properties, for example, slower reaction kinetics with steam, slower hydrogen generation rate, and good cladding thermo-physical properties; and (3) backward compatible, minimal impact on plant operations and fuel cycle, improved plant safety, and minimal economic impacts.

The ATF concepts explored by the industry include Chromium (Cr) coated cladding, Iron-Chromium-Aluminum (FeCrAl) cladding, Silicon-Carbide (SiC) ceramic cladding, Uranium silicide (U<sub>3</sub>Si<sub>2</sub>) fuel, and fully ceramic micro-encapsulated (FCM) fuel (Bragg-Sitton, 2014). The ATF program reached an important milestone when lead test assemblies using FeCrAl cladding and coated zirconium (Zr) cladding were installed in Southern Nuclear's Edwin I. Hatch Plant Unit 1 in March 2018.

This report documents the activities that investigate integrated evaluation approaches that combine the plant probabilistic risk assessment (PRA) models with multi-physics best estimate analyses and perform detailed risk and benefit assessments of introducing ATF and FLEX into current nuclear power plants to achieve both safety and operational performance enhancements. Risk analysis was conducted for the FeCrAl and Cr-coated cladding design impact on a generic Westinghouse 3-loop pressurized water reactor (PWR) for postulated station blackout (SBO) and large break loss-of-coolant-accident (LBLOCA) accident scenarios using SAPHIRE (Smith & Wood, 2011), RELAP5-3D (RELAP5-3D Code Development Team, 2018), and RAVEN (Alfonsi, et al., 2017) codes. For the postulated SBO accident scenario, the coping time difference between the FeCrAl-coated fuel cladding ATF design and the conventional fuel cladding design was also presented through carrying out the BISON fuel performance code (Hales & al., 2015).

The remaining sections of the report are organized as below: Section 2 presents an overview of the enhanced resilient plant systems analysis process. Section 3 introduces the risk analysis tools used in the project, including SAPHIRE, RELAP5-3D, RAVEN, and BISON. Section 4 provides the SBO scenario analysis using SAPHIRE and RELAP5-3D. Limit surface analysis results are also presented. Section 5 provides LBLOCA scenario analysis using the dynamic PRA approach. Sections 6 to 9 present other associated analyses conducted for the project including the risk-informed plant enhancement analysis, the risk-informed sensitivity analysis for ATF, the fuel performance analysis, and the resilience analysis in long-term SBO scenario. Section 10 provides a summary and the future work of the program.

## **2. ENHANCED RESILIENT PLANT SYSTEMS ANALYSIS**

### **2.1 ERP Analysis Process**

The ATF, combined with the optimal use of FLEX, the enhancements to plant components and systems, the incorporation of augmented or new passive cooling systems, and the improved fuel cycle efficiency are called ERP Systems.

General process to perform engineering analysis for ERP ATF and FLEX designs is described below.

Step 1: Identify and select the ERP design features to be analyzed, which include

- ATF (e.g., FeCrAl, Cr coated, or SiC cladding, doped UO<sub>2</sub> or U<sub>3</sub>Si<sub>2</sub> fuel)
- FLEX (e.g., primary FLEX injection, FLEX generators)

Step 2: Identify and select analysis tools to be used in the research. Such tools includes those for

- Classical probabilistic risk assessment (e.g., SAPHIRE, CAFTA)
- Dynamic probabilistic risk assessment (e.g., RAVEN, EMERALD)
- Thermal hydraulic analysis (e.g., RELAP5-3D, TRACE, MELCOR, MAAP)
- Severe accident analysis (e.g., MELCOR, MAAP)
- Core design and fuel performance analysis (e.g., BISON).

Step 3: Identify and select the accident scenarios to be analyzed. For example,

- Station blackout (SBO)
- Loss-of-coolant accidents (LOCA)
- Loss of feedwater (LOFW)
- Steam generator rupture (SGTR)

Step 4: Identify analysis metrics to be evaluated in the research for accident scenarios, for example,

- Time: the time for peak clad temperature (PCT) to reach the corresponding clad melting temperature, the time to generate 0.5 kilograms hydrogen
- Mass of hydrogen generated in the accident scenario
- Risk metrics: core damage frequency (CDF), large early release frequency (LERF)
- Economic: loss of plant generation, loss due to the evacuation, loss of land/life/public health

Step 6: Conduct engineering analysis and evaluate risk impact and economic impact from the ERP designs.

- Classic risk analysis
- Advanced risk analysis
- Risk-informed sensitivity analysis
- Fuel performance analysis
- Economic analysis

Figure 2-1 shows the general ERP analysis process. The remaining of this section provides an overview of various engineering analysis approaches and then presents the work conducted in FY 2018.

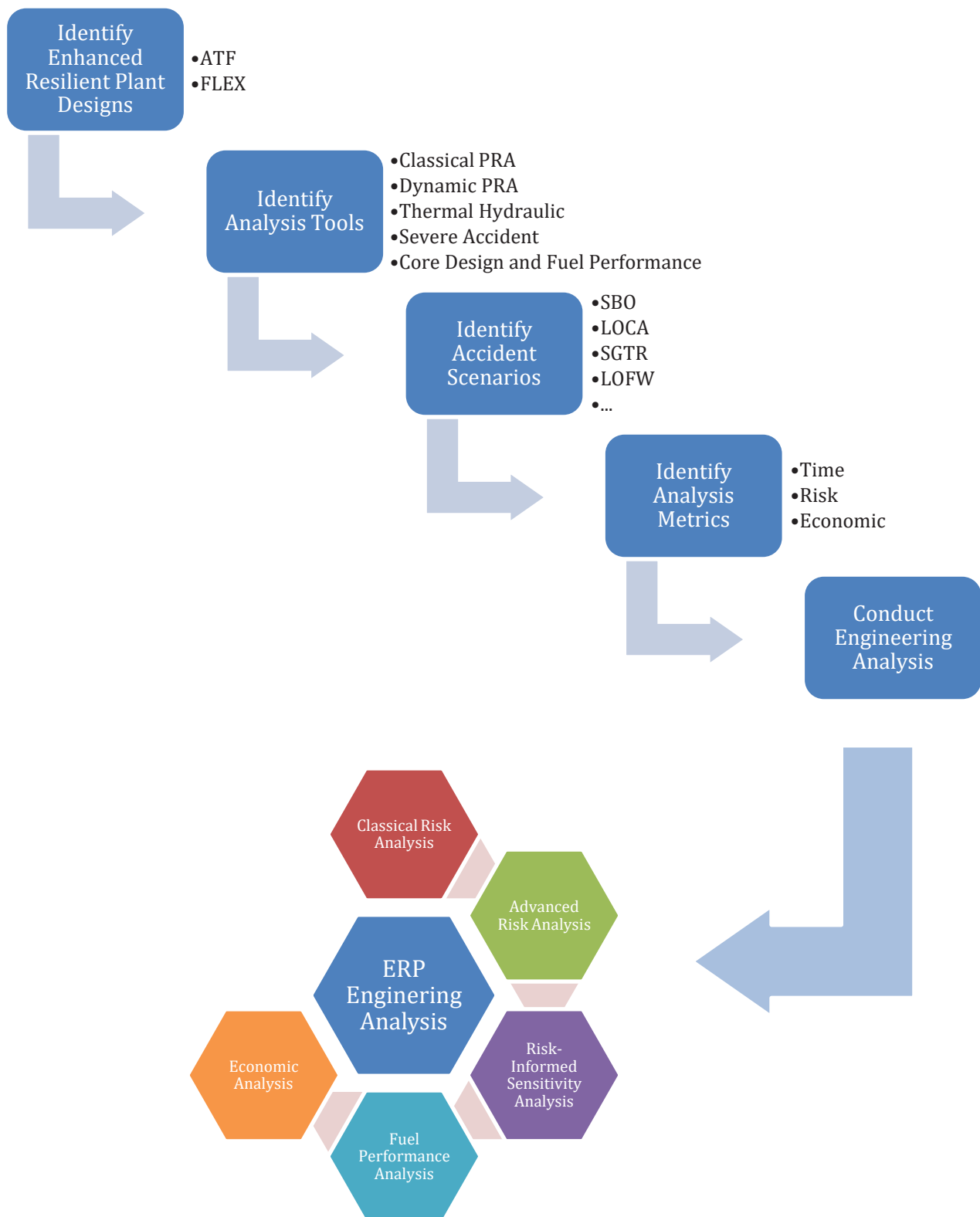


**Figure 2-1. Enhanced Resilient Plant Engineering Analysis.**



## 2.2 Classical Risk Analysis

PRA, also called Probabilistic Safety Assessment (PSA), is defined as “a qualitative and quantitative assessment of the risk associated with plant operation and maintenance that is measured in terms of frequency of occurrence of risk metrics, such as core damage or a radioactive material release and its effects on the health of the public” in the ASME/ANS PRA Standard (ASME and ANS, 2013). It is an engineering analysis approach that models a nuclear power plant (NPP) as a system and evaluates the risk and vulnerabilities associated with the plant operations. PRA answers three fundamental questions which are called the “risk triplet:”

- What can go wrong? – accident scenario
- How likely is it to occur? – frequency/probability
- What will be the outcome? – consequences

PRA systematically identifies potential nuclear power plant accident scenarios and estimate the likelihoods and consequences of these scenarios. PRA can quantify risks associated with plant performance measures and provides insights into the strengths and vulnerabilities of the design and operation of a NPP. An NPP PRA model typically starts with the identification of the hazards and a spectrum of initiating events. Event trees are then used to model the response of the plant’s systems and operators to each initiating event, with different plant system and human action combinations leading to different outcomes (e.g., OK or core damage). Fault trees are used to identify the combinations of equipment failures and human errors that could lead to system failures, and quantify the overall failure probability for each plant system represented in the event trees. Data analysis is performed to estimate the frequencies of initiating events and probabilities of the basic events representing equipment failures and unavailabilities, while human reliability analysis estimates the probabilities of human errors that are modeled in the PRA. The event trees and fault trees are linked and quantified to calculate the likelihood of all the sequences that lead to the same outcome, e.g., CDF or LERF.

PRA is an important elements of the Nuclear Regulatory Commission (NRC)’s licensing and regulatory processes. The NRC’s PRA Policy Statement issued in 1995 (Federal Register, 1995) encourages the staff and industry to increase the use of PRA in all nuclear regulatory matters to the extent supported by the state of the art in terms of methods and data to complements the deterministic approach and supports the traditional defense-in-depth philosophy. The PRA models and results, or the so called “risk-informed” approach, have since been widely used by the NRC and nuclear industry in their decision making processes. For example, the NRC uses PRA in the nuclear reactor regulatory activities such as the development of regulations and guidance, licensing decisions and certification of reactor designs, oversight of licensee operations and facilities, and the evaluation of operational experience.

In this project, PRA is used for two types of analysis, ERP Risk Analysis and Risk-Informed ERP Analysis. The objective of an ERP Risk Analysis is to evaluate the risk impact for the proposed plant enhancement designs. Under the ERP Risk Analysis, potential plant enhancement designs are given or selected (for example, ATF and/or FLEX designs). PRA can be used along with other tools to evaluate the risk and economic impact brought by these designs. This kind of risk analysis usually starts with the base PRA model which represents the as-built, as-operated plant and without considering the proposed enhancement changes. The CDF and LERF from this base model are the reference risk,  $CDF_0$  and  $LERF_0$ . Then the proposed enhancement changes are evaluated for their effects on the base PRA model, which could mean the changes on the event tree modeling, on the fault tree modeling, or on the data and human reliability analysis. The base PRA model is then modified to reflect the proposed enhancement designs and re-quantified for the ERP risk,  $CDF'$  and  $LERF'$ . The differences between the ERP risk and the reference risk  $\Delta CDF = CDF' - CDF_0$  and  $\Delta LERF = LERF' - LERF_0$  represent the risk impact from the proposed enhancement designs.

The objective of Risk-Informed ERP Analysis, on the other hand, is to use PRA and other tools to propose potential plant enhancement designs that could provide best benefits to the plant operations and safety. This kind of analysis again starts with the base PRA model that represents the as-built, as-operated plant. It reviews risk significant accident sequences and cut sets, proposes a list of potential plant enhancement designs that could

reduce the reference risk, and then sort the list by considering the advantages and disadvantages of these potential designs, for example, the potential risk impact and the potential economic impact.

Note that in both types of ERP analysis, thermal hydraulic analysis is often needed to evaluate and compare plant conditions between the as-built, as-operated plant and the enhanced resilient plant which considers the potential enhancement designs.

## **2.3 Advanced Risk Analysis**

Traditional PRA methodologies such as the event tree/fault tree method have the limitation that they do not explicitly tracing time element in the plant system and human response model, but rather static and binary logic based. In order to improve traditional station PRAs, dynamic PRA (DPRA) methodologies have been investigated by the industry. For example, simulation based PRA methodologies treat time element and the dynamical interactions among the plant systems and human actions explicitly in the PRA model by generating numerous simulations to represent accident scenarios. Significant research efforts have been spent on developing different DPRA methodologies (Siu, 1994) (Aldemir, 2013) while the methodologies have been applied in applications such as DPRA modeling of a digital feedwater control system (Aldemir & et al., 2010) and simulation-based dynamic approach for external flooding analysis (Ma & et al., 2017).

## **2.4 Risk-Informed Sensitivity Analysis**

A key aspect in the evaluation of newly proposed ATF fuel designs is the determination of potential increases in coping time with respect to advancements in fuel and cladding materials. The objective of risk-informed sensitivity analysis in this project is to search for ideal fuel cladding material parameters that could provide big increase in coping time. The analysis adjusts the material parameters such as thermal conductivity to find out the parameters needed for the new material to obtain large increase in coping time. The study can provide a qualitative understanding of the relations between coping time increases and various material properties.

## **2.5 Fuel Performance Analysis**

Fuel performance analysis uses a modern fuel performance code, BISON (Hales & al., 2015), to predict the thermo-mechanical behavior and integrity of the full-length nuclear fuel rods during accidents through a realistic cladding failure criterion model developed at INL. ATF fuel rods are designed to have similar or improved behavior in normal operation and provide increased coping time during design-basis accidents. BISON has been developing the capability to model ATF fuel rods, including FeCrAl cladding, Cr-coated cladding and  $U_3Si_2$  fuel. Currently, Cr-coated cladding model is under development by the BISON team. In this report on the ATF fuel modeling and simulations with the BISON code, the focus is on the FeCrAl cladding. In fact, BISON's capability for the FeCrAl cladding includes models for thermophysical properties as a function of temperature, volumetric swelling, and oxidation. Thermophysical properties include the thermal conductivity, specific heat, Young's modulus, Poisson's ratio, yield stress, ultimate tensile strength (UTS), and coefficient of linear thermal expansion. These empirical models are based upon the existing data for the either C35M or APMT<sup>TM</sup> alloy.

## **2.6 FY 2018 Work**

The above general analysis process could be conducted for different ATF and FLEX designs on various accident scenarios for either PWR or boiling water reactor (BWR) across multiple years (Zhang, Szilard, & Hess, 2018). In FY 2018, two accident scenarios, Station Blackout (SBO) and Large Break Loss-of-Coolant-Accident (LBLOCA), were selected to evaluate the risk impact brought by the near term concepts of ATF and FLEX. The

two near term concepts of ATF evaluated in this report are  $\text{UO}_2$  fuel/FeCrAl clad and  $\text{UO}_2$  fuel/Cr-coated Zircaloy clad. They were modeled and incorporated in the generic RELAP5-3D PWR model and were compared against the classical  $\text{UO}_2$  fuel/Zircaloy clad which was used as the reference case. The key metrics that are used to evaluate the resiliency enhancements for a nuclear power plant include:

- Time for PCT to reach the clad melting temperature
- Time to reach 0.5 kg  $\text{H}_2$  after the accident occurred
- Core damage frequency (CDF)

Other than the above ERP risk Analyses, different types of analysis were conducted for investigation purpose in FY 2018, for example, risk-informed plant enhancement analysis for SBO, risk-informed sensitivity analysis for ATF, fuel performance analysis, and resilience analysis for long term SBO.

### 3. ERP ANALYSIS TOOLS

#### 3.1 SAPHIRE

Systems Analysis Programs for Hands-on Integrated Reliability Evaluations (SAPHIRE) is a probabilistic risk and reliability assessment software tool developed and maintained by INL for the U.S. Nuclear Regulatory Commission (NRC) (Smith & Wood, 2011). SAPHIRE can be used to model nuclear power plant response to both internal hazards (for example general transients, loss of offsite power, loss of feedwater, etc.) and external hazards (for example, seismic, fire, external flooding, high wind). SAPHIRE 8, the current version, can be used to develop Level 1 PRA for core damage frequency (CDF) quantification, Level 2 PRA for containment failure and release category frequency (including large early release frequency, or LERF) evaluation for severe accidents in which core damage has occurred, and limited Level 3 PRA for release consequence analysis. SAPHIRE 8 is a powerful PRA software that has both the basic PRA modeling capabilities such as creating event trees and fault trees, defining and assigning basic event failure data, linking and solving event trees and fault trees, documenting and reporting the results, and the advanced capabilities such as integrated Level 1 and Level 2 PRA analysis, performing sensitivity and uncertainty analyses, and conducting specialized analyses for the NRC's Accident Sequence Precursor (ASP) program and Significance Determination Process (SDP).

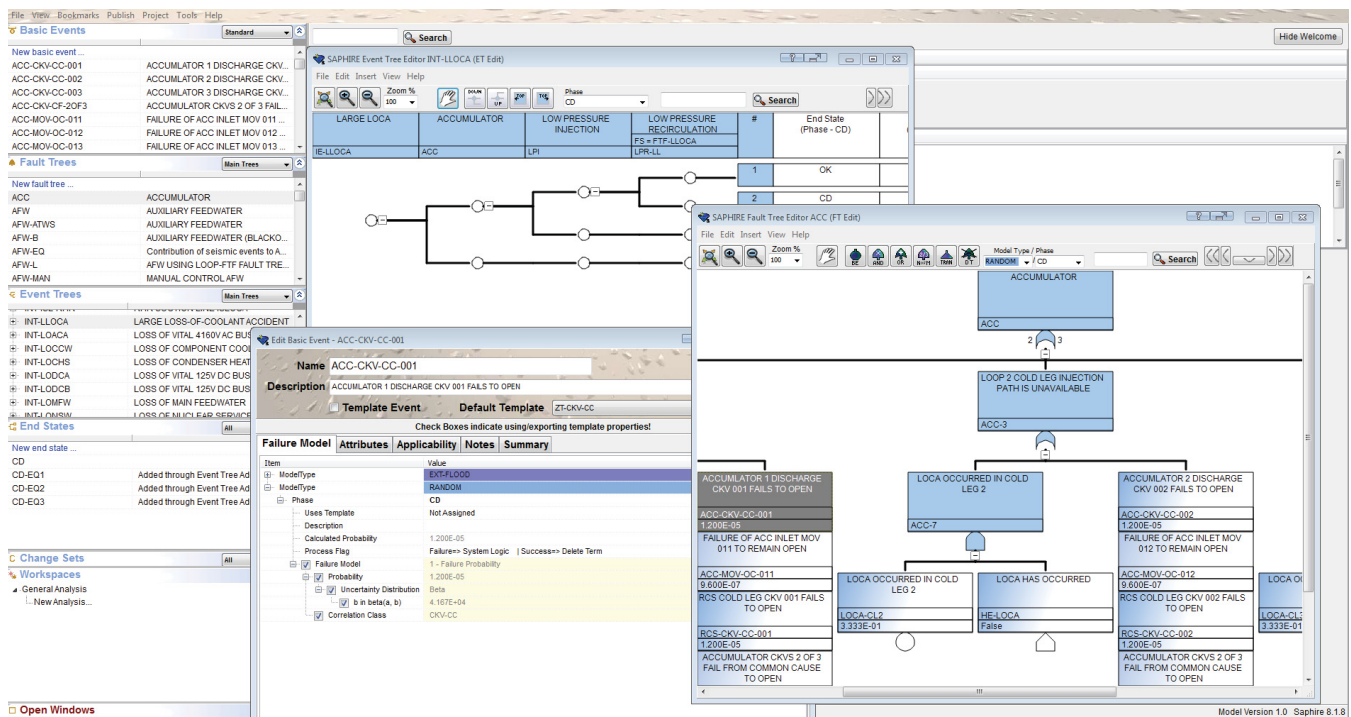


Figure 3-1. SAPHIRE 8 Graphic User Interface.

#### 3.2 RELAP5-3D

RELAP5-3D code (RELAP5-3D Code Development Team, 2018) is the INL-developed Best-Estimate (BE) system thermal-hydraulic (TH) code of the RELAP5 family. It is capable of performing transient simulations of LWR systems during normal and accidental conditions (both large and small LOCAs, ATWS, loss of feedwater, main steam line break, etc.). RELAP5-3D has also been successfully used for modeling and simulations of the following systems: fusion reactors, space reactors, gas and liquid metal reactors, cardiovascular systems.

The code solves a nonhomogeneous and non-equilibrium model (unequal velocities, unequal temperatures, UVUT) for the two-phase flow using a fast, partially implicit numerical scheme. RELAP5-3D differs from the

other RELAP5 versions thanks to a multi-dimensional TH, a 3D neutron kinetic modeling capability and an extensive library of different fluids properties. The code development and validation is based on an extensive set of experimental data and its applicability to Best-Estimate plus Uncertainty (BEPU) technology has been demonstrated (Schultz, 2015). In the ERP activities, the code is applied for the calculations of LB-LOCA and Station Blackout (SBO) accident. Simulations are run inside the code applicability range, i.e. until the code predicts the onset of the extensive fuel damage. The applicability range of RELAP5-3D is shown in Figure 3-2.

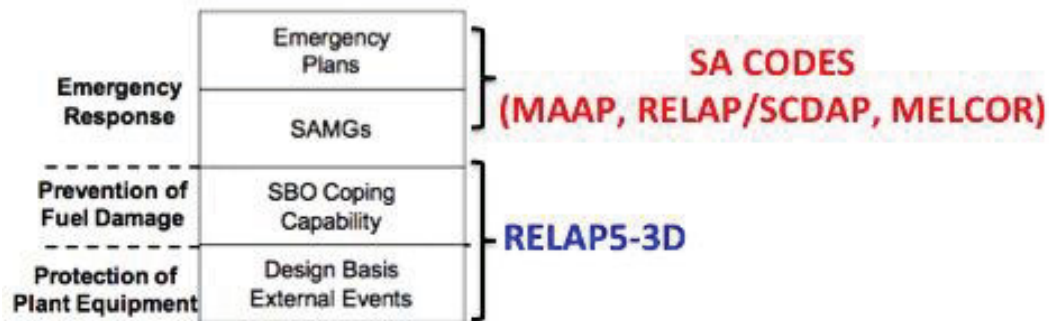


**Figure 3-2. RELAP5-3D Role in LOOP and SBO Calculations.**

References to the applicability of RELAP5 codes in simulating the above scenarios can be found in the open literature, e.g. in (Prosek & Cizelj, 2013), (Matev, 2006). For LBLOCA and SBO, the clad temperature failure criteria reported in Table 3-1 were adopted. It should be noted that for ATF, there are still not available fuel failure criteria like the 1477 K criterion for Zry-LBLOCA. Therefore, for ATF it was decided to adopt the oxide shell failure temperatures as fuel failure criterion (Robb, Howell, & Ott, 2017).

**Table 3-1. Failure Criteria for Different Fuel Clads**

Clad Type	Failure Criteria	
	LB-LOCA	SBO
Zircaloy	PCT>1477 K	PCT>2100 K
ATF - FeCrAl	PCT>1804 K	PCT>1804 K
ATF - Cr	PCT>1804 K	PCT>1804 K

Concerning ATF modeling and simulation, it should be noted that MELCOR (Gauntt, et al., 2005), MAAP (EPRI, 2012), and TRACE (NRC, 2012) codes have been utilized previously to estimate the performance of various candidate ATF designs including FeCrAl and Cr-coated cladding materials. In order to perform an effective study of the ATF candidate with the RELAP5-3D code, some code modifications to the oxidation model had to be implemented. The following paragraphs provide a description of the system modeling and of the new oxidation model.

### 3.2.1 The INL Generic PWR Model

The RELAP5-3D model used in this study is a generic 2.5 GWth Westinghouse 3-loop PWR, representative of the US LWR fleet. The base model can simulate the thermal-hydraulic parameters of the primary side and of some parts of the secondary side (Figure 3-3 to Figure 3-4). The reference base model with Zircaloy clad was

modified to include FeCrAl and Cr-coated as additional cladding material based on parameters from (Holzwarth & Stamm, 2002) and (Field, Snead, Yamamoto, & Terrani, 2017). The RELAP5-3D NPP model, also called IGPWR, is described in detail in (Szilard, Coleman, Prescott, Parisi, & Smith, 2016). In the table below the main design parameters are provided. The 3-loop unit was chosen because of the large amount of publicly available data, e.g. (Dominion, 2007) and (NRC, 2012), which allowed to develop and validate a realistic plant model.

**Table 3-2. Relevant Design Parameters of the IGPWR**

Parameter	Value (SI units)	Value (British units)
Core Power [ $\text{MW}_{\text{th}}$ ]	2,546	
Reactor Inlet / Outlet Temperature [ $^{\circ}\text{C}$ / $^{\circ}\text{F}$ ]	282 / 319	540 / 606
Number of Fuel Assemblies	157	
Rod Array	15x15	
RCS Coolant Flow [ $\text{kg/s}$ / $\text{lb}_m/\text{hr}$ ]	12,738	101.6E+8
Nominal RCS Pressure [ $\text{MPa}$ / $\text{psia}$ ]	15.5	2,250
Number of SG	3	
Secondary Pressure [ $\text{MPa}$ / $\text{psia}$ ]	5.405	785
Secondary Side Water Mass @ HFP [ $\text{kg}$ / $\text{lb}_m$ ]	41,639	91,798
SG Volume [ $\text{m}^3$ / $\text{ft}^3$ ]	166	5,868
SG Steam Flow rate @ HFP [ $\text{kg/s}$ / $\text{lb}_m/\text{hr}$ ]	473.0	3.756E+6
FW Temperature [ $^{\circ}\text{C}$ / $^{\circ}\text{F}$ ]	228	443
Main FW pump [ $\text{m}^3/\text{s}$ / $\text{gpm}$ ]	2 x 6.513 (at 518 m)	2 x 13,800 (at 1,700 feet)
Turbine-driven AFW pump [ $\text{m}^3/\text{s}$ / $\text{gpm}$ ]	1 x 0.3304 (at 832 m)	1 x 700 (at 2,730 feet)
Emergency Condensate Storage Tank [ $\text{m}^3$ / $\text{ft}^3$ ]	416	14,691
Accumulator Water Volume [ $\text{m}^3$ / $\text{ft}^3$ ]	3 x 27.61	3 x 975
Accumulator Pressure [ $\text{MPa}$ / $\text{psig}$ ]	4.14-4.59	600-665
High Head Safety Injection [ $\text{m}^3/\text{s}$ / $\text{gpm}$ ]	3 x 0.0708 (at 1,767 m)	3 x 150 (at 5,800 ft)
Low Head Safety Injection [ $\text{m}^3/\text{s}$ / $\text{gpm}$ ]	2 x 1.416 (at 68.6 m)	2 x 3,000 (at 225 ft)
Containment Volume [ $\text{m}^3$ / $\text{ft}^3$ ]	50,970	1,800,000
Containment Design Pressure [ $\text{MPa}$ / $\text{psig}$ ]	0.31	45
Containment Operating Pressure [ $\text{MPa}$ / $\text{psia}$ ]	0.062 to 0.071	9 to 10.3



The RELAP5-3D model developed for analyzing LB-LOCA and SBO-like events is based on an input-deck describing:

- reactor pressure vessel (RPV);
- three main circulation circuits (MCC), including the main coolant pumps (MCP) and the steam generators (SG);
- pressurizer (PRZ), and its main valves (PORV and SV);
- connections for the emergency core cooling system (ECCS) and the auxiliary feed-water (AFW);
- secondary part of the SGs up to the SG outlet, including the main valves (PORV and SV);
- main feed-water (MFW)
- ECCS including High and Low Pressure Injection Systems (HPIS and LPIS) and accumulators

The sketches of the RPV and of the MCC, including the secondary side of the SGs, are given in Figure 3-3. Three independent TH channels representing the central, the middle and the periphery of the core are used. A sketch of the three-channel core region subdivision is given in Figure 3-4, together with the number of the fuel assemblies and their relative radial power. 214 hydraulic volumes connected by 257 junctions and coupled to 240 heat structures compose the RELAP5-3D nodalization. The total number of mesh points, discretizing the heat structures, is 1312. The model is based on a Surry NPP nodalization developed for the RELAP/SCDAP code for SBO analyses (Bayless, 1987). The model has been upgraded and changed to reflect the current plant configuration (e.g., power uprate) and to be compatible with the RELAP5-3D code syntax.

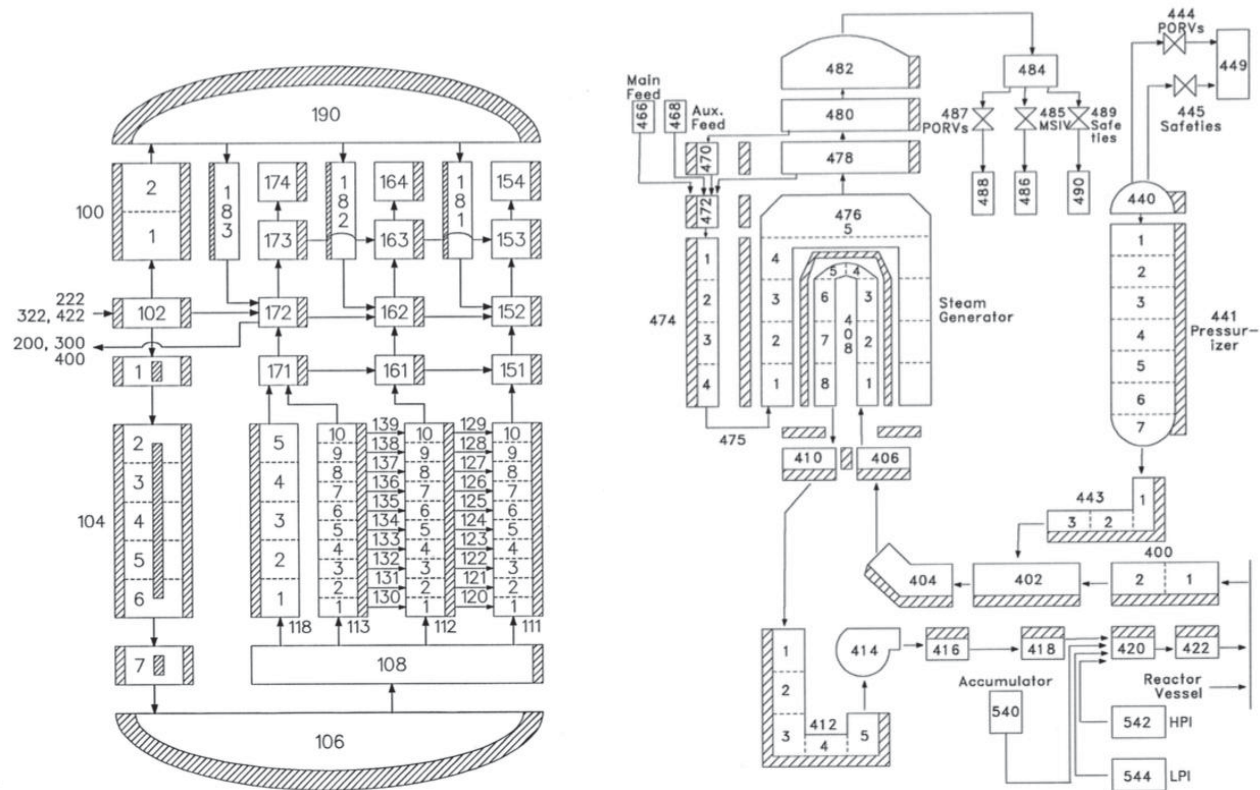


**Figure 3-3. RELAP5-3D RPV Model (left) and MCC & SG Models (right).**

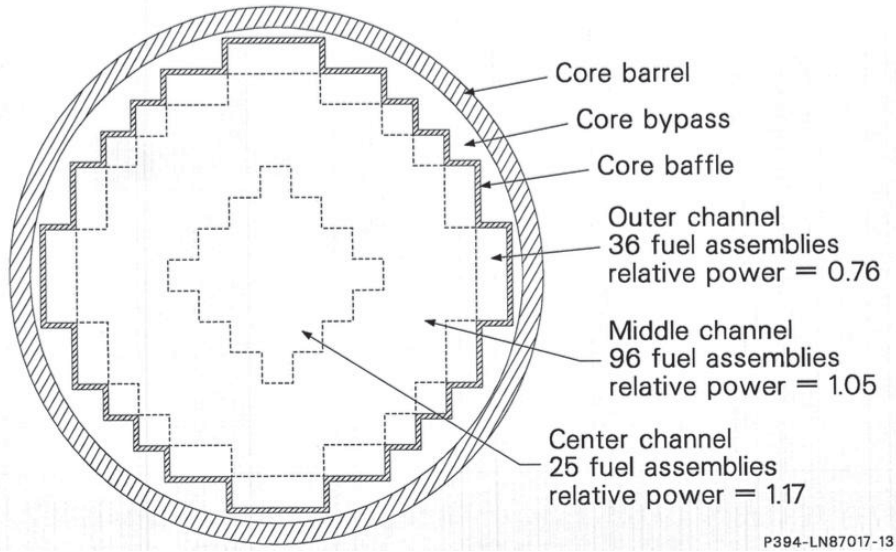


**Figure 3-4. RELAP5-3D Core Model.**

The possible operator actions (SG cool-down, feed and bleed, AFW flow control, HPIS/LPIS actuation) are implemented through the RELAP5-3D control logic system. RELAP5-3D control variables calculate the derived parameters for the control logic system and for the transients' analyses.

### 3.2.2 Model Qualification

Steady state and on-transient validation has been achieved. Deviations of calculated values are negligible, resulting in an excellent agreement. (Parisi, et al., 2016) provides the trend of the main parameters and the on-transient calculations with code-to-code (RELAP5-3D vs. MELCOR code) validation.

A null-transient of 1000 s was calculated for validating the steady-state solution. The steady state validation table is reported below.



**Table 3-3. RELAP5-3D Steady State Values**

Parameter	Reference Value	RELAP5-3D Value	Deviation (%)	References
Reactor Power (W)	2,546	2,546	imposed	(NRC, 2012)
PRZ pressure (MPa)	15.5	15.5	imposed	(NRC, 2012)
Total RCS coolant loop flow rate (Kg/s)	12,738	12,738	0.0	(NRC, 2012)
HL Temperature (K)	591.8	593.1	0.2	(Virginia Electric and Power Company, 2010)
		593.1	0.2	
		593.1	0.2	
CL Temperature (K)	555.6	557.3	0.3	(Virginia Electric and Power Company, 2010)
		557.3	0.3	
		557.3	0.3	
Feedwater Temperature (K)	501.5	501.5	imposed	(Virginia Electric and Power Company, 2010)
		501.5	imposed	
		501.5	imposed	
Steam flow rate per SG (Kg/s)	473	470.1	-0.6	(Virginia Electric and Power Company, 2010)
		470.7	-0.5	
		471.0	-0.4	
Steam pressure at the Outlet Nozzle (MPa)	5.405	5.405	imposed	(Virginia Electric and Power Company, 2010)
		5.405	imposed	
		5.405	imposed	
Liquid Mass per SG (Kg)	41,639	41,640	0.0	(NRC, 2012)
		41,638	0.0	
		41,638	0.0	
Steam Temperature (K)	542	542	0.0	(Virginia Electric and Power Company, 2010)
		542	0.0	
		542	0.0	

### 3.2.3 Metal-Water Reactor Model in RELAP5-3D

The capability of modeling a thin coating layer to the outside of fuel cladding was added to RELAP5-3D in this project. This coding change only affects cylindrical heat structures. The coating layer as in the ATF designs is designed to protect the fuel cladding from oxidizing and degrading under high temperature conditions. This oxidation reaction is of concern because it weakens the Zirconium cladding and also releases additional heat, which can increase the temperature in the reactor. The presence of the coating means that the coating will react instead of the cladding. A slow reacting coating material should protect the cladding in the reactor and lengthen the lifetime of the reactor.

It should be noted that the change in outer fuel radius does not affect the flow geometry in the reactor core. The additional thickness in the cladding does not contribute to the heat conduction through the cladding. This change will protect the outer layer of the cladding from oxidation, the amount of heat generated due to the chemical reaction will be added to the heat structure, and the amount of chemical reaction product generated will be calculated.

A correlation developed by (Cathcart & et al., 1977) is used to model the metal-water reaction model in RELAP5-3D which uses a parabolic rate law. This default correlation was developed for the Zirconium-Steam reaction. The coding has been generalized to allow the user to model coolant-structure chemical interactions for which the parabolic rate law applies. The Cathcart correlation used in RELAP5-3D to calculate the thickness of the cladding converted to oxide is shown in Equation 1.

$$\Delta r^{n+1} = [(\Delta r^n)^2 + (K\Delta t)e^{-(\Delta E/RT)}]^{1/2} \quad (1)$$

where the superscript n+1 refers to the new time value and n refers to the old time value.

K is a reaction rate constant ( $9.166 \times 10^{-7} \text{ m}^2/\text{s}$ , derived from the Cathcart model)

$\Delta t$  is the time step size (s)

$\Delta E$  is the activation energy (35,890 cal/mole for the Cathcart model)

R is the gas constant (1.986 cal/K-mole)

T is the cladding temperature (K).

The amount of heat added (Q) to the outer surface of the cladding due to oxidation is calculated by Equation 2.

$$Q = \rho\pi[(r_o - \Delta r^n)^2 - (r_o - \Delta r^{n+1})^2] \frac{H}{W} \quad (2)$$

where  $r_o$  is the initial radius of unreacted cladding (cladding outer radius)

$\rho$  is the cladding density ( $6,500 \text{ kg/m}^3$  for Zirconium)

H is the reaction heat release ( $5.94 \times 10^8 \text{ J/(kg-mole)}$ )

W is the molecular weight of cladding ( $91.22 \text{ kg/(kg-mole)}$  for Zirconium).

Lastly the total Hydrogen mass generated by the metal water reaction is calculated by multiplying the mass of Zirconium reacted by the ration of the molecular weight of 4 Hydrogen atoms to 1 Zirconium atom.

For the coating, the calculation of the thickness of the coating converted to oxide matches what is done for the cladding. The user can enter an initial coating thickness, material density, activation energy, reaction rate constant, reaction heat release, coating material molecular weight, and the molecular weight of the reaction product (typically Hydrogen) divided by the coating material molecular weight.

At higher temperatures the oxidation parameters can change significantly for both coated-cladding and other ATF cladding types (e.g., full FeCrAl cladding). To account for this, additional input was added. The user can

input a threshold temperature at which a transition occurs, followed by the usual input of material density, activation energy, reaction rate constant, reaction heat release, coating material molecular weight (although this should be a constant), and the molecular weight of the reaction product divided by the coating material molecular weight. Additional input was also added to allow the user to specify a transition temperature for the base-cladding or the full ATF cladding (FeCrAl). However this option only allows the user to input a transition reaction rate constant.

The logic path for the metal-water reaction coding is shown in Figure 3-5 – one potential logic path is described here. When a coating layer is applied to the cladding, the coding first checks if the coating has oxidized through the entire thickness. If that is the case, the code will switch to performing the metal-water reaction calculations for the cladding material only. If the clad has broken, then the metal-water reaction will be calculated for both the inner and outer surfaces of the cladding. If the outer surface heat structure temperature is greater than the specified transition temperature then the coding will switch to using the high-temperature parameters for the calculations. Other logic paths behave as shown in the figure.

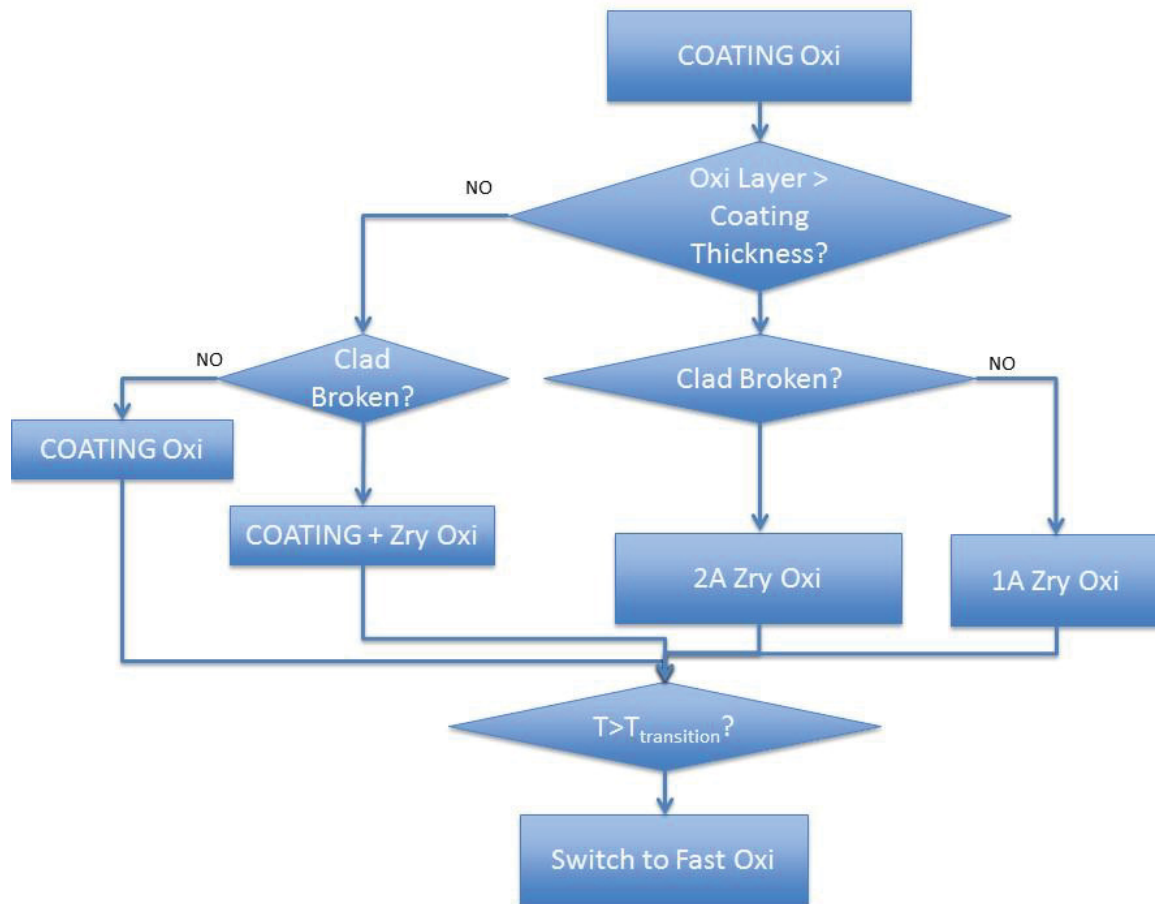


**Figure 3-5. Logic Path for the Metal-Water Reaction Model Coding.**

The changes to the input are as follows:

<b>1CCCG002 Card, Coating Metal-Water Reaction Control</b>	
W1(R)	Initial unreacted coating thickness on cladding's outer surface (m, ft).
W2(R)	Coating material density (kg/m <sup>3</sup> ). This quantity is optional, if not entered or 0.0 the default value for zirconium (6,500 kg/m <sup>3</sup> ) is used.
W3(R)	Coating activation energy (cal/mole). This quantity is optional, if not entered or 0.0 the default value for the Cathcart model (35,890 cal/mole) is used.
W4(R)	Coating reaction rate constant (variable K) (m <sup>2</sup> /s). This quantity is optional, if not entered or 0.0 the default value for the Cathcart model (2.252 x 10 <sup>-6</sup> m <sup>2</sup> /s) is used.
W5(R)	Coating reaction heat release (J/kg-mole). This quantity is optional, if not entered or 0.0 the default value for the zirconium-steam reaction (5.94 x 10 <sup>8</sup> J/kg-mole) is used.
W6(R)	Coating material molecular weight (kg/kg-mole). This quantity is optional, if not entered or 0.0 the default value for zirconium (91.22 kg/kg-mole) is used.
W7(R)	Molecular weight of reaction product divided by Word 6. This quantity is optional, if not entered or 0.0 the default value for the zirconium-steam reaction (0.0442) is used.
<b>1CCCG005 Card, High-Temperature Coating Metal-Water Reaction Control</b>	
W1(R)	Coating material transition temperature (K, F).
W2(R)	Coating material density (kg/m <sup>3</sup> ). This quantity is optional, if not entered or 0.0 the default value for zirconium (6,500 kg/m <sup>3</sup> ) is used.
W3(R)	Coating activation energy (cal/mole). This quantity is optional, if not entered or 0.0 the default value for the Cathcart model (35,890 cal/mole) is used.
W4(R)	Coating reaction rate constant (variable K) (m <sup>2</sup> /s). This quantity is optional, if not entered or 0.0 the default value for the Cathcart model (2.252 x 10 <sup>-6</sup> m <sup>2</sup> /s) is used.
W5(R)	Coating reaction heat release (J/kg-mole). This quantity is optional, if not entered or 0.0 the default value for the zirconium-steam reaction (5.94 x 10 <sup>8</sup> J/kg-mole) is used.
W6(R)	Coating material molecular weight (kg/kg-mole). This quantity is optional, if not entered or 0.0 the default value for zirconium (91.22 kg/kg-mole) is used.

W7(R)	Molecular weight of reaction product divided by Word 6. This quantity is optional, if not entered or 0.0 the default value for the zirconium-steam reaction (0.0442) is used.
<b>1CCCG003 Card, Cladding Metal-Water Reaction Control</b>	
W8(R)	Initial oxide thickness on cladding's inner surface (m, ft). This quantity is optional for rectangular heat structures. This word must be entered to activate the calculation of the oxide thickness on the inner surface of a rectangular heat structure. The code sets this value to 0.0 for cylindrical or spherical heat structures.
W9(R)	Cladding material transition temperature (K, F).
W10(R)	Cladding reaction rate constant (variable K) ( $\text{m}^2/\text{s}$ ) at high-temperatures. This quantity is optional, if not entered or 0.0 the default value for the Cathcart model ( $2.252 \times 10^{-6} \text{ m}^2/\text{s}$ ) is used.

### 3.3 RAVEN

RAVEN (Alfonsi, et al., 2017) is a generic software framework to perform parametric and probabilistic analysis based on the response of complex system codes. It is capable of communicating directly with the system codes that currently used to perform plant safety analyses. The provided Application Programming Interfaces (APIs) allow RAVEN to interact with any code as long as all the parameters that need to be perturbed are accessible by input files or via python interfaces. For example, RAVEN can be coupled to RELAP5-3D system TH code via an API to perform sensitivity and uncertainty analysis. RAVEN is capable of investigating system response and exploring input spaces using various sampling schemes such as Monte Carlo, grid, or Latin hypercube. However, RAVEN's strength lies in its system feature discovery capabilities such as: constructing limit surfaces, separating regions of the input space leading to system failure, and using dynamic supervised learning techniques.

RAVEN has the capability to run on High Performance Computing machines (HPC), which allows the execution of hundreds of parallel serial runs. RAVEN strength lies also in its system feature discovery capabilities such as: constructing limit surfaces, separating regions of the input space leading to system failure, and using dynamic supervised learning techniques.

Dynamic PRA approach heavily relies on multi-physics system simulator codes (e.g., RELAP5-3D) coupled with stochastic analysis tools (e.g., RAVEN). From a PRA point of view, this type of simulation can be described by using two sets of variables:

- $\mathbf{c} = \mathbf{c}(t)$  represents the status of components and systems of the simulator (e.g., status of emergency core cooling system, AC system)
- $\boldsymbol{\theta} = \boldsymbol{\theta}(t)$  represents the temporal evolution of a simulated accident scenario, i.e.,  $\boldsymbol{\theta}(t)$  represents a single simulation run. Each element of  $\boldsymbol{\theta}$  can be for example the values of temperature or pressure in a specific node of the simulator nodalization.

From a mathematical point of view, a single simulator run can be represented as a single trajectory in the phase space. The evolution of such a trajectory in the phase space can be described as follows:

$$\begin{cases} \frac{\partial \boldsymbol{\theta}(t)}{\partial t} = \mathcal{H}(\boldsymbol{\theta}, \mathbf{s}, \mathbf{c}, t) \\ \frac{\partial \mathbf{c}(t)}{\partial t} = \mathcal{C}(\boldsymbol{\theta}, \mathbf{s}, \mathbf{c}, t) \end{cases} \quad (3)$$

where:

- $\mathcal{H}$  is the actual simulator code that describes how  $\boldsymbol{\theta}$  evolves in time
- $\mathcal{C}$  is the operator which describes how  $\mathbf{c}$  evolves in time, i.e., the status of components and systems at each time step
- $\mathbf{s}$  is the set of stochastic parameters.

Starting from the system located in an initial state,  $\boldsymbol{\theta}(t = 0) = \boldsymbol{\theta}(0)$ , and the set of stochastic parameters (which are generally generated through a stochastic sampling process), the simulator determines at each time step the temporal evolution of  $\boldsymbol{\theta}(t)$ . At the same time, the system control logic<sup>1</sup> determines the status of the system and components  $\mathbf{c}(t)$ . The coupling between these two sets of variables is shown in Figure 3-6.

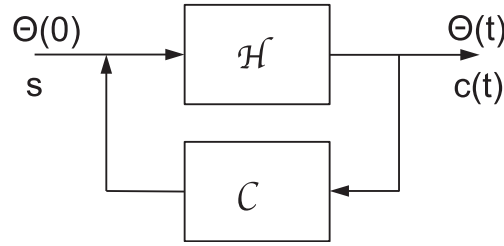


**Figure 3-6. Relationship between Simulator Physics Code ( $\mathcal{H}$ ) and Control Logic ( $\mathcal{C}$ ).**

By using the RISMC approach, the Dynamic PRA analysis is performed by:

1. Associating a probabilistic distribution function (pdf) to the set of parameters  $\mathbf{s}$  (e.g., timing of events)
2. Performing stochastic sampling of the pdfs defined in Step 1
3. Performing a simulation run given  $\mathbf{s}$  sampled in Step 2, i.e., solve the system of equations (3)
4. Repeating Steps 2 and 3  $M$  times and evaluating user defined stochastic parameters such as core damage (CD) probability ( $P_{CD}$ ).

The RISMC project has developed in the past years a statistical framework in order to perform advanced (i.e., Dynamic) PRA analyses: RAVEN (Risk Analysis and Virtual control ENvironment). RAVEN is a software framework that allows the user to perform generic statistical analysis. By statistical analysis we include:

- Sampling of codes: either stochastic (e.g., Monte-Carlo and Latin Hypercube Sampling) or deterministic (e.g., grid and Dynamic Event Trees)
- Generation of Reduced Order Models also known as Surrogate models
- Create connection/dependencies among multiple models (e.g., codes or ROMs) through the ensemble models feature
- Post-processing of the sampled data and generation of statistical parameters (e.g., mean, variance, covariance matrix)

<sup>1</sup> Which is usually integral part of the system simulator

These features are particularly relevant for the multi-unit PRA models and they have been extensively employed both on desktop/laptop machines and High Performance Computing (HPC) systems. Figure 3-7 shows a general overview of the elements that comprise the RAVEN statistical framework:

- Model: it represents the pipeline between input and output space. It comprises both codes (e.g., RELAP5-3D) and also Reduced Order Models
- Sampler: it is the driver for any specific sampling strategy (e.g., Monte-Carlo, LHS, DET)
- Database: the data storing entity
- Post-processing module: module that performs statistical analyses and visualizes results

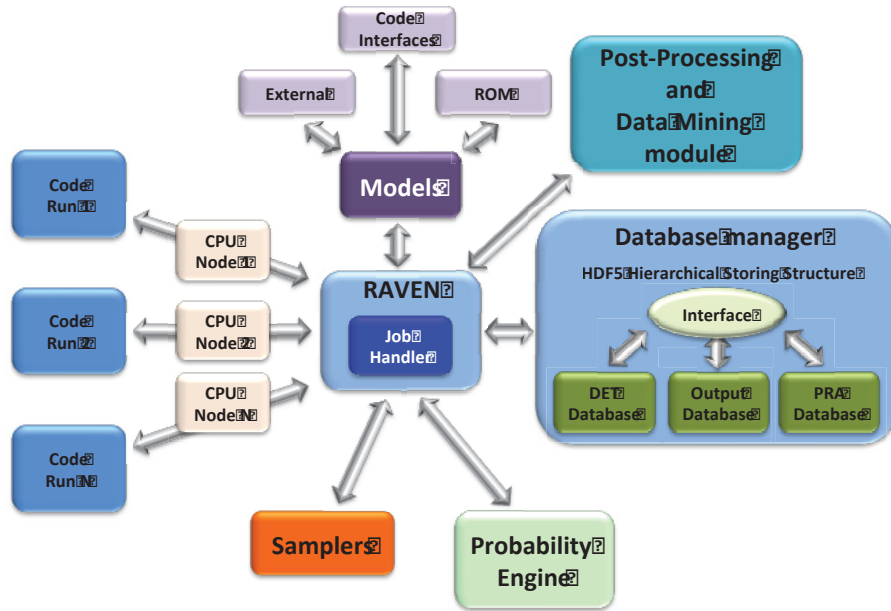


**Figure 3-7. Scheme of RAVEN Statistical Framework Components.**

In some cases multiple models need to be interfaced with each other since the initial conditions of some are dependent on the outcomes of others. In order to solve this problem in the RAVEN framework, a new model category (e.g., class), named *EnsembleModel*, was implemented. This class is able to assemble multiple models of other categories (i.e. Code, External Model, ROM), identifying the input/output connections, and, consequentially the order of execution and which sub-models can be executed in parallel.

### 3.4 BISON

BISON (Hales & al., 2015) is a modern finite element-based, multidimensional fuel performance code developed at INL. As a nuclear fuel performance code, it is applicable to a variety of fuel forms including light water reactor fuel rods, TRISO particle fuel, and metallic rod and plate fuel. It solves the fully-coupled equations of thermomechanics and species diffusion, for 1D spherical, 1D layered, 2D axisymmetric, 2D plane strain, or 3D geometries. Fuel models are included to describe temperature and burnup dependent thermal properties, fission product swelling, densification, thermal and irradiation creep, fracture, and fission gas production and release. Plasticity, irradiation growth, and thermal and irradiation creep models are implemented for clad materials. Models are also available to simulate gap heat transfer, mechanical contact, and the evolution of the gap/plenum pressure with plenum volume, gas temperature, and fission gas addition. BISON has been coupled to the mesoscale fuel performance code Marmot, demonstrating fully-coupled multiscale fuel performance capability. BISON is based on the MOOSE (Gaston, Hansen, & Newman, 2009) framework and can therefore efficiently

solve problems using standard workstations or very large high-performance computers. BISON has been adopted as the fuel performance tool of choice for either model development or application by multiple DOE NE programs (NEAMS and CASL being the primary examples). More recently, significant work has been performed on BISON development and validation for the ATF designs, for example FeCrAl-coated cladding and  $U_3Si_2$  fuel. Cr-coated cladding model is currently being developed into BISON.



## 4. SBO SCENARIO ANALYSIS

### 4.1 Generic PWR SBO PRA Model

This project uses a generic internal events PRA model developed using SAPHIRE 8 for a typical pressurized water reactor (PWR) plant for the station blackout (SBO) accident scenario analysis. The generic PWR SBO PRA model starts with the occurrence of a loss of offsite power (LOOP) event. There are four different LOOP categories (Grid-Related or GR, Plant-Centered or PC, Switchyard-Centered or SC, and Weather-Related or WR) (Eide, Gentillon, Wierman, & Rasmuson, 2005) that have been analyzed separately by splitting the LOOP event tree over these categories. Four LOOP event trees (LOOPGR, LOOPPC, LOOPSC, and LOOPWR) are developed in the PRA model for the corresponding LOOP categories. The event tree structure is the same for all four LOOP event trees. The only differences are the initiating event frequencies and the AC power non-recovery probabilities.

The SBO SAPHIRE model includes the LOOP initiating event tree, the SBO main event tree, and the four SBO sub-event trees (SBO-1, SBO-2, SBO-3, SBO-4). Figure 4-1 shows a chart that represents the flow logic of these event trees. Figure 4-2 presents the SAPHIRE SBO main event tree, while the complete SBO event tree model is provided in Appendix A.

The four LOOP event trees (LOOPGR, LOOPPC, LOOPSC, LOOPWR) are quantified with SAPHIRE 8. Table 4-1 presents the quantification results. For each of the four LOOP event trees, there are 222 accident (or core damage) sequences. 76 of the 222 LOOP accident sequences are SBO sequences in which onsite emergency diesel generators fail to supply emergency power to vital buses for the safety equipment. 36 of the 76 Grid-Related SBO accident sequences have non-zero (or greater than  $1\text{E-}12$ , which was set as the quantification truncation level) core damage frequency (CDF). 17 Plant-Centered, 29 Switchyard-Centered, and 23 Weather-Related SBO sequences have non-zero CDF. The total Grid-Related SBO CDF is  $3.77\text{E-}7/\text{year}$  ( $1.50\text{E-}8/\text{year}$  for Plant-Centered SBO,  $1.18\text{E-}7$  for Switchyard-Centered SBO, and  $3.12\text{E-}7$  for Weather-Related SBO). The total SBO CDF for all four LOOP categories is  $8.21\text{E-}7/\text{year}$ .

**Table 4-1. Overview of LOOP/SBO Event Trees Quantification Results**

LOOP Category	Description	Number of LOOP Seq.	Number of SBO Seq.	Number of Non-Zero SBO Seq.	SBO CDF (per year)
LOOPGR	Grid-Related	222	76	36	$3.77\text{E-}07$
LOOPPC	Plant-Centered	222	76	17	$1.50\text{E-}08$
LOOPSC	Switchyard-Centered	222	76	29	$1.18\text{E-}07$
LOOPWR	Weather-Related	222	76	23	$3.12\text{E-}07$
Total		888	304	105	$8.21\text{E-}07$

Table 4-2 shows the 36 non-zero Grid-Related SBO accident sequence results. These non-zero SBO sequences were reviewed to develop scenarios that are simulated and analyzed by RELAP5-3D. Each scenario starts with the occurrence of a SBO event. It then looks at:

- (1) whether the turbine-driven auxiliary feedwater (TDAFW) system could provide flow to the steam generators (SGs) to remove decay heat;
- (2) whether the reactor cooling system (RCS) power-operated relief valves (PORVs) are closed when the pressure is lower than the set point;
- (3) whether operator could rapid depressurize secondary side (RSD);
- (4) what is the reactor coolant pump (RCP) seal leakage rate (for example, 21, 76, 182, 300, or 400 gallons per minute per RCP);
- (5) whether the AC power could be recovered within the defined period (1, 2 or 4 hours);

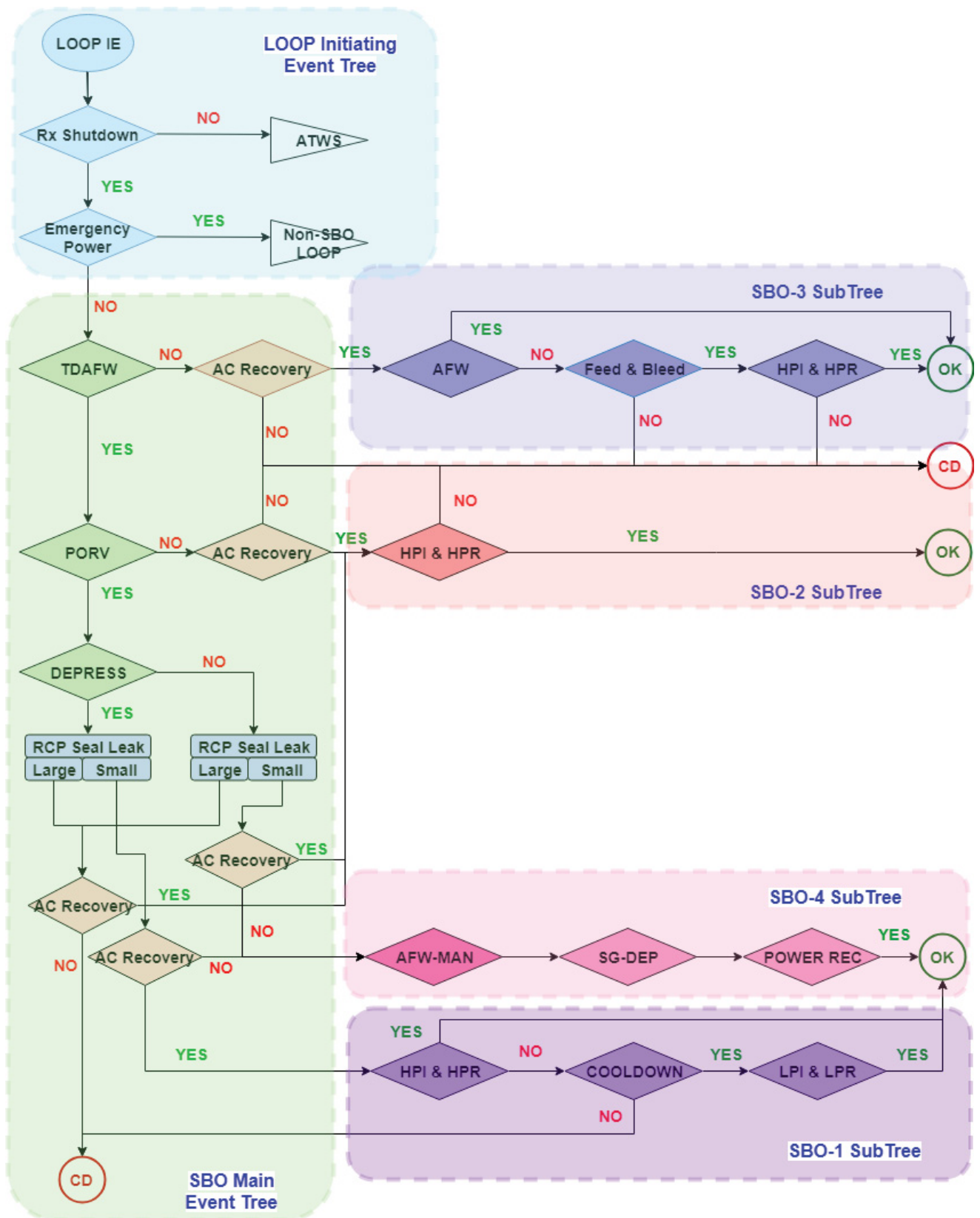


Figure 4-1. SBO Model Event Tree Logic.

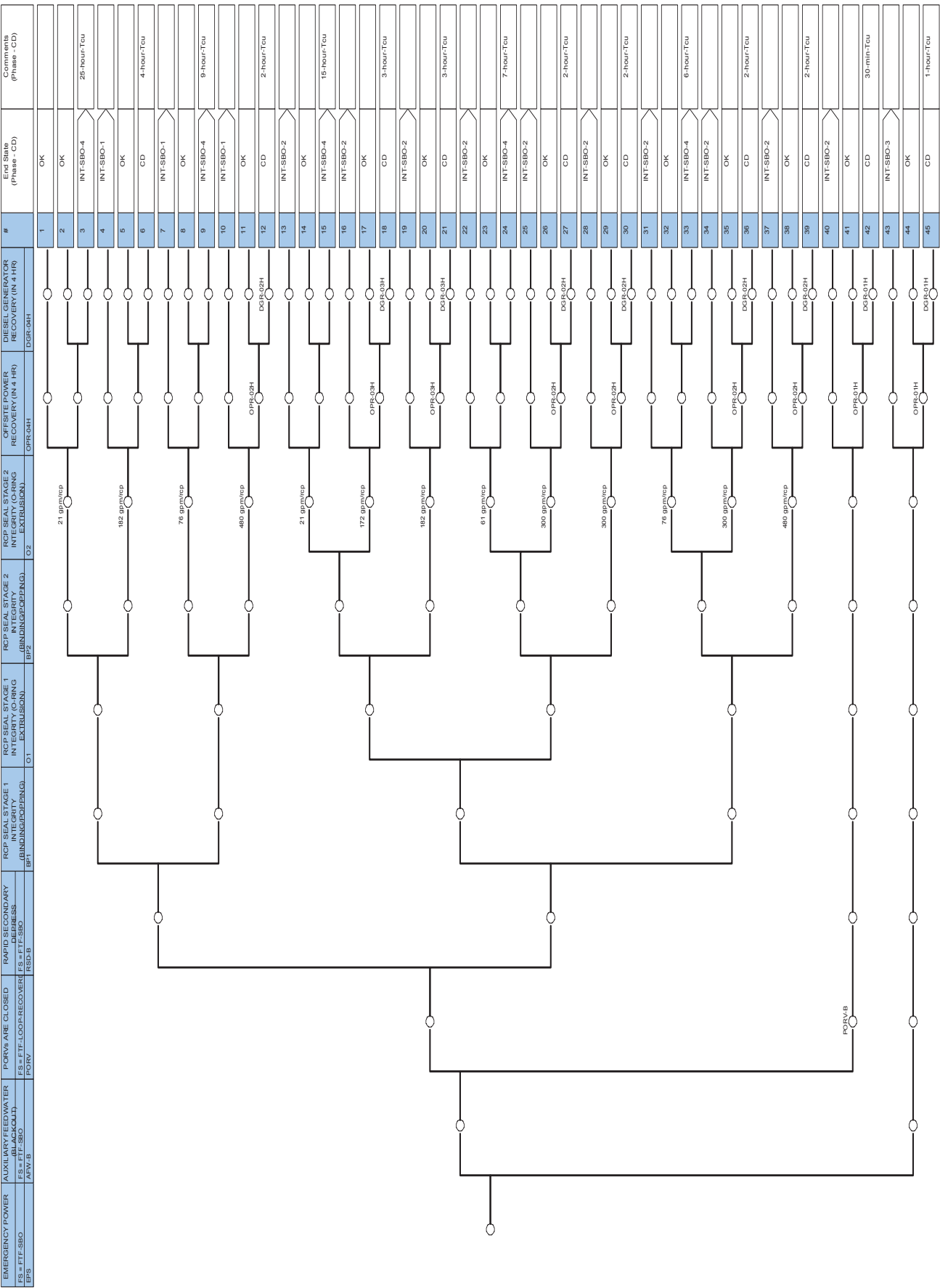


Figure 4-2. Generic PWR SBO Main Event Tree.

**Table 4-2. Grid-Related SBO Sequence Results**

<b>SBO Sequence</b>	<b>CDF</b>	<b>Cut Set Count</b>	<b>%</b>
INT-LOOPGR:16-03-10	1.57E-07	819	41.6%
INT-LOOPGR:16-06	1.30E-07	774	34.6%
INT-LOOPGR:16-45	5.42E-08	925	14.4%
INT-LOOPGR:16-04-7	1.08E-08	149	2.9%
INT-LOOPGR:16-04-2	1.01E-08	665	2.7%
INT-LOOPGR:16-12	4.37E-09	110	1.2%
INT-LOOPGR:16-42	2.32E-09	160	0.6%
INT-LOOPGR:16-03-04	2.23E-09	88	0.6%
INT-LOOPGR:16-09-10	1.91E-09	86	0.5%
INT-LOOPGR:16-27	7.49E-10	132	0.2%
INT-LOOPGR:16-09-04	7.16E-10	72	0.2%
INT-LOOPGR:16-07-7	5.19E-10	18	0.1%
INT-LOOPGR:16-18	4.10E-10	98	0.1%
INT-LOOPGR:16-07-2	4.01E-10	51	0.1%
INT-LOOPGR:16-30	3.47E-10	93	0.1%
INT-LOOPGR:16-21	1.74E-10	56	0.0%
INT-LOOPGR:16-43-07	7.52E-11	27	0.0%
INT-LOOPGR:16-10-2	5.84E-11	10	0.0%
INT-LOOPGR:16-15-10	3.96E-11	15	0.0%
INT-LOOPGR:16-24-10	3.96E-11	15	0.0%
INT-LOOPGR:16-43-06	3.77E-11	14	0.0%
INT-LOOPGR:16-04-8	2.01E-11	9	0.0%
INT-LOOPGR:16-13-3	2.01E-11	18	0.0%
INT-LOOPGR:16-22-3	2.01E-11	18	0.0%
INT-LOOPGR:16-24-04	1.92E-11	5	0.0%
INT-LOOPGR:16-16-3	1.83E-11	18	0.0%
INT-LOOPGR:16-04-4	8.37E-12	3	0.0%
INT-LOOPGR:16-13-2	5.76E-12	2	0.0%
INT-LOOPGR:16-22-2	5.76E-12	2	0.0%
INT-LOOPGR:16-16-2	5.26E-12	2	0.0%
INT-LOOPGR:16-36	4.84E-12	2	0.0%
INT-LOOPGR:16-40-2	4.69E-12	2	0.0%
INT-LOOPGR:16-25-2	4.38E-12	2	0.0%
INT-LOOPGR:16-19-2	2.63E-12	2	0.0%
INT-LOOPGR:16-39	2.42E-12	2	0.0%
INT-LOOPGR:16-28-2	2.19E-12	2	0.0%
Total	3.77E-07	4466	100.0

- (6) if AC power could not be recovered, whether the TDAFW could continue to run without overfill the SGs after DC battery depletes (AFW-MAN), whether steam generator could be depressurized, and whether late power recovery is successful (Late OPR);
- (7) if AC power is recovered in time, whether high pressure injection (HPI) system can provide makeup water to the RCS, and

- (8) Whether high pressure or low pressure recirculation (HPR or LPR) is available to provide long-term cooling for the reactor.

Table 4-3 shows the reviewing results of the PRA SBO accident sequences as well as the preliminary grouping of the sequences into RELAP5-3D scenarios.

**Table 4-3. PRA SBO Sequences to RELAP5-3D Scenarios**

<b>PRA SBO Sequence Results</b>				<b>RELAP5-3D Scenario</b>
<b>Sequence</b>	<b>CDF</b>	<b>Cut Set Count</b>	<b>%</b>	<b>Scenario</b>
INT-LOOPGR:16-03-10	1.57E-07	819	41.6%	SBO-1.0
INT-LOOPGR:16-06	1.30E-07	774	34.6%	SBO-3.0
INT-LOOPGR:16-45	5.42E-08	925	14.4%	SBO-7.0
INT-LOOPGR:16-04-7	1.08E-08	149	2.9%	Same as SBO-3.0, 16-06
INT-LOOPGR:16-04-2	1.01E-08	665	2.7%	SBO-3.3
INT-LOOPGR:16-12	4.37E-09	110	1.2%	SBO-4.0
INT-LOOPGR:16-42	2.32E-09	160	0.6%	SBO-6.0
INT-LOOPGR:16-03-04	2.23E-09	88	0.6%	SBO-1.2
INT-LOOPGR:16-09-10	1.91E-09	86	0.5%	SBO-2.0
INT-LOOPGR:16-27	7.49E-10	132	0.2%	SBO-5.1
INT-LOOPGR:16-09-04	7.16E-10	72	0.2%	SBO-2.2
INT-LOOPGR:16-07-7	5.19E-10	18	0.1%	Same as SBO-2.0, 16-09-10
INT-LOOPGR:16-18	4.10E-10	98	0.1%	Use SBO-3.1, 16-19-2
INT-LOOPGR:16-07-2	4.01E-10	51	0.1%	SBO-2.3
INT-LOOPGR:16-30	3.47E-10	93	0.1%	Same as SBO-5.1, 16-27
INT-LOOPGR:16-21	1.74E-10	56	0.0%	SBO-3.1
INT-LOOPGR:16-43-07	7.52E-11	27	0.0%	SBO-7.3
INT-LOOPGR:16-10-2	5.84E-11	10	0.0%	SBO-4.3
INT-LOOPGR:16-15-10	3.96E-11	15	0.0%	SBO-1.1
INT-LOOPGR:16-24-10	3.96E-11	15	0.0%	SBO-2.1
INT-LOOPGR:16-43-06	3.77E-11	14	0.0%	Use SBO-7.3, 16-43-07
INT-LOOPGR:16-04-8	2.01E-11	9	0.0%	Small CDF
INT-LOOPGR:16-13-3	2.01E-11	18	0.0%	Small CDF
INT-LOOPGR:16-22-3	2.01E-11	18	0.0%	Small CDF
INT-LOOPGR:16-24-04	1.92E-11	5	0.0%	Use SBO-2.2, 16-09-4
INT-LOOPGR:16-16-3	1.83E-11	18	0.0%	Small CDF
INT-LOOPGR:16-04-4	8.37E-12	3	0.0%	Small CDF
INT-LOOPGR:16-13-2	5.76E-12	2	0.0%	Small CDF
INT-LOOPGR:16-22-2	5.76E-12	2	0.0%	Small CDF
INT-LOOPGR:16-16-2	5.26E-12	2	0.0%	Small CDF
INT-LOOPGR:16-36	4.84E-12	2	0.0%	Same as SBO-5.1, 16-27
INT-LOOPGR:16-40-2	4.69E-12	2	0.0%	SBO-6.3
INT-LOOPGR:16-25-2	4.38E-12	2	0.0%	Small CDF
INT-LOOPGR:16-19-2	2.63E-12	2	0.0%	Small CDF
INT-LOOPGR:16-39	2.42E-12	2	0.0%	SBO-4.1
INT-LOOPGR:16-28-2	2.19E-12	2	0.0%	Small CDF
Total	3.77E-07	4466	100.0%	

The scenarios considered for RELAP5-3D thermal hydraulic analysis are listed below:

- SBO-1.0: LOOP occurs, both EDG fail, TDAFP success, No PORV remained opened, 21gpm/RCP leakage, Rapid Secondary Depressurization success, No offsite power recovery and TDAFP stops after DC battery depletes. -> Core Damage Timing.
- SBO-1.1: Same as SBO-1.0, except that Rapid Secondary Depressurization fails. (small CDF)
- SBO-1.2: Same as SBO-1.0, however, TDAFP continue to run for 24 hours. -> Core Damage or not?
- SBO-2.0: Same as SBO-1.0, except that 21gpm -> 76gpm.
- SBO-2.1: Same as SBO-2.0, except that Rapid Secondary Depressurization fails. (small CDF)
- SBO-2.2: Same as SBO-2.0, however, TDAFP continue to run for 24 hours. -> Core Damage or not?
- SBO-2.3: Same as SBO-2.0, however, Offsite Power Recovered at 4 hours, When should Cooldown/LPI/LPR start to prevent CD?
- SBO-3.0: Same as SBO-1.0, except that 21gpm -> 182gpm.
- SBO-3.1: Same as SBO-3.0, except that Rapid Secondary Depressurization fails.
- SBO-3.3: Same as SBO-3.0, however, Offsite Power Recovered at 4 hours, When should Cooldown/LPI/LPR start to prevent CD?
- SBO-4.0: Same as SBO-1.0, except that 21gpm -> 480gpm.
- SBO-4.1: Same as SBO-4.0, except that Rapid Secondary Depressurization fails. (small CDF)
- SBO-4.3: Same as SBO-4.0, however, Offsite Power Recovered at 4 hours, When should Cooldown/LPI/LPR start to prevent CD?
- SBO-5.1: Same as SBO-1.0, except that Rapid Secondary Depressurization fails, 21gpm -> 300gpm.
- SBO-5.3: Same as SBO-5.1, however, Offsite Power Recovered at 4 hours, When should HPI/HPRR start to prevent CD? (small CDF)
- SBO-6.0: LOOP occurs, both EDG fail, TDAFP success, PORV remained opened, No offsite power recovery and TDAFP stops after DC battery depletes. -> Core Damage Timing.
- SBO-6.3: Same as SBO-6.0, however, Offsite Power Recovered at 1 hour, When should HPR start to prevent CD?
- SBO-7.0: LOOP occurs, both EDG fail, TDAFP fails, No offsite power recovery. -> Core Damage Timing.
- SBO-7.3: Same as SBO-7.0, however, Offsite Power Recovered at 1 hour, AFW success -> When should HPI/HPR start to prevent CD?

Of them, scenarios SBO-1.1, SBO-2.1, SBO-4.1, and SBO-5.3 are excluded from detailed analysis due to very small CDF. A total of 15 scenarios, from SBO-1.0 to SBO-7.3, are provided to RELAP5-3D analyst for thermal hydraulic analysis (see Table 4-4). The Scenario column in the table represents the plant conditions and responses to those scenario-related questions. For example, AFW (or No AFW) indicates that the TDAFW could (or could not) provide flow to the SGs to remove decay heat. Scenario SBO-1.0 (AFW, PORV Closed, RSD, 21gpm/RCP, 4Hours No, No AFW-MAN) represents a SBO scenario in which the TDAFP automatically actuates and supplies sufficient cooling water to the SGs, all PORVs are closed as designed when RCS pressure is lower than the valve set point, the RCS depressurization through secondary side (i.e., the operation of SG relief valves) is successful, the leakage rate of RCP seal is 21 gpm per pump, AC power is not recovered within 4 hours, TDAFP cannot continue to provide cooling water to the SGs after DC battery depletes at 4 hour. Core damage occurs due to the decay heat not being removed. Scenarios SBO-2.0, SBO-3.0, and SBO-4.0 are similar with SBO-1.0, only with different RCP leak rates at 76, 182, and 480 gpm per RCP, respectively.

Each of the scenarios in Table 4-4 is then run with RELAP5-3D, first with the current Zr-based fuel cladding design as the base case and then with the ATF design (the FeCrAl design or the Cr-coated design). The times of peak cladding temperature (PCT) to reach melting point, the times to generate a half kilogram hydrogen, and the total amount of hydrogen generated when the run is terminated are compared between different cladding designs for each scenario. The estimated time differences for PCT to reach melting point from RELAP5-3D are fed back to the PRA model to evaluate the risk impacts from the proposed ATF design.



**Table 4-4. Grid-Related SBO Sequence Results**

RELAP5 Scenario	Scenario							
SBO-1.0	AFW	PORV Closed	RSD	21gpm/RCP	4Hrs No	No AFW-MAN		
SBO-1.2	AFW	PORV Closed	RSD	21gpm/RCP	4Hrs No	AFW-MAN	No SG Depre.	No Late OPR
SBO-2.0	AFW	PORV Closed	RSD	76gpm/RCP	4Hrs No	No AFW-MAN		
SBO-2.2	AFW	PORV Closed	RSD	76gpm/RCP	4Hrs No	AFW-MAN	No SG Depre.	No Late OPR
SBO-2.3	AFW	PORV Closed	RSD	76gpm/RCP	4Hrs Yes	HPI	Cooldown	No LPR
SBO-3.0	AFW	PORV Closed	RSD	182gpm/RCP	4Hrs No			
SBO-3.1	AFW	PORV Closed	No RSD	182gpm/RCP	3Hrs No			
SBO-3.3	AFW	PORV Closed	RSD	182gpm/RCP	4Hrs Yes	HPI	Cooldown	No LPR
SBO-4.0	AFW	PORV Closed	RSD	480gpm/RCP	2Hrs No			
SBO-4.3	AFW	PORV Closed	RSD	480gpm/RCP	2Hrs Yes	HPI	Cooldown	No LPR
SBO-5.1	AFW	PORV Closed	No RSD	300gpm/RCP	2Hrs No			
SBO-6.0	AFW	PORV Opened	NA	NA	1Hr No			
SBO-6.3	AFW	PORV Opened	NA	NA	1Hr Yes	HPI	No HPR	
SBO-7.0	No AFW	NA	NA	NA	1Hr No			
SBO-7.3	No AFW	NA	NA	300gpm/RCP	1Hr Yes	AFW	No HPI	

## 4.2 RELAP5-3D Analysis

### 4.2.1 SBO Control Logic

The RELAP5-3D IGPWR model was used for the simulation of the previous PRA branches of SBO. Special provisions were implemented in the RELAP5-3D input deck for simulating the operator actions, the black-start of the TDAFW, the ECST level, the SG depressurization procedure, etc. (see Table 4-5).

**Table 4-5. RELAP5-3D Control Logic for SBO**

Procedure/Event	RELAP5-3D Control Logic
SGs depressurization	Start at $t=+5,400$ s (+1.5 hr), depressurize and cool-down with 100 F/hr (~55 C/hr) rate
Battery depletion	Selected by the safety analyst (4-8 hr). Disable TD-AFW injection and SG/PRZ PORVs
TD-AFW black-start	Restart TD-AFW and SG PORVs
Feed & Bleed on Secondary Side	Inject water from the ECST and bleed steam via SG PORVs. Keep the SGs depressurized at 0.923 MPa. Stop if ECST water or batteries are depleted.
Kerr pump injection on the primary side	Inject ~ 4 Kg/s of borated water from RWST after successful primary side depressurization. Injection continuing until: $P_{\text{primary}} \leq 2.0$ MPa.
ECCS injection	HPI/LPI + Recirculation mode if AC available. Accumulators injection if $P_{\text{primary}} < 4.0$ MPa
MCP Seal LOCA	21-480 gpm, depending on the transient

#### 4.2.2 Creep Model

Since the primary system could operate at quite high temperatures for long periods, a creep rupture model was implemented in the RELAP5-3D SBO input-deck. The creep rupture criterion is based on the Larson-Miller model (Larson & Miller, 1952) and it is calculated at every time steps by RELAP5-3D for different parts of the MCC (hot and cold legs, SG tubes, PRZ surge line). The Larson-Miller model provides the time to rupture,  $t_R$ , in seconds:

$$t_R(s) = 10^{\left(\frac{P_{LM}}{T} - 7.042\right)} \quad (4)$$

with  $P_{LM}$  being the Larson-Miller parameter calculated by:

$$P_{LM} = 4.812 \times 10^4 - 4.725 \times 10^3 \log_{10} \sigma_e \quad (5)$$

where  $\sigma_e$  is the effective stress in Pa. Being  $\sigma_e$  calculated in pipelines (cylindrical structures), the effective stress is obtained according to the following equation:

$$\sigma_e = \frac{(P_i r_i - P_o r_o)}{(r_o - r_i)} \approx \frac{(P_i r_i)}{(r_o - r_i)} \quad (6)$$

where  $P$  is the pressure on the structure,  $r$  is the radius and the subscripts 'o' and 'i' indicate the external and internal values. RELAP5-3D determines the creep damage of the selected parts of the MCC using the following equation (RELAP5-3D Code Development Team, 2003) :

$$D_c(t + \Delta t) = D_c + \frac{\Delta t}{t_R(t)} \quad (7)$$

where:

$D_c(t)$  = creep damage at time  $t$ ,

$\Delta t$  = time step at current problem time (s),

$t_R(t)$  = time to rupture according to the Larson-Miller model

$t$  = problem time (s)

When the value of  $D_c$  is equal to one, creep rupture occurs and a special trip valve simulates the corresponding pipe rupture.

#### 4.2.3 Clad Oxidation Kinetics and Fuel Geometry

The SBO RELAP5-3D input deck then uses the special cards developed for simulating the oxidation kinetics of ATF (both coated and non-coated clads, see Section 3.2). The ATF oxidation parameters were obtained from selected publications (e.g., (Holzwarth & Stamm, 2002), (Robb, Howell, & Ott, 2017)) and implemented in the RELAP5-3D input deck. The main parameters for the oxidation kinetics and the fuel pin geometries are reported in Table 4-6.

For the FeCrAl clad, a transition temperature of 1773 K was selected. When the code calculates such temperature, the oxidation kinetics parameters are switched to the stainless-steel oxidation parameter (i.e., rapid oxidation). The failure criterion for both Cr and FeCrAl is the PCT reaching 1804 K (see Section 3.2).

The outer radius of the fuel rod is identical for all three types of clads (Zry, Cr-coated, FeCrAl). FeCrAl clad thickness was half of the reference Zry clad thickness; this was assumed for compensating the increased neutron capture of FeCrAl (George, Terrani, Powers, Worrall, & Maldonado, 2015). Consequently, in order to keep the gas gap and the outer radius constant, fuel pellet radius was increased. RELAP5-3D performs also a simplified clad deformation calculation (RELAP5-3D Code Development Team, 2018). The empirical model included in RELAP5-3D has been taken from the FRAP-T6 code. The purpose of the model is to take into account a possible plastic deformation of the clad during an accidental condition. The model can inform the user of a possible clad



rupture and of a possible flow blockage due to the hydraulic channel flow area reduction. Further investigation by specialized fuel pin mechanics codes are needed if extensive plastic deformation or rupture of the clad are detected.

**Table 4-6. RELAP5-3D Parameters for the Fuel Clads**

Parameter	Clad Type		
	Zry	Cr-coated	FeCrAl
Reaction Rate Constant (m <sup>2</sup> Metal/s)	9.166E-7	1.409E-5	2.444E-5
Reaction Heat Release (J/Kg mole)	5.94E+8	6.48E+7	6.73E+7
Activation Energy (cal/mole)	35,890	66,890	82,218
Clad Density (kg/m <sup>3</sup> )	6,500	7,190	6,860
Clad Molecular Weight (kg/kg mole)	91.22	51.99	53.96
Ratio Molecular Weight Reactant/Clad	0.042	0.058	0.112
Clad thickness (μm)	617	617	309
Clad coating thickness (μm)	N/A	20	N/A
Gas Gap thickness (μm)	95	95	95
Pellet outer radius (mm)	4.6469	4.6469	4.9555
Fuel pin outer radius (mm)	5.3594	5.3594	5.3594

#### 4.2.4 Sample RELAP5-3D results for LT-SBO sequence

In Table 4-7 and Table 4-8, we provide sample results of the Long Term Station Blackout (LT-SBO scenarios SBO-1.0 and SBO-1.3<sup>2</sup>). Figure 4-3 through Figure 4-16 show the trend of the main TH parameters. PCT trend for the three different clad types is given in Figure 4-9 and Figure 4-16. Pictures of the results of the other transients are reported in Appendix B. The LT-SBO scenarios SBO-1.0 and SBO-1.3 are initiated by the LOOP and the complete loss of AC power to safety buses. SBO involves the LOOP concurrent with the failure of the onsite emergency AC power system. It does not include the loss of available AC power to safety buses fed by station batteries through inverters (NRC, 2017).

DC power is not lost and after the seal LOCA at 21 gpm, the operator is able to perform reactor cool-down using feed-and-bleed procedure on the secondary side, reducing the leak rate and allowing the accumulators injection. After the batteries are depleted (~4 hours for SBO-1.0 and ~8 hours for SBO-1.3), the SGs dry up and the reactor re-pressurizes. Continuous loss of inventory and loss of cooling lead to the core uncover and ultimately to the fuel damage.

<sup>2</sup> SBO-1.3 scenario is an additional SBO scenario developed for the risk-informed plant enhancement analysis in Section 6.

**Table 4-7. Sequence of Events for LT-SBO-1.0, Zry clad.**

EVENT DESCRIPTION	TIME [hh:mm]
Initiating event <sub>SEP</sub> – LOOP and failure of the onsite emergency AC power systems.	00:00
Reactor trip, MSIVs close, RCP seals initially leak at 21 gpm/pump (~1 Kg/s)	00:00
TD-AFW auto initiates at full flow	00:01
Operators control AFW to maintain level	00:15
First SG SRV opening	00:25
Operator performs controlled cooldown of secondary at ~100 F/hr (~55.5 C/hr)	01:30
Accumulators begin to inject	02:30
Secondary pressure reduced to ~0.9 MPa	03:40
Offsite Power is not recovered, battery depleted	04:00
SGs empty	08:16
System re-pressurize, PRZ SRV open	9:01
RPV water level starts to decrease, core uncover	9:30
Core Damage	10:32

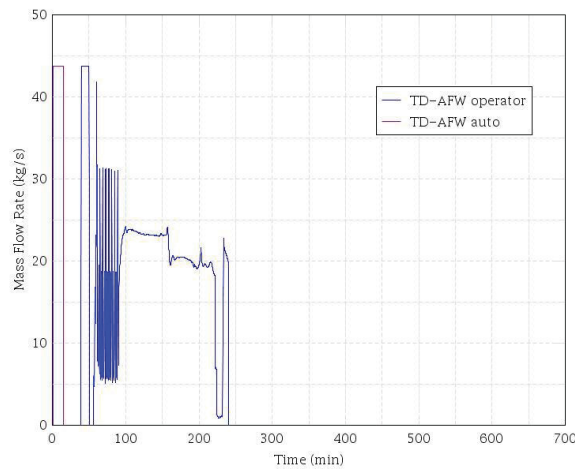


**Figure 4-3. LT\_SBO 1.0 Zry – TD-AFW Mass Flow.**

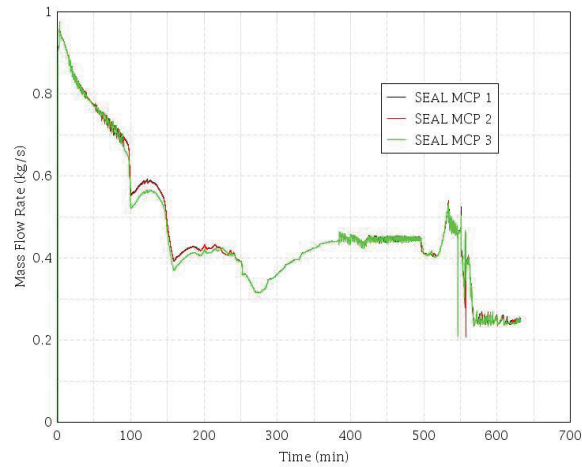


**Figure 4-4. LT\_SBO 1.0 Zry – MCP Seal Leakage Mass Flow.**

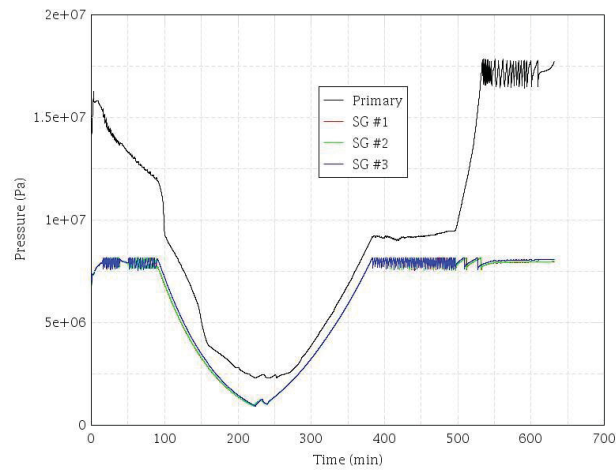


**Figure 4-5. LT\_SBO 1.0 Zry – Primary and Secondary Sides Pressures.**

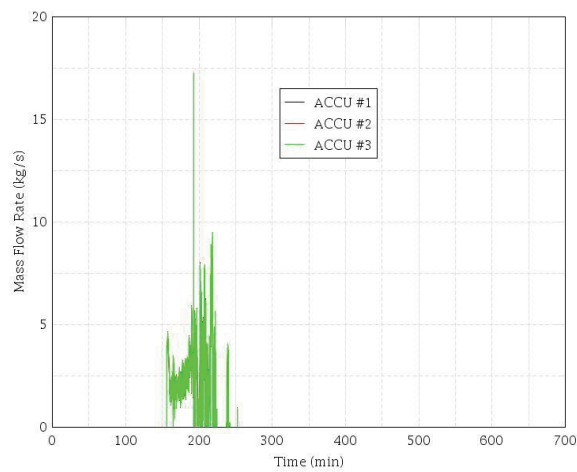


**Figure 4-6. LT\_SBO 1.0 Zry –Accumulators Mass Flow.**

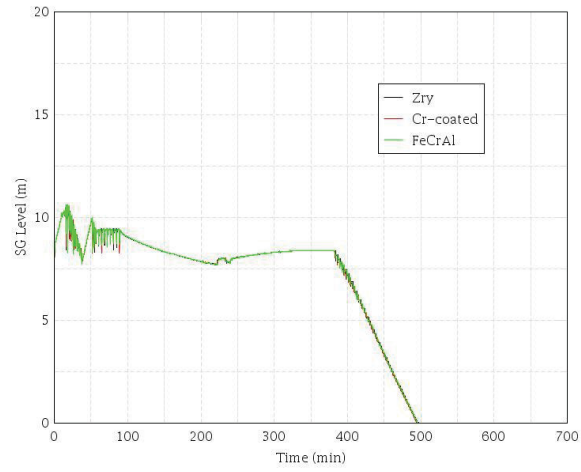


**Figure 4-7. LT\_SBO 1.0 Zry – SG Levels.**

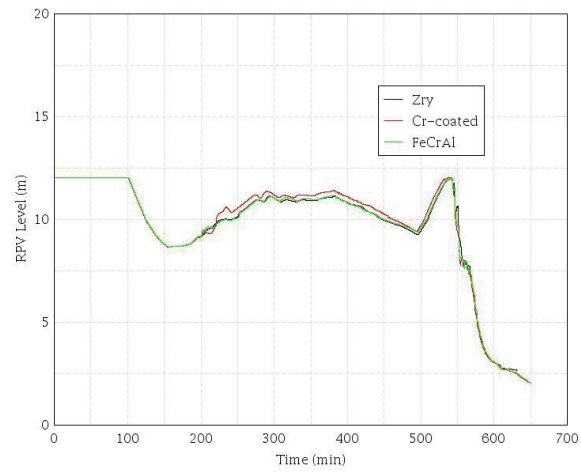


**Figure 4-8. LT\_SBO 1.0 – RPV Water Level for Zry, Cr-Coated, FeCrAl Clads.**

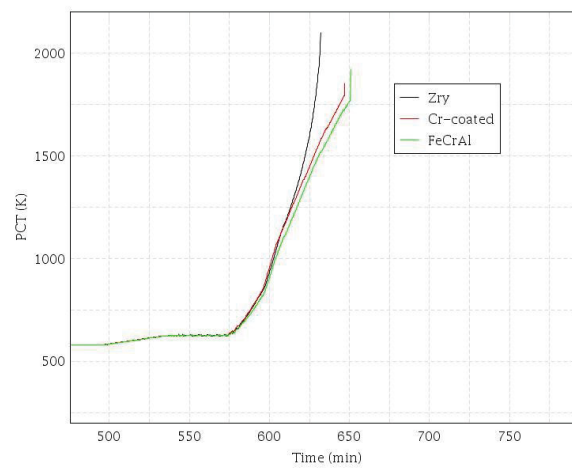


**Figure 4-9. LT\_SBO 1.0 – PCT for Zry, Cr-Coated, FeCrAl Clads.**

**Table 4-8. Sequence of Events for LT-SBO-1.3, Zry clad.**

EVENT DESCRIPTION	TIME [hh:mm]
Initiating event <sub>SEP</sub> – LOOP and failure of the onsite emergency AC power systems.	00:00
Reactor trip, MSIVs close, RCP seals initially leak at 21 gpm/pump (~1 Kg/s)	00:00
TD-AFW auto initiates at full flow	00:01
Operators control AFW to maintain level	00:15
First SG SRV opening	00:25
Operator performs controlled cooldown of secondary at ~100 F/hr (~55.5 C/hr)	01:30
Accumulators begin to inject	02:30
Secondary pressure reduced to ~0.9 MPa	03:40
Primary pressure decreased below 2.0 MPa	05:50
Offsite Power is not recovered, battery depleted	08:00
SGs empty	12:57
System re-pressurize, PRZ SRV open	13:34
RPV water level starts to decrease, core uncover	14:28
Core Damage	15:40

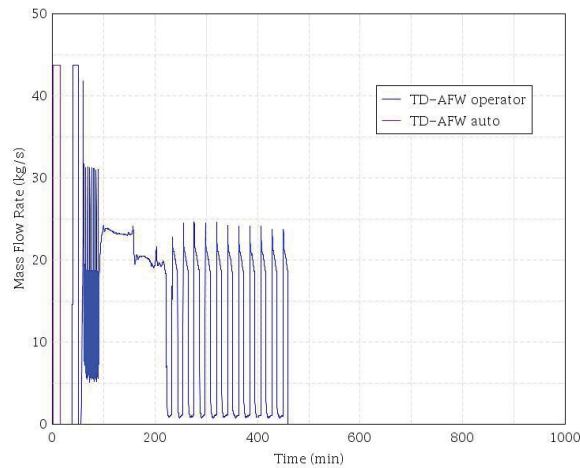


**Figure 4-10. LT\_SBO 1.3 Zry – TD-AFW Mass Flow.**

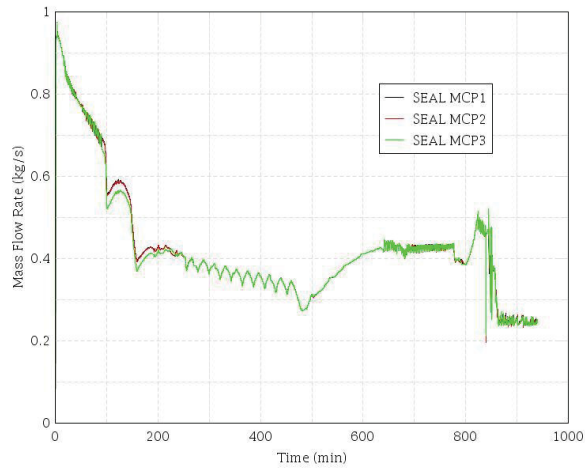


**Figure 4-11. LT\_SBO 1.3 Zry – MCP Seal Leakage Mass Flow.**

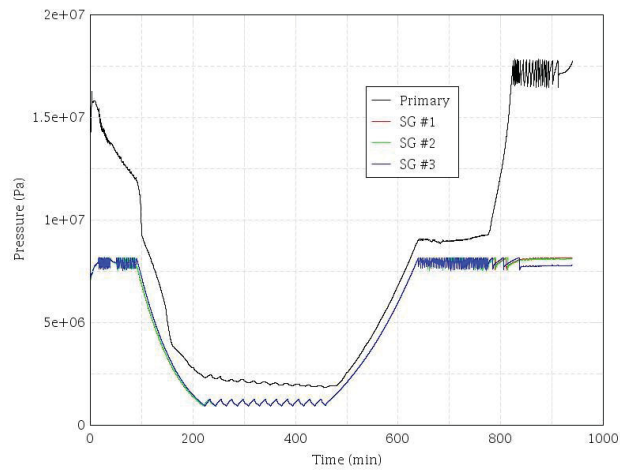


**Figure 4-12. LT\_SBO 1.3 Zry – Primary and Secondary Sides Pressures.**

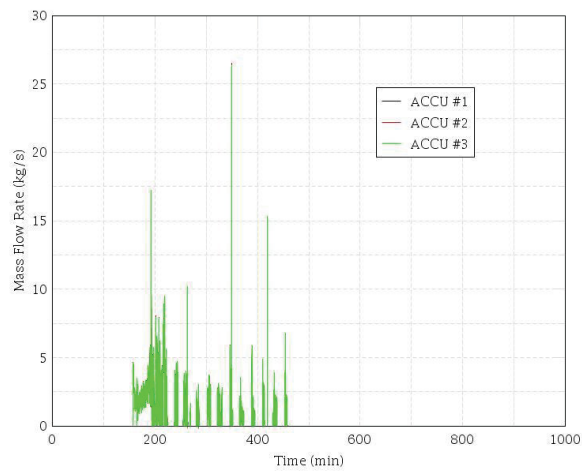


**Figure 4-13. LT\_SBO 1.3 Zry –Accumulators Mass Flow.**

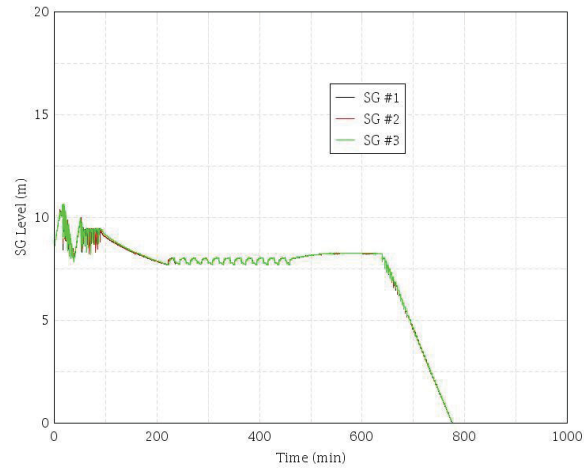


**Figure 4-14. LT\_SBO 1.3 Zry – SG Levels.**

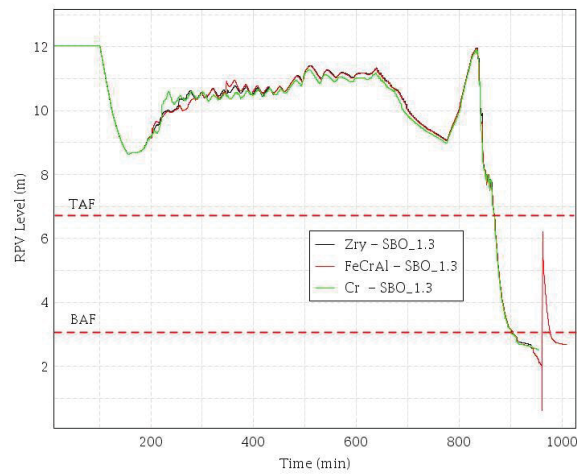


**Figure 4-15. LT\_SBO 1.3 – RPV Water Level for Zry, Cr-Coated, FeCrAl Clads.**

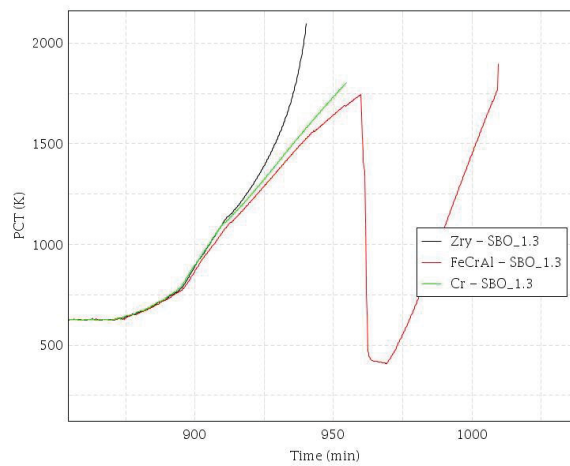


**Figure 4-16. LT\_SBO 1.3 – PCT for Zry, Cr-Coated, FeCrAl Clads.**

FeCrAl PCT trend resulted different than Zry and Cr-coated PCT trends because surge line creep failure caused a sudden depressurization of the primary side and the injection of the remaining water in the accumulators. After water boil-off, the FeCrAl clad temperatures start to raise again, finally reaching the failure temperature roughly 1 hour and 10 minutes later than the Zry clad.

## **4.3 SBO Analysis Results**

### **4.3.1 RELAP5-3D Results**

The following tables presents the RELAP5-3D simulation results for time to core damage, the equivalent clad reacted (ECR), the timing of the start of significant hydrogen production (0.5 Kg) and the total hydrogen generated for SBO scenarios and for Zircaloy and ATF clads (FeCrAl and Cr-coated).

The RELAP5-3D simulations estimate only marginal increase of the coping time with Cr-coated and FeCrAl in most scenarios, from about 3-6 minutes in short term SBO (SBO-7.0, see Table 4-9 and Table 4-11) to about twenty minutes in long term SBO with a battery life of 4 hours (for example, SBO-1.0). The maximum increase of the coping time is 1 hour in long term SBO with a battery life of 8 hours (SBO-1.3 for FeCrAl fuel). The timing to core damage is dictated by the timing of the core uncover, the decay power level and the oxidation kinetics. FeCrAl is showing here some slight advantage on Cr-coated.

The reason of this is due to the fact that RELAP5-3D predicted clad breaching in all SBO cases, except SBO-1.3 with Cr-coated clad. The Cr-coated clad breaching leads to the Zirconium oxidation of the internal surface of the clad, with a consequent higher oxidation energy and hydrogen gas releases. Calculations suggest that an internal surface coating would be eventually beneficial.

As expected, the ECR is generally lower for both FeCrAl and Cr-coated clads compared to Zircaloy clads. This parameter is generally affected by the timing of clad breaching.

A clear benefit for adopting the ATF clads is more evident in Table 4-10 and Table 4-12. Hydrogen production can be one or two order of magnitude lower than the Zircaloy clad cases. The timing of significant hydrogen production is also another good indicator of the ATF performances.

Cr-coated and FeCrAl release the same significant quantity of hydrogen (0.5 Kg) between roughly half an hour to one hour and half later compared to the Zircaloy clad cases. This could result in some benefits/relieves for the Accident Management procedures and for the accidental loads on the severe accidents mitigation SSCs (e.g., hydrogen recombiners, containment venting pipes, containment shell, etc.).

Finally, all the RELAP5-3D analyses highlight the complex fuel pin mechanics behavior during the different SBO branches (clad rupture, oxidation, channel flow area reduction). This indicates the need in the future to perform coupled TH – fuel pin mechanics codes analyses for assessing with more details fuel transient dynamics.



**Table 4-9. RELAP5-3D Results for SBO Scenarios without AC Power Recovery – Zry vs. FeCrAl – Clad Performance**

	Scenario Description				Time to Core Damage $t_{CD}$ (hh:mm)			ECR (%)	
					Zry	FeCrAl	$\Delta t$	Zry	FeCrAl
SBO-1.0	TDAFW runs 4 hrs	PORV Closed	Depress.	21 gpm	10:32	10:51	<b>0:19</b>	35.8	11.7
SBO-1.3	TDAFW runs 8 hrs	PORV Closed	Depress.	21 gpm	15:40	16:49	<b>1:09</b>	39.4	9.1
SBO-2.0	TDAFW runs 4 hrs	PORV Closed	Depress.	76 gpm	10:17	10:36	<b>0:19</b>	40.0	4.8
SBO-3.0	TDAFW runs 4 hrs	PORV Closed	Depress.	182 gpm	10:22	10:43	<b>0:21</b>	41.2	11.7
SBO-3.1	TDAFW runsr 4 hrs	PORV Closed	No Depress.	182 gpm	7:10	7:26	<b>0:16</b>	38.7	11.7
SBO-4.0	TDAFW runsr 4 hrs	PORV Closed	Depress.	480 gpm	5:25	5:46	<b>0:21</b>	54.3	11.7
SBO-5.1	TDAFW runsr 4 hrs	PORV Closed	No Depress.	300 gpm	4:42	4:51	<b>0:03</b>	32.0	11.7
SBO-6.0	TDAFW runsr 4 hrs	PORV Opened	NA	21 gpm	1:16	1:23	<b>0:07</b>	24.8	11.7
SBO-6.1	TDAFW runsr 4 hrs	PORV Opened	Depress.	21 gpm	5:19	5:40	<b>0:21</b>	27.0	11.7
SBO-7.0	No TDAFW	NA	NA	21 gpm	2:35	2:41	<b>0:06</b>	37.9	11.7

**Table 4-10. RELAP5-3D Results for SBO Scenarios without AC Power Recovery – Zry vs. FeCrAl – H<sub>2</sub> Production**

	Scenario Description				Timing of 0.5 Kg H2 production tH2 (hh:mm)			Total Hydrogen (kg)	
					Zry	FeCrAl	Δt	Zry	FeCrAl
SBO-1.0	TDAFW runs 4 hrs	PORV Closed	Depress.	21 gpm	10:01	10:45	<b>0:44</b>	98.1	3.0
SBO-1.3	TDAFW runs 8 hrs	PORV Closed	Depress.	21 gpm	15:02	15:35	<b>0:51</b>	110.8	2.8
SBO-2.0	TDAFW runs 4 hrs	PORV Closed	Depress.	76 gpm	9:45	10:31	<b>0:46</b>	98.8	1.6
SBO-3.0	TDAFW runs 4 hrs	PORV Closed	Depress.	182 gpm	9:48	10:37	<b>0:49</b>	77.1	2.8
SBO-3.1	TDAFW runs 4 hrs	PORV Closed	No Depress.	182 gpm	6:47	7:23	<b>0:36</b>	48.1	2.4
SBO-4.0	TDAFW runs 4 hrs	PORV Closed	Depress.	480 gpm	5:10	5:46	<b>0:36</b>	17.6	2.0
SBO-5.1	TDAFW runs 4 hrs	PORV Closed	No Depress.	300 gpm	4:26	4:51	<b>0:25</b>	31.5	2.0
SBO-6.0	TDAFW runs 4 hrs	PORV Opened	NA	21 gpm	1:07	1:23	<b>0:16</b>	17.7	1.9
SBO-6.1	TDAFW runs 4 hrs	PORV Opened	Depress.	21 gpm	1:17	5:40	<b>4:23</b>	23.6	2.0
SBO-7.0	No TDAFW	NA	NA	21 gpm	2:11	2:39	<b>0:28</b>	88.0	2.4

**Table 4-11. RELAP5-3D Results for SBO Scenarios without AC Power Recovery – Zry vs. Cr-coated – Clad Performance**

	Scenario Description				Time to Core Damage $t_{CD}$ (hh:mm)			ECR (%)	
					Zry	Cr-coated	$\Delta t$	Zry	Cr-coated
SBO-1.0	TDAFW runs 4 hrs	PORV Closed	Depress.	21 gpm	10:32	10:47	<b>0:15</b>	35.8	1.3
SBO-1.3	TDAFW runs 8 hrs	PORV Closed	Depress.	21 gpm	15:40	15:55	<b>0:15</b>	39.4	1.0
SBO-2.0	TDAFW runs 4 hrs	PORV Closed	Depress.	76 gpm	10:17	10:29	<b>0:12</b>	40.0	1.1
SBO-3.0	TDAFW runs 4 hrs	PORV Closed	Depress.	182 gpm	10:22	10:30	<b>0:08</b>	41.2	1.4
SBO-3.1	TDAFW runsr 4 hrs	PORV Closed	No Depress.	182 gpm	7:10	7:19	<b>0:09</b>	38.7	19.6
SBO-4.0	TDAFW runsr 4 hrs	PORV Closed	Depress.	480 gpm	5:25	5:29	<b>0:04</b>	54.3	12.7
SBO-5.1	TDAFW runsr 4 hrs	PORV Closed	No Depress.	300 gpm	4:42	4:47	<b>0:05</b>	32.0	14.6
SBO-6.0	TDAFW runsr 4 hrs	PORV Opened	NA	21 gpm	1:16	1:18	<b>0:02</b>	24.8	10.7
SBO-6.1	TDAFW runsr 4 hrs	PORV Opened	Depress.	21 gpm	5:19	5:21	<b>0:02</b>	27.0	12.0
SBO-7.0	No TDAFW	NA	NA	21 gpm	2:35	2:38	<b>0:03</b>	37.9	7.3

**Table 4-12. RELAP5-3D Results for SBO Scenarios without AC Power Recovery – Zry vs. Cr-coated – H<sub>2</sub> Production**

	Scenario Description				Timing of 0.5 Kg H <sub>2</sub> production t <sub>H2</sub> (hh:mm)			Total Hydrogen (kg)	
					Zry	Cr-coated	Δt	Zry	Cr-coated
SBO-1.0	TDAFW runs 4 hrs	PORV Closed	Depress.	21 gpm	10:01	N/A	N/A	98.1	0.3
SBO-1.3	TDAFW runs 8 hrs	PORV Closed	Depress.	21 gpm	15:02	N/A	N/A	110.8	<0.1
SBO-2.0	TDAFW runs 4 hrs	PORV Closed	Depress.	76 gpm	9:45	N/A	N/A	98.8	0.3
SBO-3.0	TDAFW runs 4 hrs	PORV Closed	Depress.	182 gpm	9:48	10:28	<b>0:40</b>	77.1	10.6
SBO-3.1	TDAFW runs 4 hrs	PORV Closed	No Depress.	182 gpm	6:47	7:09	<b>0:22</b>	48.1	12.7
SBO-4.0	TDAFW runs 4 hrs	PORV Closed	Depress.	480 gpm	5:10	5:18	<b>0:08</b>	17.6	6.2
SBO-5.1	TDAFW runs 4 hrs	PORV Closed	No Depress.	300 gpm	4:26	4:31	<b>0:05</b>	31.5	8.1
SBO-6.0	TDAFW runs 4 hrs	PORV Opened	NA	21 gpm	1:07	1:09	<b>0:02</b>	17.7	5.2
SBO-6.1	TDAFW runs 4 hrs	PORV Opened	Depress.	21 gpm	1:17	5:11	<b>3:54</b>	23.6	5.0
SBO-7.0	No TDAFW	NA	NA	21 gpm	2:11	2:37	N/A	88.0	11.3

### 4.3.2 Risk Impact Evaluation

With only marginal increase of the time to core damage with FeCrAl and Cr-coated against the conventional Zry cladding design based on the RELAP5-3D simulation results (see Table 4-9 and Table 4-11), the risk benefit on behalf of the CDF as the risk metrics would be very small. The less than an hour time difference does not warrant a change of the PRA SBO model (event tree, fault tree, success criteria, or human reliability analysis). Instead, a simplified approach using a multiplication factor, called coping time factor  $F_{CT}(m/n)$ , is developed in this report to estimate the risk impact of the ATF design with the small increase of the coping time. If a SBO sequence that includes top events of AC power recovery (either offsite power recovery or diesel generator recovery) within  $n$  hours has a base case core damage frequency of  $CDF_0$ , with the increase of coping time for  $m$  hours with the ATF design, the time to core damage is delayed by  $m$  hours, and the base case top events of AC power recovery within  $n$  hours become as AC power recovery within  $(m+n)$  hours. The failure probability for operator to recover AC power is thus smaller which would lead to a reduced core damage frequency,  $CDF'$ , by the factor of  $F_{CT}(m/n)$ :

$$CDF' = F_{CT}(m/n) * CDF_0 \quad (8)$$

The coping time factor  $F_{CT}(m/n)$  can be estimated from the ratio of the probabilities of operator fails to recover AC power within different time periods. Table 4-13 shows the probabilities of operator fails to recover offsite power ( $P_{OPR}$ ), the probabilities of operator fails to recover diesel generators ( $P_{DGR}$ ) within specified time periods from 1 hour to 8 hours. The probability of operator fails to recover AC power is calculated by

$$P_{ACR} = P_{OPR} * P_{DGR} \quad (9)$$

The column of  $P(n+1)/P(n)$  in Table 4-13 presents the ratio of the probability of operator fails to recover AC power,  $P_{ACR}$ , within  $n+1$  hours to that of within  $n$  hours. The last 2 columns of the table proportionally assigns the ration of the failure probabilities if the coping time is increased by 0.5 hours or 0.25 hours. The coping time factor  $F_{CT}(m/n)$  is estimated by rounding up these ratios with the results presented in Table 4-14.

The factor  $F_{CT}(m/n)$  can then be applied to the PRA SBO sequence results. Table 4-15 and Table 4-16 show the estimated CDF for the analyzed SBO sequences with FeCrAl and Co-coated cladding designs, respectively. The results show that the marginal coping time increase brought by the FeCrAl and Cr-coated designs would lead to about 4% and 2% CDF reductions, respectively. However, this should not be misinterpreted as that ATF brings no risk benefits. Actually the hydrogen production with ATF is one or two order of magnitude lower than the Zircaloy clad. And the timing to release significant hydrogen production (0.5 Kg) with ATF is about 0.5 hour to 1.5 hours later than that with Zircaloy.

**Table 4-13. Failure Probabilities for Operator to Recover AC Power**

Operator Action	$P_{OPR}$	$P_{DGR}$	$P_{ACR}$	$P(n+1)/P(n)$	$P(n+0.5)/P(n)$	$P(n+0.25)/P(n)$
Operator Fails to Recover in $n = 1$ Hour	6.11E-01	7.86E-01	4.80E-01	51%	75%	88%
Operator Fails to Recover in $n = 2$ Hours	3.56E-01	6.87E-01	2.45E-01	57%	78%	89%
Operator Fails to Recover in $n = 3$ Hours	2.27E-01	6.14E-01	1.39E-01	61%	81%	90%
Operator Fails to Recover in $n = 4$ Hours	1.54E-01	5.57E-01	8.56E-02	65%	82%	91%
Operator Fails to Recover in $n = 5$ Hours	1.09E-01	5.09E-01	5.56E-02	68%	84%	92%
Operator Fails to Recover in $n = 6$ Hours	8.05E-02	4.68E-01	3.77E-02	70%	85%	93%
Operator Fails to Recover in $n = 7$ Hours	6.10E-02	4.33E-01	2.64E-02	72%	86%	93%
Operator Fails to Recover in $n = 8$ Hours	4.73E-02	4.02E-01	1.90E-02	74%	87%	93%
Operator Fails to Recover in $n = 9$ Hours	3.74E-02	3.74E-01	1.40E-02			

**Table 4-14. Estimated Coping Time Factor**

Coping Time Factor	$F_{CT}(1.0/n)$	$F_{CT}(0.5/n)$	$F_{CT}(0.25/n)$
Operator Fails to Mitigate Accident in n = 1 Hour	0.55	0.75	0.90
Operator Fails to Mitigate Accident in n = 2 Hours	0.60	0.80	0.90
Operator Fails to Mitigate Accident in n = 3 Hours	0.65	0.85	0.90
Operator Fails to Mitigate Accident in n = 4 Hours	0.65	0.85	0.95
Operator Fails to Mitigate Accident in n = 5 Hours	0.70	0.85	0.95
Operator Fails to Mitigate Accident in n = 6 Hours	0.70	0.85	0.95
Operator Fails to Mitigate Accident in n = 7 Hours	0.75	0.90	0.95
Operator Fails to Mitigate Accident in n = 8 Hours	0.75	0.90	0.95

**Table 4-15. CDF Estimation for FeCrAl**

	Time to Core Damage $t_{CD}$			Power Recovery	$CDF_0$	$F_{CT}$	$CDF'$	$\Delta CDF$	$\Delta CDF\%$
	Zr	FeCrAl	$\Delta t$						
SBO-1.0	10:32	10:51	<b>0:19</b>	4 Hrs	1.57E-07	0.95	1.49E-07	-7.83E-09	-5%
SBO-2.0	10:17	10:36	<b>0:19</b>	4 Hrs	1.91E-09	0.95	1.81E-09	-9.53E-11	-5%
SBO-3.0	10:22	10:43	<b>0:21</b>	4 Hrs	1.30E-07	0.95	1.24E-07	-6.52E-09	-5%
SBO-3.1	7:10	7:26	<b>0:16</b>	3 Hrs	5.84E-10	0.90	5.26E-10	-5.84E-11	-10%
SBO-4.0	5:25	5:46	<b>0:21</b>	2 Hrs	4.37E-09	0.90	3.93E-09	-4.37E-10	-10%
SBO-5.1	4:42	4:51	<b>0:09</b>	2 Hrs	1.10E-09	1.00	1.10E-09	0.00E+00	0%
SBO-6.0	1:16	1:23	<b>0:07</b>	1 Hrs	2.32E-09	1.00	2.32E-09	0.00E+00	0%
SBO-6.1	5:19	5:40	<b>0:21</b>	1 Hrs	NA	NA	NA	NA	NA
SBO-7.0	2:35	2:41	<b>0:06</b>	1 Hrs	5.42E-08	1.00	5.42E-08	0.00E+00	0%
Total					3.51E-07		3.37E-07	-1.49E-08	-4%

**Table 4-16. CDF Estimation for Cr-Coated**

	Time to Core Damage $t_{CD}$			Power Recovery	$CDF_0$	$F_{CT}$	$CDF'$	$\Delta CDF$	$\Delta CDF\%$
	Zr	Cr-coated	$\Delta t$						
SBO-1.0	10:32	10:47	0:15	4 Hrs	1.57E-07	0.95	1.49E-07	-7.83E-09	-5%
SBO-2.0	10:17	10:29	0:12	4 Hrs	1.91E-09	0.95	1.81E-09	-9.53E-11	-5%
SBO-3.0	10:22	10:30	0:08	4 Hrs	1.30E-07	1.00	1.30E-07	0.00E+00	0%
SBO-3.1	7:10	7:19	0:09	3 Hrs	5.84E-10	1.00	5.84E-10	0.00E+00	0%
SBO-4.0	5:25	5:29	0:04	2 Hrs	4.37E-09	1.00	4.37E-09	0.00E+00	0%
SBO-5.1	4:42	4:47	0:05	2 Hrs	1.10E-09	1.00	1.10E-09	0.00E+00	0%
SBO-6.0	1:16	1:18	0:02	1 Hrs	2.32E-09	1.00	2.32E-09	0.00E+00	0%
SBO-6.1	5:19	5:21	0:02	1 Hrs	NA	NA	NA	NA	NA
SBO-7.0	2:35	2:38	0:03	1 Hrs	5.42E-08	1.00	5.42E-08	0.00E+00	0%
Total					3.51E-07		3.44E-07	-7.93E-09	-2%

## 4.4 Limit Surface Search Results

### 4.4.1 Background

The RAVEN code, coupled to the RELAP5-3D code, was used for performing exploration of the SBO accident space and for determining the effects of some of the aleatory uncertainties. As it can be inferred from Table 4-5, the accident dynamic and its outcome (safe/failed conditions) can be influenced by several aleatory factors. Batteries time, SG depressurization and emergency crew recovery timings as well as MCP leakage rate are just an example of some of those influential parameters.

RAVEN code allows to systematically perturbing selected RELAP5-3D input deck parameters and then, thorough the use of trained Reduced order Models (ROMs), RAVEN can derive the Limit Surface for the selected transient. Here we define a Limit Surface (LS) as the surface, in the n-dimensional space of our problem, identifying the safe and failed conditions for the fuel.

Exploration of the n-dimensional space of the problem using ROM is not computationally expensive and several algorithms from machine learning are available. The workflow of the LS search is presented in Figure 4-17.

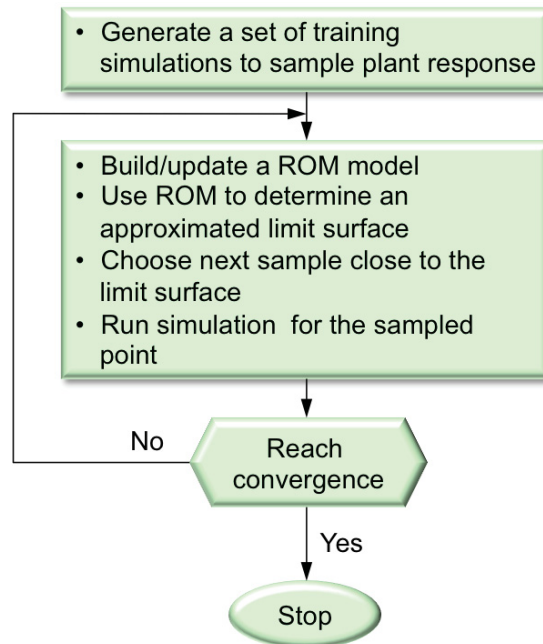


**Figure 4-17. Limit Surface Search workflow in RAVEN.**

Among the multiple ROM algorithms available, we selected the k-nearest neighbors algorithm (Altman, 1992) classifier from the Scikit-Learn external Python library (Scikit-Learn, 2017).

Several runs were performed for assessing the effect of the convergence parameters. It should be noted that the LS algorithm identifies, more than the real LS, a region that bound the LS. The identification of the different points of the regions (fail/safe) is performed using a “goal function”, which in this case is:

$$\text{if } (CladTemp_i < Failure\ Temperature\ Criterion) \text{ then goal function} = 1; \text{ else} = -1$$

for all the selected  $i$  values of the clad temperatures calculated by RELAP5-3D. The different failure temperature criteria adopted in this report for the different clad types are given in Table 3-1. A convergence acceleration of the LS search was also pursued in RAVEN using an adaptive refined sub-grid (Alfonsi, et al., 2017).

#### 4.4.2 Two-dimensional Limit Surface Search

The first LS search was applied to SBO-3.0 sequence (182 gpm of MCP seal leakage, depressurization successful at  $t=1.5$  hour). It should be noted that for the reference SBO-3.0 sequence there is no success path, the batteries are assumed to be depleted at  $t=4$  hours and no recovery actions are implemented. We investigated this sequence assuming a battery life between 4 and 8 hours. With the loss of DC power, we assumed that the TD-AFW flow stop because of the unavailability of power for regulating the steam flow to the turbine and to monitor the SG level.

We assumed possible recovery actions starting between 10 and 15.5 hours. The recovery actions include: TD-AFW black-start and use of mobile generators for supplying information to the operator and control the TD-AFW. We also assumed that at  $t=+4.5$  hours, a Kerr pump is available and connected to the primary side, ready for the injection flow (NRC, 2012). The condition for a successful Kerr pump injection (primary system pressure  $< 2.0$  MPa) is checked by RELAP5-3D at every time step. The parameters that were sampled for the LS derivation are reported in Table 4-17.

**Table 4-17. Parameters for the 2D Limit Surface Search – Case 1**

Parameters	Range	Distribution type
Battery lifetime	14,400-28,800 s (4-8 hrs)	Uniform
Recovery Action timing	36,000-55,800 s (10-15.5 hrs)	Uniform

The results of the LS calculations for the Zry, Cr-coated and FeCrAl clads are shown in Figure 4-18. The figure shows some increase of coping time for ATF clads (i.e., time available for the emergency crew recovery actions), at the top zones of the LS. However, this extra coping time (~1 hour at maximum), it is minimal and it is going to be included in the RELAP5-3D code uncertainties bands.



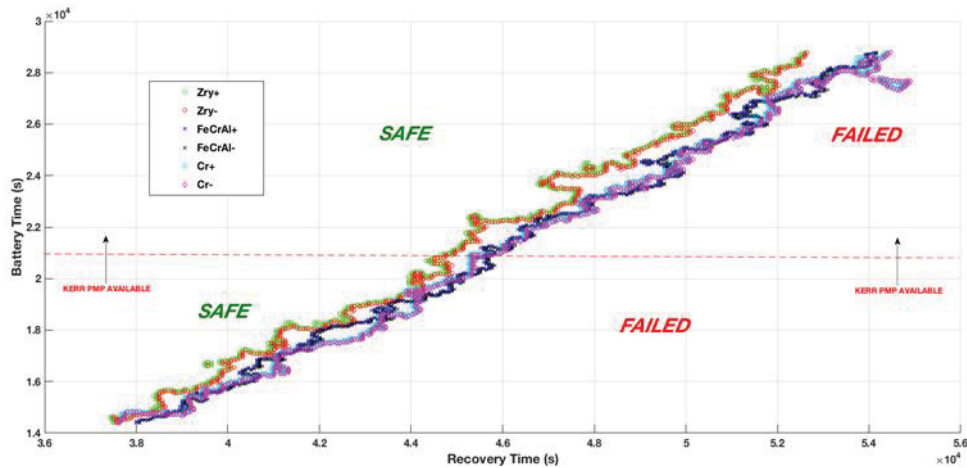


**Figure 4-18. 2D Limit Surface – Case 1.**

Limit Surface Integral was also used as a metric for evaluating the Safe conditions area vs. the Failed conditions area. The algorithm computing the integral is using Monte Carlo technique and the parameters specified in Table 4-17 as integration intervals. The LS integral results presented in Table 4-18 show some sensible improvement on the failure probability for ATF fuels, with maximum of -10.0% for Cr-coated clads.

**Table 4-18. LS Integral for SBO-3.0. Case 1.**

Clad Type	Failure Probability	Variation vs. Zry
Zry	0.5220	N/A
Cr-Coated	0.4698	-10.0%
FeCrAl	0.4735	-9.3%

A second LS search was performed, increasing the variability of the battery lifetime to 5 hours (battery lifetime between 3 and 8 hours) and assuming the Kerr pump injection at  $t=3.5$  hours (same boundary condition used in (NRC, 2012), see Table 4-19.

**Table 4-19. Parameters for the 2D Limit Surface Search – Case 2**

Parameters	Range	Distribution type
Battery lifetime	10,800-28,800 s (3-8 hrs)	Uniform
Recovery Action timing	36,000-55,800 s (10-15.5 hrs)	Uniform

The exploration of the SBO accident space is reported in Figure 4-19. Also in this case, results shows a slight improvement in using the ATF: LSs are almost overlapped, with FeCrAl and Cr-coated clads identifying a slightly larger “safe area” (see Table 4-20).

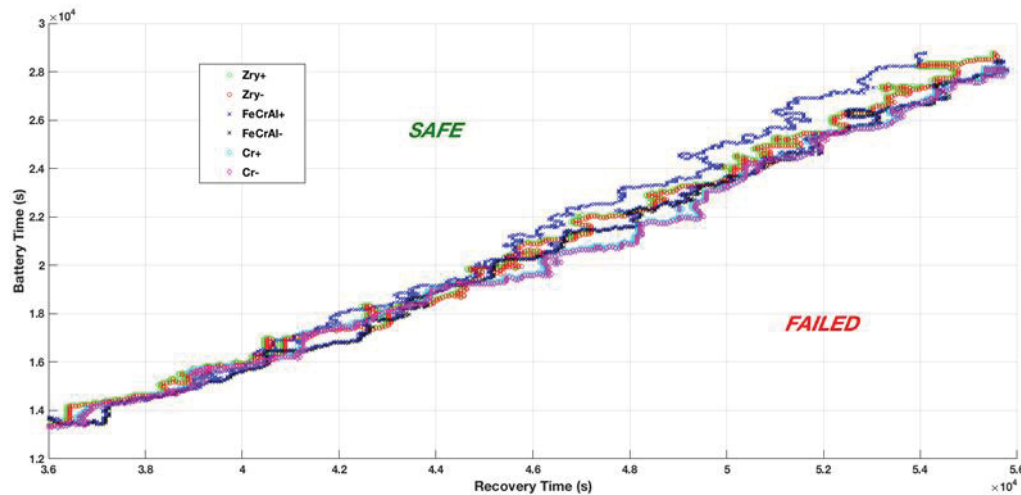


Figure 4-19. 2D Limit Surface – Case 2.

Table 4-20. Parameters for the 2D Limit Surface Search – Case 2

Clad Type	Failure Probability	Variation vs. Zry
Zry	0.5618	N/A
Cr-Coated	0.5268	-6.2%
FeCrAl	0.5327	-5.2%

#### 4.4.3 Three-dimensional Limit Surfaces Search

Further investigation of the accidental domain was performed by increasing the number of dimensions from two to three (see Table 4-21 and Table 4-22). The variables perturbed in the 2D LS were kept the same for both cases. The additional variables that were perturbed are:

- case 1. Kerr pump injection time (assumed constant at 16,200 s in the 2D LS case). SG depressurization time was kept constant at  $t=5,400$  s.
- case 2. SG depressurization time (assumed constant at 5,400 s in the 2D LS case). Kerr pump injection time was kept constant at  $t=16,200$  s.

**Table 4-21. Parameters for the 3D Limit Surface Search – SBO-3.0 – Case 1**

Parameters	Range	Distribution type
Battery lifetime	14,400-28,800 s (4-8 hrs)	Uniform
Recovery Action time	36,000-55,800 s (10-15.5 hrs)	Uniform
Kerr pump Injection time	7200-16,200 s (2-4.5 hrs)	Uniform

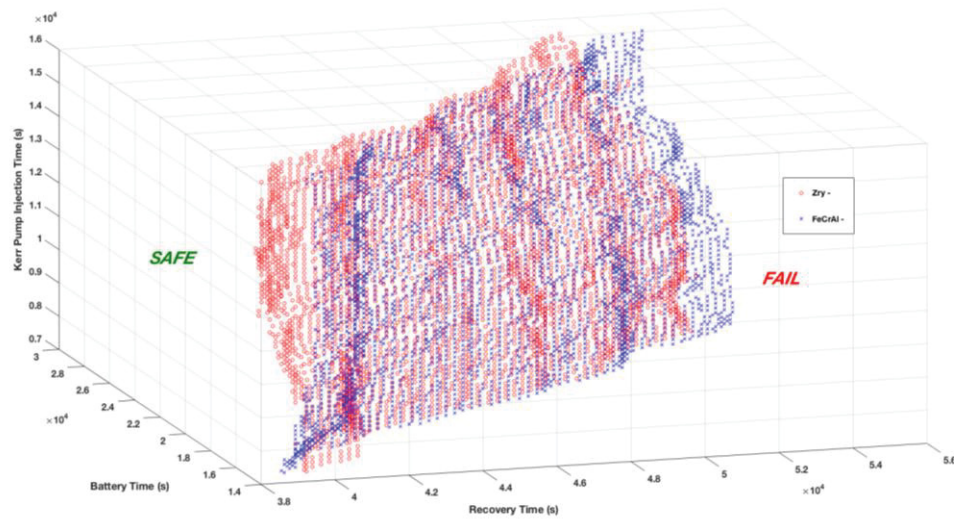


**Figure 4-20. 3D Limit Surface – Case 1.**

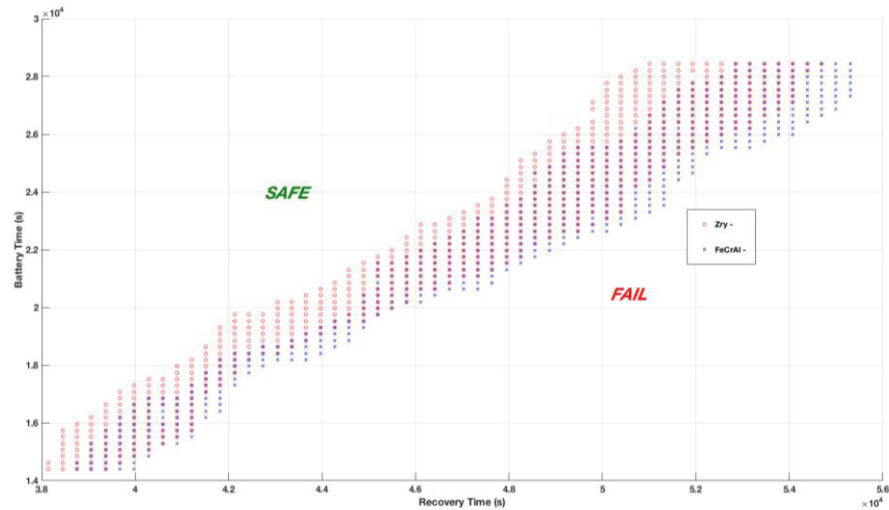


**Figure 4-21. 2D projections of 3D Limit Surface – Case 1.**

**Table 4-22. Parameters for the 3D Limit Surface Search – SBO-3.0 – Case 2**

Parameters	Range	Distribution type
Battery lifetime	14,400-28,800 s (4-8 hrs)	Uniform
Recovery Action timing	36,000-55,800 s (10-15.5 hrs)	Uniform
SG depressurization time	3,600-12,600 (1-4.5 hrs)	Uniform

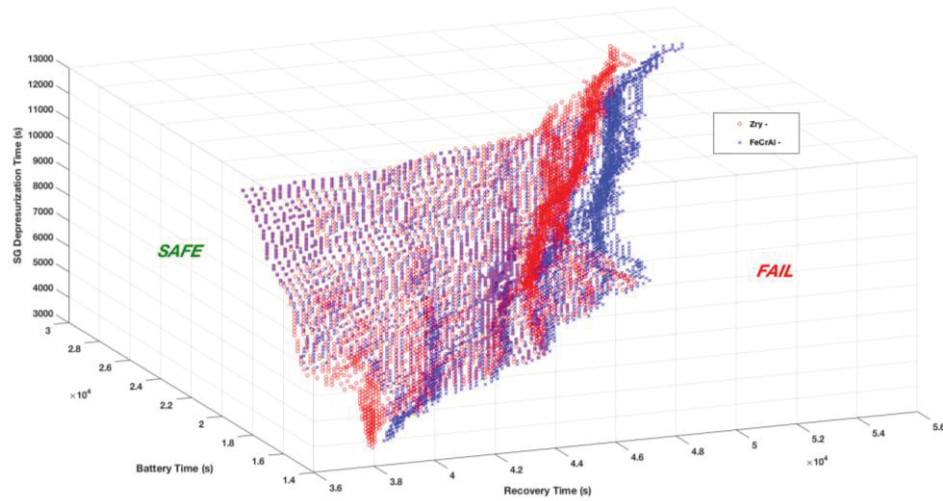


**Figure 4-22. 3D Limit Surface – Case 2.**

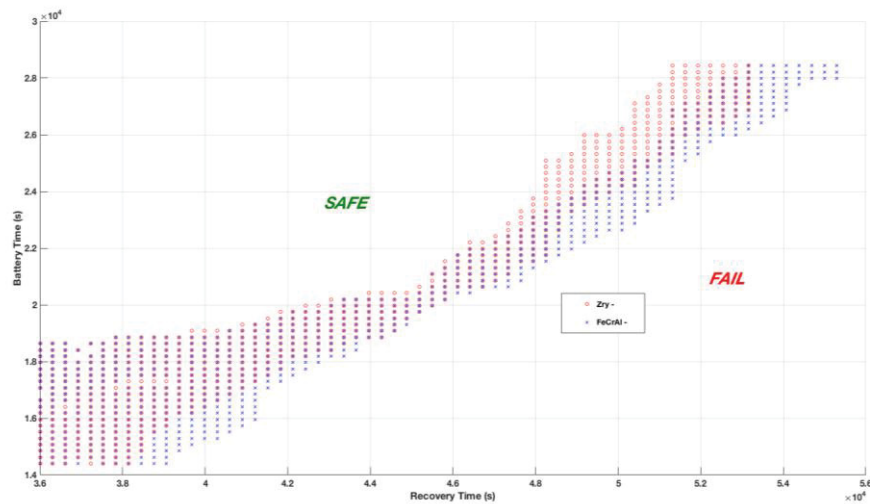


**Figure 4-23. 2D projections of 3D Limit Surface – Case 2.**

From the figures reported above, it can be qualitatively assessed the better performance of the FeCrAl compared to the Zry clad. An exact quantification of the improvement can be obtained using again the LS integral algorithm. Results for both cases are reported in Table 4-23.

**Table 4-23. LS Integral for SBO-3.0. 3D Case**

<b>Clad Type</b>	<b>Case 1</b>		<b>Case 2</b>	
	<b>Failure Probability</b>	<b>Variation vs. Zry</b>	<b>Failure Probability</b>	<b>Variation vs. Zry</b>
Zry	0.4957	N/A	0.5267	N/A
Cr-Coated	0.4453	-10.2%	0.5156	-2.1%
FeCrAl	0.4429	-10.6%	0.4846	-8.0%

As for the 2D LS, there is a sensible reduction of the failed conditions area, with a maximum reduction of~ 10% for case 1 (anticipation of Kerr pump injection).

## 5. LBLOCA SCENARIO ANALYSIS

This section presents the LBLOCA analysis for the same 3-loop PWR system of Westinghouse design with a large-dry containment described in Section 3.2.1 (see Figure 5-1). The initiating event is a LBLOCA on the cold-leg RPV where the break occurs on the pressurizer loop. Under these accident conditions, the system experiences a sudden sub-cooled blowdown and primary system pressure drops from about 15.5 MPa down to the containment pressure ( $\sim 0.1$  MPa).

In order to compensate the large loss of coolant inventory into the vessel and prevent core damage, two emergency core-cooling systems are employed: High Pressure Injection (HPI), Accumulator (ACC), and Low Pressure Injection (LPI) Systems. ACC system consists of pressurized water tanks that are employed at the beginning of the transient and can dump large inventory of sub-cooled water into the vessel. The HPI and LPI systems are activated when primary system pressure falls below the injection set points and by using pumps a large amount of water is transferred from the Reactor Water Storage Tank (RWST) directly into the vessel.

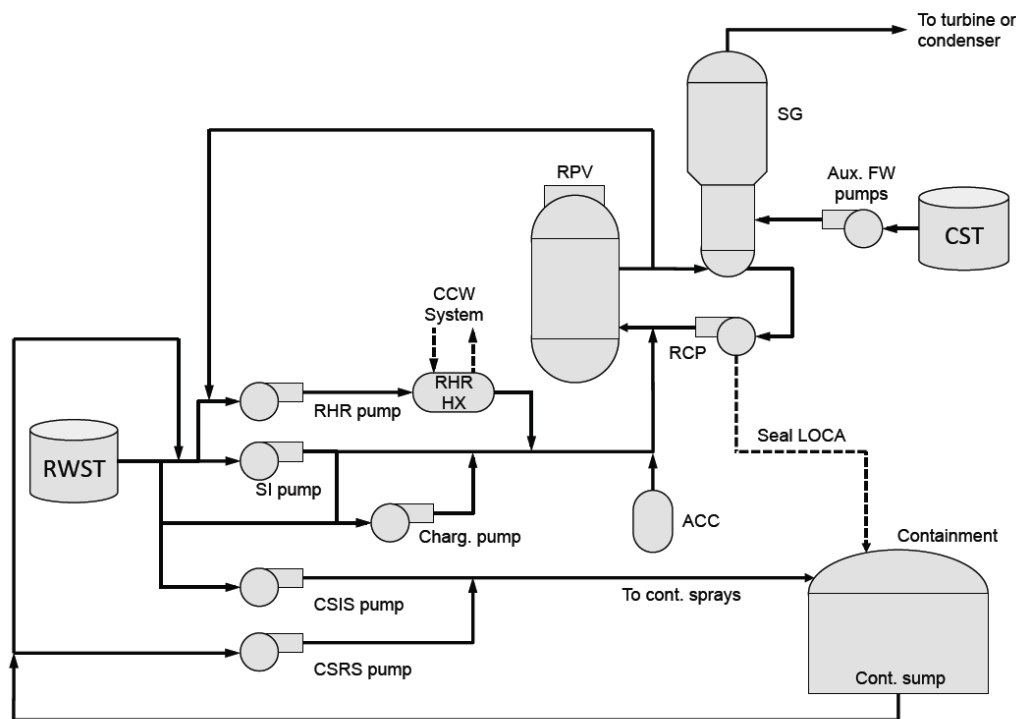


**Figure 5-1. PWR Scheme.**

The large amount of water that leaves the primary system and is collected in the containment and, thus, its temperature and pressure increase. In order to cool it down, the Containment Spray (CS) system is employed. Similarly to the HPI and LPI, through pumps RWST water is sprayed from the top level of the containment.

Once RWST is empty, both CS and HPI/LPI switch from injection mode to recirculation mode: water collected at the base of the containment and through the sump and is injected back into the vessel (through the HPI/LPI) and into the containment (through the CS).

## 5.1 RELAP5-3D Model

The IGPWR RELAP5-3D model described in Section 3.2.1 is used for LBLOCA analysis. The model represents a 2.5 GWth Westinghouse 3-loop PWR and includes the RPV, the 3 loops and the primary and secondary sides of the SGs. Four independent channels are used for representing the reactor core. Three

channels model the active core and one channel models the core bypass. Different power values are assigned to the three core channels in order to take into account the radial power distribution. Passive and active heat structures simulate the heat transfer between the coolant and fuel, the structures and the secondary side of the PWR plant.

For the transient calculation, a horizontal LBLOCA on the cold-leg RPV nozzle was considered. The break occurs on the pressurizer loop. Several LBLOCA cases were completed, including some considered by Westinghouse for LBLOCA spectrum analysis: 2A (Double-Ended Guillotine Break - DEGB),

In this scenario, depressurization of the primary vessel occurs very quickly and large amount of water inventory is lost due to the break. In order to compensate for the loss of water inventory and provide cooling to the core to avoid core damage, several systems are modeled:

- ACC which consists of water tanks that are employed right at the beginning of the transient in order to flood the RPV
- LPI system which is an injection system that transfers cold water from RWST to RPV
- Low Pressure Recirculation (LPR) system which is employed once the RWST tank is empty; this system is still composed by the same components of the LPI system but water source is now the water collected inside the containment through the containment sump. Thus, the water lost from the RPV is collected at the bottom of the containment, it is cooled down through heat-exchangers and it is injected back into the RPV (i.e., low pressure recirculation mode).
- Containment cooling system which controls containment thermodynamic behavior (temperature and pressure) in order to maintain its structural integrity

## 5.2 LBLOCA Analysis

The overall LBLOCA Dynamic PRA was performed by considering the following variables:

- Number of ACC trains available (out of 3)
- Activation time of the ACC trains
- Number of HPI trains available (out of 3)
- Activation time of the HPI trains
- Number of HPI trains available for recirculation (out of 3)
- Switch time of the HPI trains to recirculation mode
- Number of LPI trains available (out of 2)
- Activation time of the LPI trains
- Number of LPI trains available for recirculation (out of 2)
- Switch time of the LPI trains to recirculation mode

By sampling this set of stochastic parameters, the initial and boundary conditions in the RELAP5-3D input file are set and the simulation can be run. The Dynamic PRA analysis has been performed by generating a large number of simulation runs by employing a Monte-Carlo sampling method available in RAVEN. Simulation datasets were separately generated for the three considered fuel types.

In order to precisely measure and better visualize the different impact of each fuel type to the simulation end state we have restructured the generated datasets (one for each fuel type) to match a tree structure, i.e., the LBLOCA Event Tree (see Figure 5-2).

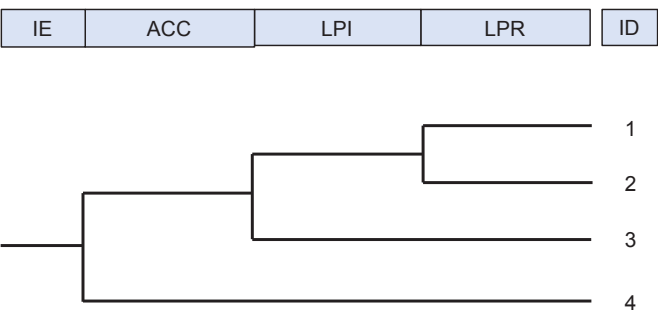


**Figure 5-2. LBLOCA Event Tree.**

Note that the LBLOCA Event Tree of Figure 5-2 is that 1) the HPI system is not explicitly queried and 2) the Branch 3 queries only the ACC system. In order to give a more refined analysis of the generated transients, the LBLOCA Event Tree of Figure 5-2 has been expanded to explicitly consider the HPI system and by querying all the injection systems (HPI and LPI) in Branch 4 of the original Event Tree of Figure 5-2. The resulting expanded LBLOCA Event is shown in Figure 5-3.

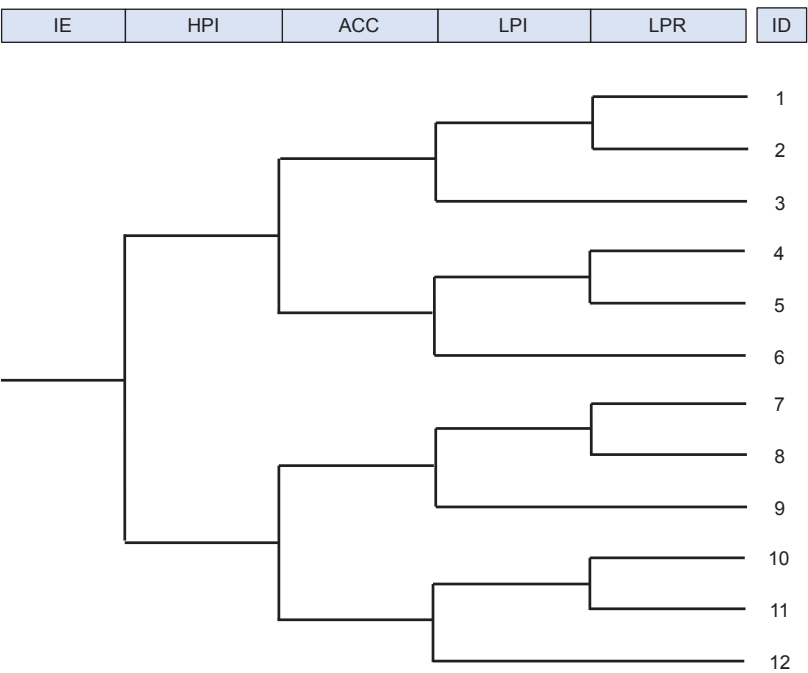


**Figure 5-3. Expanded LBLOCA Event-Tree Structure.**

The matching between simulated transients and Event-Tree was performed by associating each transient simulated by RELAP5-3D to a specific branch of the LOCA ET as follows (see Figure 5-4):

- Identify the ET branching conditions in the transient temporal evolution (e.g., successful activation of the ACC system)



- Determine the successful/unsuccessful outcome of each branching condition
- Identify the ET branch that matches the set of branching condition outcomes; if no match is found, then the ET requires a review (e.g., additional branches/branching conditions)

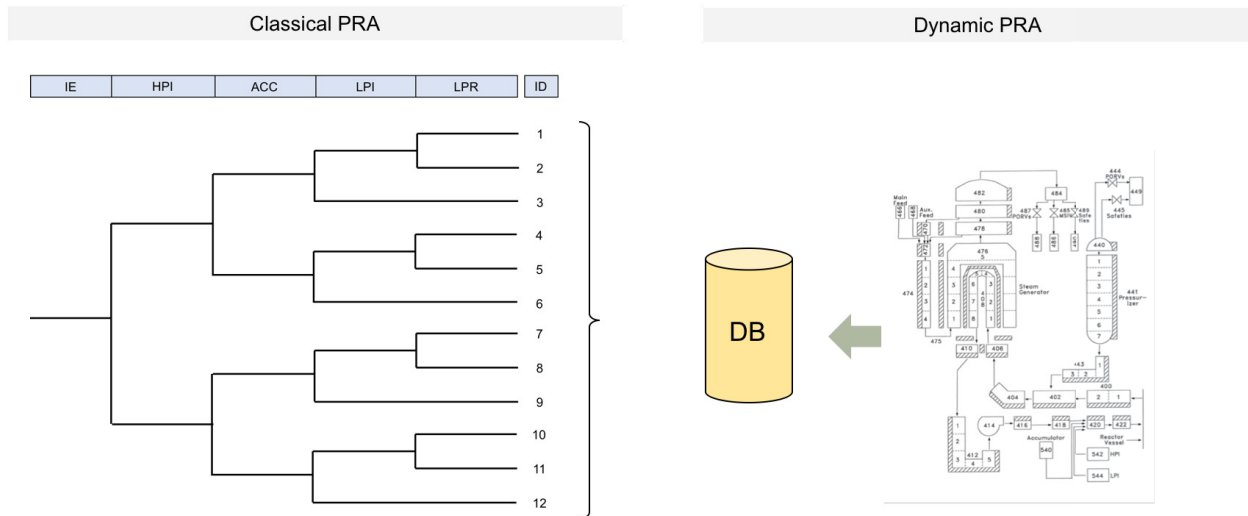


**Figure 5-4. Scheme of the Classical and Dynamic PRA Integration for the LBLOCA Test Case.**

### 5.3 Results

By following this “simulated transient to Event Tree” matching data analysis step we were able to identify the first difference in term of performances for the three considered fuel types. Figure 5-5 summarize the outcome of the simulations associated to each of the 12 branches of Figure 5-4 for each fuel model.

Note that different outcome are recorded for the simulations contained in Branches 4 and 10. While Zr fuel cannot withstand a LBLOCA scenario without the initial activation of the ACC system, the Cr and the FeCrAl can avoid CD condition if the LPI system is available. Thus, a first conclusion can be withdrawn from Figure 5-5 in terms of importance from a risk perspective of the ACC system: its failure does not preclude the system to reach a safe condition. Note the HPI system alone is not sufficient to reach a safe condition for all three fuel types; instead, the LPI system is sufficient and necessary condition.

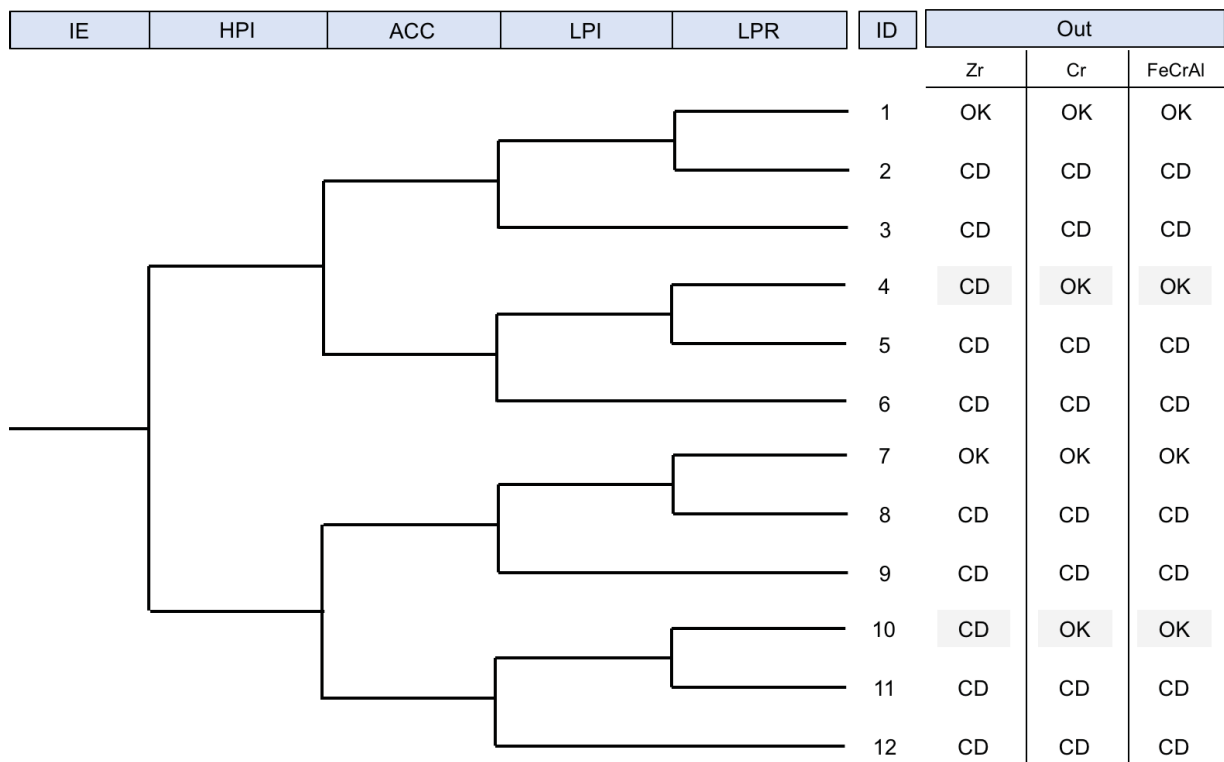


**Figure 5-5. Outcome of the Simulations associated to Each Branch of the Expanded LBLOCA Event-Tree for the Three Considered Fuel Types.**

Furthermore, we have focused our attention to the branches leading to CD by measuring the time at which the simulations reach CD condition. The objective is to evaluate how much time can be gained by employing ATF; from a PRA perspective, this gained time can be employed to increase the probability to perform water injection in the vessel through auxiliary systems (e.g., FLEX systems).

Table 5-1, Table 5-2, and Table 5-3 provide the histogram of the time at which CD condition is reached for Branches 2, 3, 5, 6, 8, 9, 10, 11 and 12 of expanded Event-Tree of Figure 5-5. By observing the time distributions for Branches 3, 6, 9 and 12, it is possible to notice that without the ACC and LPI systems the time reaches CD very quickly (about 400 seconds). With ATF fuels, a margin of about 100-200 seconds can be gained; however, such time gain is too small to allow any FLEX equipment to be connected. On the other hand, by observing the time distributions for Branches 2, 5, 8, 11 and 12, it is possible to notice that a bigger difference in terms of time to reach CD for the ATF fuels when compared to the Zr fuel. This is more evident for the FeCrAl fuel type where on average about 600 seconds can be gained from Zr fuel.

Table 5-1. Time to Reach CD Condition for Branches 2, 3 and 5 of the Expanded Event-Tree of Figure 5-5

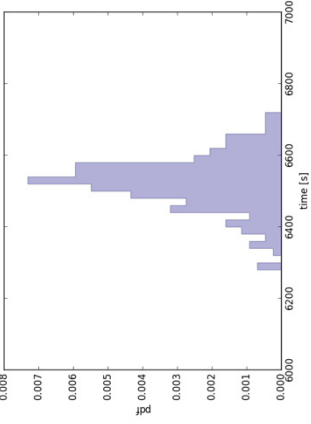
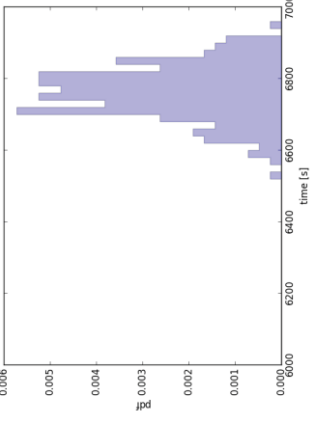
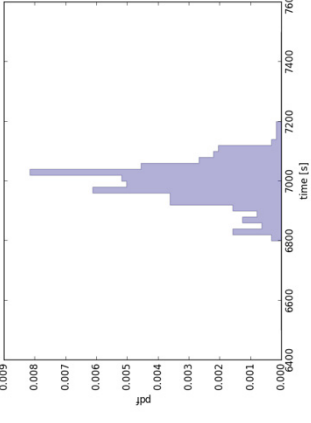
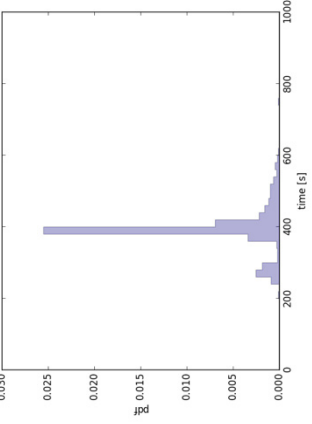
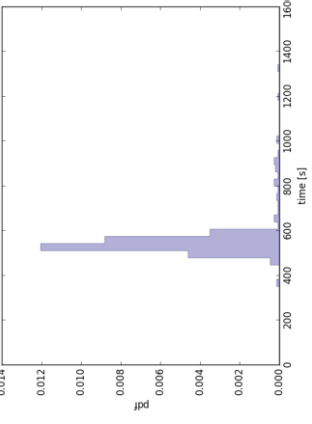
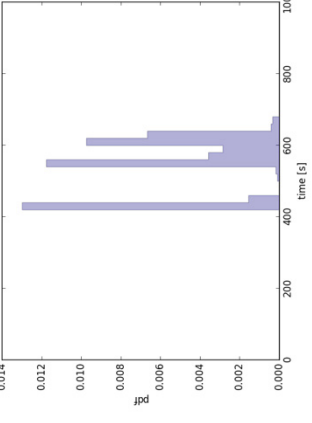
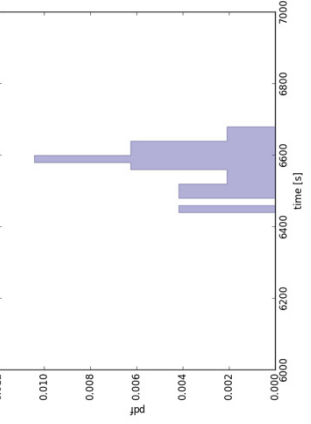
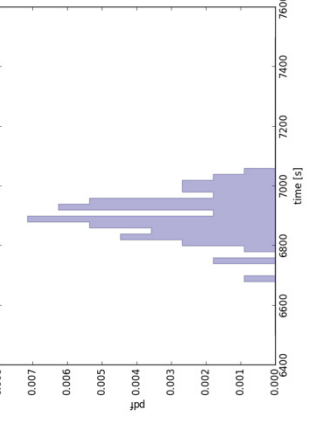
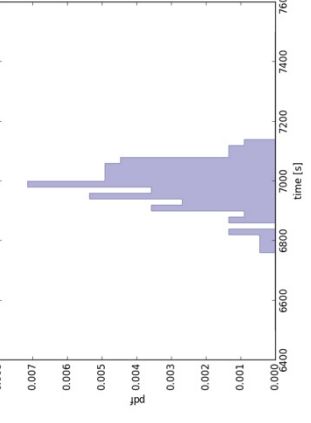
Branch	Zr	Cr	FeCrAl
2			
3			
5			

Table 5-2. Time to Reach CD Conditions for Branches 6, 8 and 9 of the Expanded Event-Tree of Figure 5-5.

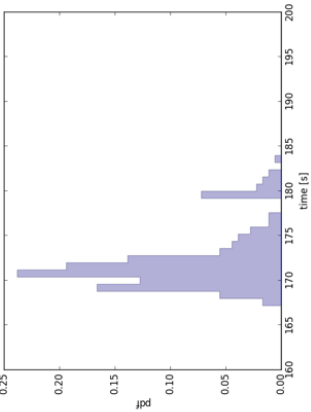
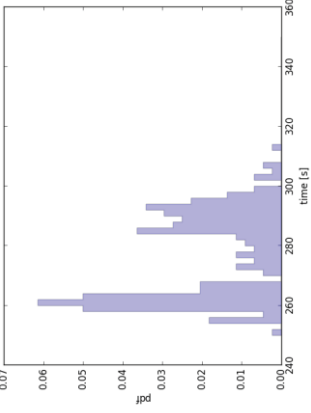
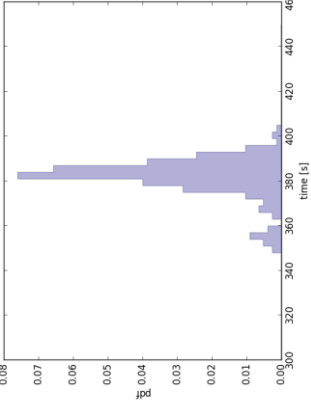
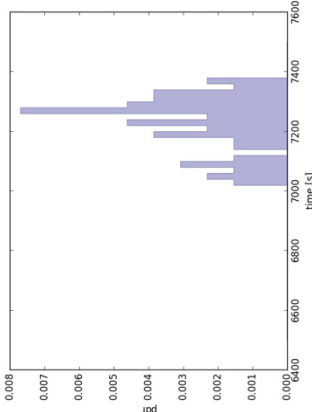
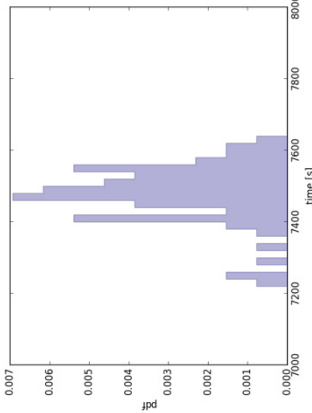
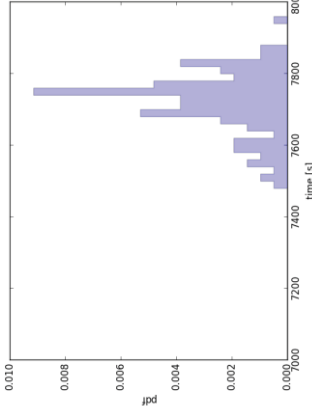
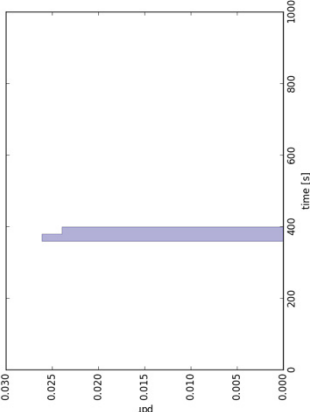
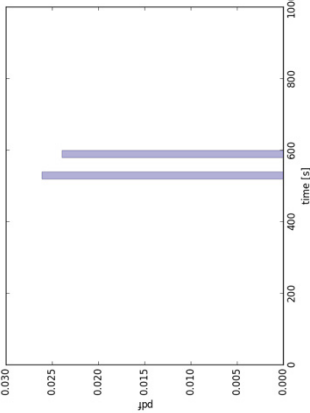
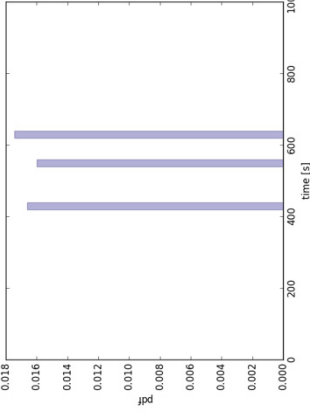
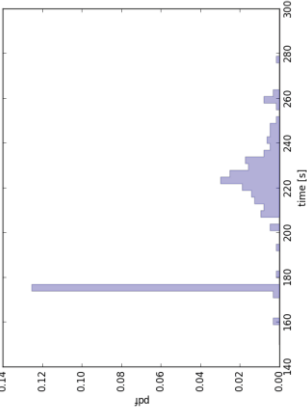
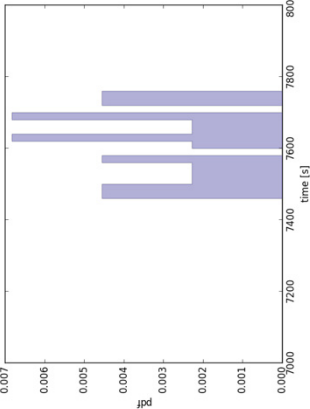
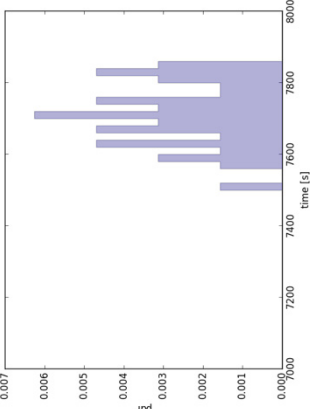
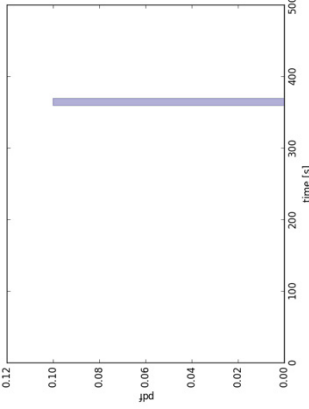
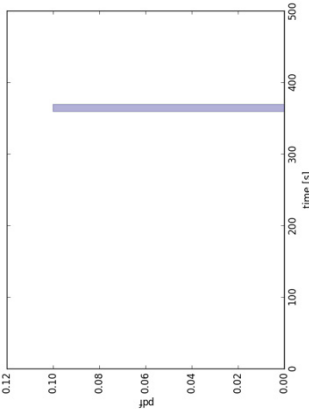
Branch	Zr	Cr	FeCrAl
6			
8			
9			

Table 5-3. Time to Reach CD Conditions for Branches 10, 11 and 12 of the Expanded Event-Tree of Figure 5-5.

Branch	Zr	Cr	FeCrAl
10		NA	NA
11			
12			

## 6. RISK-INFORMED PLANT ENHANCEMENT ANALYSIS

This section introduces how a risk-informed approach is applied to investigate and optimize the potential plant enhancements that would improve plant resiliency. The same generic PWR SBO PRA model as in Section 4 is used to describe the approach. The risk-informed resiliency plant enhancement approach includes the following steps:

1. For the analyzed scenario (either a general transient, design basis accident, or beyond design basis), develop a list of risk significant accident sequences for further analysis, with criteria such as cumulative CDF contribution greater than 90% or 95%, individual sequence CDF greater than  $1\text{E-}7$  or  $1\text{E-}8$  per year.
2. Develop top event list for each selected risk significant accident sequence, focusing on the failure top events (or down branch in the event tree) which would present potential plant design changes that improve plant resiliency.
3. Develop a preliminary list of potential plant design changes by reviewing the top events, the cut sets, and the basic event importance measures of each selected risk significant accident sequence. These potential plant changes could effectively reduce the likelihood of the occurrence of the top event failures and/or enhance plant resiliency with additional mitigation equipment or strategies.
4. Review the preliminary list of potential plant enhancements (from the standpoint of feasibility, risk impact, and economic impact) and select an optimized list of enhancements for further analysis.
5. Develop plant accident scenarios with the selected potential plant design enhancements. Conduct necessary thermal hydraulic analysis on the scenarios to demonstrate the safety impact from the enhancements (for example, increased safety margin, extended accident coping time, etc.).
6. Revise PRA model properly and quantify the model for the risk impact from the plant change candidates.
7. Document and report the risk-informed resiliency plant design results to stakeholder and decision makers.

Using the SBO model as a case study, Table 6-1 presents risk significant grid-related SBO accident sequences that contribute more than 95% of the total grid related SBO CDF (Step 1). A generic PWR SBO SAPHIRE model was reviewed for top events, especially the failed top events, for each risk significant sequence (Step 2). For example, the INT-LOOPGR:16-03-10 sequence includes 2 failed top events: AC power is not recovered within 4 hours, and failure to manual control TDAFW to provide flow to SGs after battery depletes. The INT-LOOPGR:16-45 sequence also includes 2 failed top events: TDAFW fails to provide flow to SGs following SBO, and AC power is not recovered within 1 hour.

Step 3 reviews the results in Table 6-1 and the cut sets and importance measures for each of the six SBO sequences. The importance measures used in this step are Risk Reduction Worth (RRW) and Fussell-Vesely (FV) which focus on the risk contributions by the basic event and the risk reduction if the basic event would not fail. Table 6-2 shows the most important basic events and their association with the sequence top events which also means the potential plant enhancement that could reduce the basic event failure probability and the sequence CDF. Table 6-3 presents a preliminary list of potential plant design enhancements based on previous analysis. Note that Table 6-3 also considers potential plant enhancement as Item 0 that could reduce the occurrence of the initiating event, SBO in this case study.

**Table 6-1. Risk Significant Grid-Related PWR SBO Sequences**

SBO Sequence	CDF	%	AFW (1)	PORVs	Rapid Sec. Depress.	RCP Leakage (2)	AC Power Recovery (3)	Manual AFW (4)	HPI (5)	Pri & Sec Cooldown	LPI (6)	LPR (7)
INT-LOOPGR:16-03-10	1.57E-07	41.6%	AFW	PORV Closed	RSD	21	4Hrs No	No AFW- MAN				
INT-LOOPGR:16-06	1.30E-07	34.6%	AFW	PORV Closed	RSD	182	4Hrs No					
INT-LOOPGR:16-45	5.42E-08	14.4%	No AFW	NA	NA	NA	1Hr No					
INT-LOOPGR:16-04-7	1.08E-08	2.9%	AFW	PORV Closed	RSD	182	4Hrs Yes		No HPI	Cooldown	No LPI	NA
INT-LOOPGR:16-04-2	1.01E-08	2.7%	AFW	PORV Closed	RSD	182	4Hrs Yes		HPI	Cooldown	NA	No LPR
INT-LOOPGR:16-12	4.37E-09	1.2%	AFW	PORV Closed	RSD	480	2Hrs No					

Table 6-2. Sequence Cut Set and Importance Measure Review for Potential Plant Enhancement

Basic Event	Failure Prob.	Description	Area for Enhancement
<b>INT-LOOPGR:16-03-10</b>			
EPS-XHE-XL-NR04H	5.57E-01	OPERATOR FAILS TO RECOVER EMERGENCY DIESEL IN 4 HOURS	E3. AC Power Recovery
OEP-XHE-XL-NR04HGR	1.54E-01	OPERATOR FAILS TO RECOVER OFFSITE POWER IN 4 HOURS (GRID-RELATED)	E3. AC Power Recovery
AFW-XHE-XM-TDPBD	3.00E-01	OPERATOR FAILS TO CONTROL AFW TDP AFTER BATTERY DEPLETION	E4. TDAFP Black Run
<b>INT-LOOPGR:16-06</b>			
RCS-MDP-LK-BP2	2.00E-01	RCP SEAL STAGE 2 INTEGRITY (BINDING/POPPING OPEN) FAILS	E2. RCP Seal
EPS-XHE-XL-NR04H	5.57E-01	OPERATOR FAILS TO RECOVER EMERGENCY DIESEL IN 4 HOURS	E3. AC Power Recovery
OEP-XHE-XL-NR04HGR	1.54E-01	OPERATOR FAILS TO RECOVER OFFSITE POWER IN 4 HOURS (GRID-RELATED)	E3. AC Power Recovery
<b>INT-LOOPGR:16-45</b>			
EPS-XHE-XL-NR01H	7.86E-01	OPERATOR FAILS TO RECOVER EMERGENCY DIESEL IN 1 HOUR	E3. AC Power Recovery
OEP-XHE-XL-NR01HGR	6.11E-01	OPERATOR FAILS TO RECOVER OFFSITE POWER IN 1 HOUR (GRID-RELATED)	E3. AC Power Recovery
AFW-TDP-FS-C	7.00E-03	TURBINE DRIVEN FEED PUMP C FAILS TO START	E1. TDAFP
AFW-TDP-TM-C	5.00E-03	AFW TDP PUMP C IS IN TEST OR MAINTENANCE	E1. TDAFP
AFW-TDP-FR-C	4.10E-03	TURBINE DRIVEN FEED PUMP C FAILS TO RUN	E1. TDAFP
<b>INT-LOOPGR:16-04-7</b>			
RCS-MDP-LK-BP2	2.00E-01	RCP SEAL STAGE 2 INTEGRITY (BINDING/POPPING OPEN) FAILS	E2. RCP Seal
NSW-MDP-CF-START	1.40E-05	NSCW PUMPS FAIL FROM COMMON CAUSE TO START	E5&E6. SW System
<b>INT-LOOPGR:16-04-2</b>			
RCS-MDP-LK-BP2	2.00E-01	RCP SEAL STAGE 2 INTEGRITY (BINDING/POPPING OPEN) FAILS	E2. RCP Seal
LPI-XHE-XM-ERROR	2.00E-03	OPERATOR FAILS TO INITIATE LOW PRESSURE RECIRCULATION	E7. LPR XHE
<b>INT-LOOPGR:16-12</b>			
RCS-MDP-LK-BP1	1.25E-02	RCP SEAL STAGE 1 INTEGRITY (BINDING/POPPING OPEN) FAILS	E2. RCP Seal
RCS-MDP-LK-BP2	2.00E-01	RCP SEAL STAGE 2 INTEGRITY (BINDING/POPPING OPEN) FAILS	E2. RCP Seal
OEP-XHE-XL-NR02HGR	3.56E-01	OPERATOR FAILS TO RECOVER OFFSITE POWER IN 2 HOURS (GRID-RELATED)	E3. AC Power Recovery
EPS-XHE-XL-NR02H	6.87E-01	OPERATOR FAILS TO RECOVER EMERGENCY DIESEL IN 2 HOURS	E3. AC Power Recovery



**Table 6-3. Preliminary List of Potential Plant Enhancements**

Enhancement	Description	Sub-Category
E0	IE-SBO Occurrence	E0.a Reduced LOOP frequency
		E0.b Increased EDG reliability/redundancy
E1	TDAFP	E1.a Feed & Bleed capability during SBO
		E1.b Additional TDAFP capability
E2	RCP Seal	E2.a RCP Shutdown Seal
		E2.b RCP seal cooling capability during SBO
E3	AC Power Recovery	E3.a Additional on-site power capability
		E3.b Additional off-site power capability
		E3.c Increased battery capability
E4	TDAFP Black Run	E4.a SG level self-regulating capability
		E4.b TDAFP Black Run capability
E5	HPI Failure - SW	E5.a Service water supporting system
E6	LPI Failure - SW	E6.a Service water supporting system
E7	LPR Failure	E7.a LPR operator action performance

In Step 4, the preliminary list of potential plant enhancements in Table 6-3 is reviewed. The following enhancement categories are chosen for further analysis:

- E3 AC Power Recovery
  - E3.a Additional on-site power capability, for example, additional diesel generator
  - E3.b Additional off-power capability, for example, the ability to connect to additional off-site power source(s)
  - E3.c Increased battery capability, for example, increase battery life from 4 hours to 8 hours through measures such as load shedding and/or additional battery
- E2 RCP Seal
  - E2.a Adopt RCP Shutdown Seal which could basically eliminate the likelihood of RCP seal leak during a loss of AC power
  - E2.b RCP seal cooling capability during SBO scenario, which would require a diesel-driven pump to provide cooling to RCP seals during SBO
- E1 and E4 TDAFP Capability
  - E1.a Feed & Bleed capability during SBO
  - E1.b Additional TDAFP capability
  - E4.a SG level self-regulating capability
  - E4.b TDAFP Black Run capability

Most of the above potential enhancements may not warrant the need to perform additional thermal hydraulic (T-H) analysis as they could be covered by existing T-H analyses. For example, with additional on-site or off-site power capability, the likelihood to recover AC power within the defined timeline (for example, within 4 hours) could increase, but no additional T-H analysis is necessary. For RCP Shutdown Seal or increased seal cooling capability, the existing T-H analysis for 21gpm/RCP could be used as a surrogate for such enhancement and no additional analysis is needed. The one may need additional T-H analysis is Enhancement E3.c in which battery life is increased from 4 hours to 8 hours. This could be run as a sensitivity case as the previous SBO scenario SBO-1.0 in Section 4. SBO-1.3 listed below is thus created for RELAP5-3D analysis.

- SBO-1.0: LOOP occurs, both EDG fail, TDAFP success, No PORV remained opened, 21gpm/RCP leakage, Rapid Secondary Depressurization success, No offsite power recovery and TDAFP stops after DC battery depletes. -> Core Damage Timing.

- **SBO-1.3:** LOOP occurs, both EDG fail, TDAFP success, No PORV remained opened, 21 gpm (or 76, 182, 480 gpm)/RCP leakage, Rapid Secondary Depressurization success, No offsite power recovery and TDAFP stops after DC battery depletes in 8 hours. -> Core Damage Timing.

Scenario SBO-1.3 has been analyzed with RELAP5-3D with the results included in Section 4.3. Due to the short timing available in FY 2018, Steps 3 and 6 of this approach did not proceed as planned. The approach in this section would be continuously pursued in next year.

## 7. RISK-INFORMED SENSITIVITY ANALYSIS FOR ATF

In this section we presented a risk-informed sensitivity analysis for ATF. A key aspect in the evaluation of the ATF designs is the determination of potential increases in coping time with respect to advancements in fuel and cladding materials. The purpose of the analysis is to obtain a qualitative understanding of the relations between coping time increases and various material properties. The fuel cladding material parameters such as thermal conductivity are adjusted to find out the parameters needed for the new material to maximize coping time. For this particular sensitivity analysis, one at a time methods (OAT) are used in place of the increasingly more common global sensitivity analysis methods. OAT was selected in order to better elucidate the behavior of the coping time with respect to various inputs (i.e. linear, asymptotic, sporadic, etc.).

RELAP5-3D was used to model a PWR SBO scenario. The RELAP5-3D input deck included the primary coolant loop which was comprised of the reactor core, steam generators, pressurizers, and pumps. A nodalization of the primary coolant loop is shown in Figure 7-1. The core assemblies utilized standard uranium dioxide fuel with Zircaloy cladding. The core was modeled by treating each assembly as two heat structures: one representing the hot rod and the other as an average of all remaining rods. Each heat structure contained six axial elements and 8 radial elements (5 for the fuel, 1 for the gap, and 2 for the clad). The core sub-channels were modeled as six hydraulic components, with every assembly heat structure being attached to exactly one of the components. Both the dynamic gap model and oxidation models within RELAP5-3D were activated.

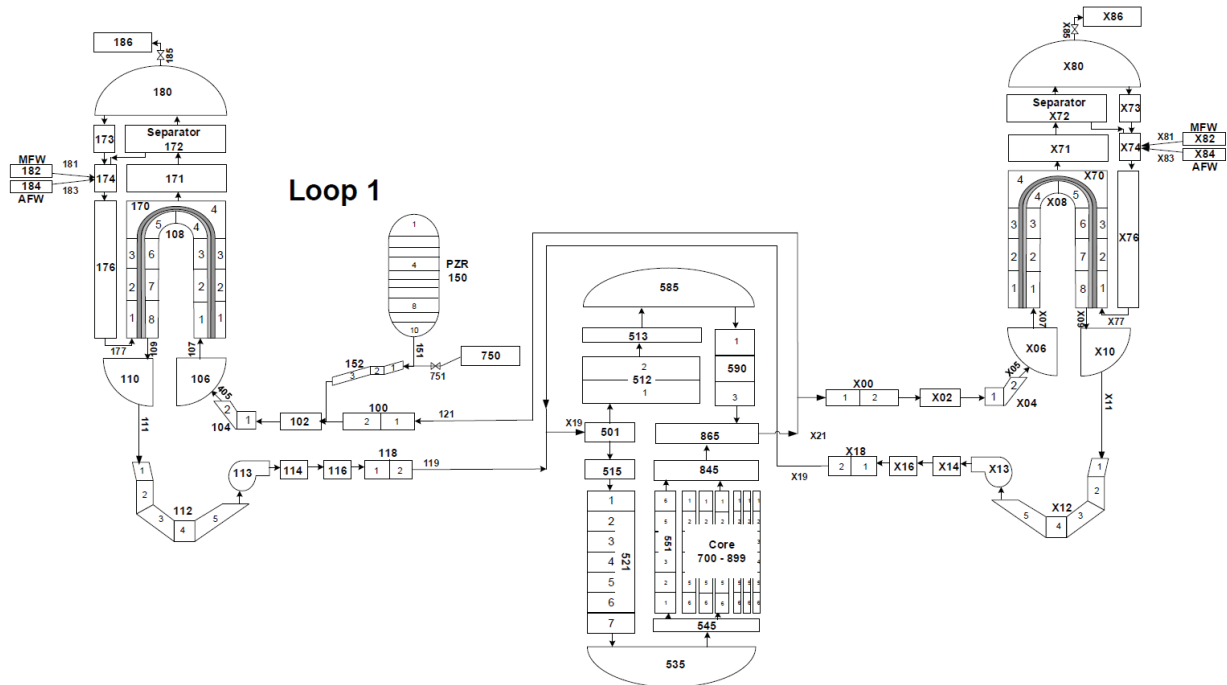


**Figure 7-1. Relap5-3D Coolant Primary Coolant Loop.**

Each RELAP5-3D case consisted of a steady state initialization, followed by a transient (SBO) with scram. Decay heat then raised the coolant temperature until boil off, followed by drastic increases in cladding temperatures. The failure criteria was set as any clad temperature in excess of 1478 K (2200°F).

Due to considerable research being performed on the incorporation of new fuel and cladding materials, only material properties for ATF concepts were subject to analysis. Other potential impactful inputs on coping time such as fuel dimensions, as well as inputs outside of fuel performance (i.e. coolant properties and decay heat), are left for future work.

The selected inputs include thermal conductivity and volumetric heat capacity for both fuel and cladding, as well as the cladding side oxidation parameters of activation energy, rate, and heat release. One of primary

purpose of ATF is to minimize the exothermic oxidation process, which in turn reduces heat release and by extension coolant and cladding temperature rises. It is therefore of value to study the effects of oxidation on coping time increases. The pertinent inputs were altered as shown in Table 7-1.

**Table 7-1. Multiplicative Factors of Material Properties for Sensitivity Analysis of Coping Time**

Material Property	Lower Bound	Upper Bound	Distribution
Fuel Thermal Conductivity	1	10	Uniform
Fuel Volumetric Heat Capacity	1	10	Uniform
Clad Thermal Conductivity	1	10	Uniform
Clad Volumetric Heat Capacity	1	10	Uniform
Clad Oxidation Activation Energy	1	10	Uniform
Clad Oxidation Rate	0.1	1	Uniform
Clad Oxidation Heat Release	0.1	1	Uniform

For each parameter of Table 7-1, a sample of 300 multiplicative factors was generated. In each instance, the multiplicative factor was applied to the nominal RELAP5-3D input deck. RELAP5-3D was executed with each input files, after which post processors acquired all coping times. A nominal case was also executed which served as reference in the determination of all coping time increases reported in this work.

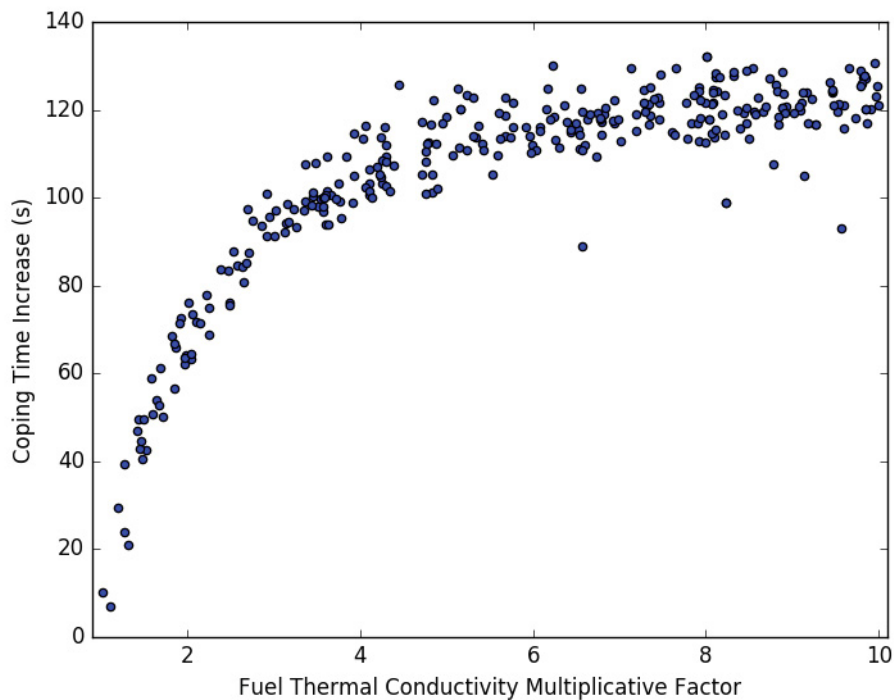


**Figure 7-2. Coping Time versus Fuel Thermal Conductivity.**

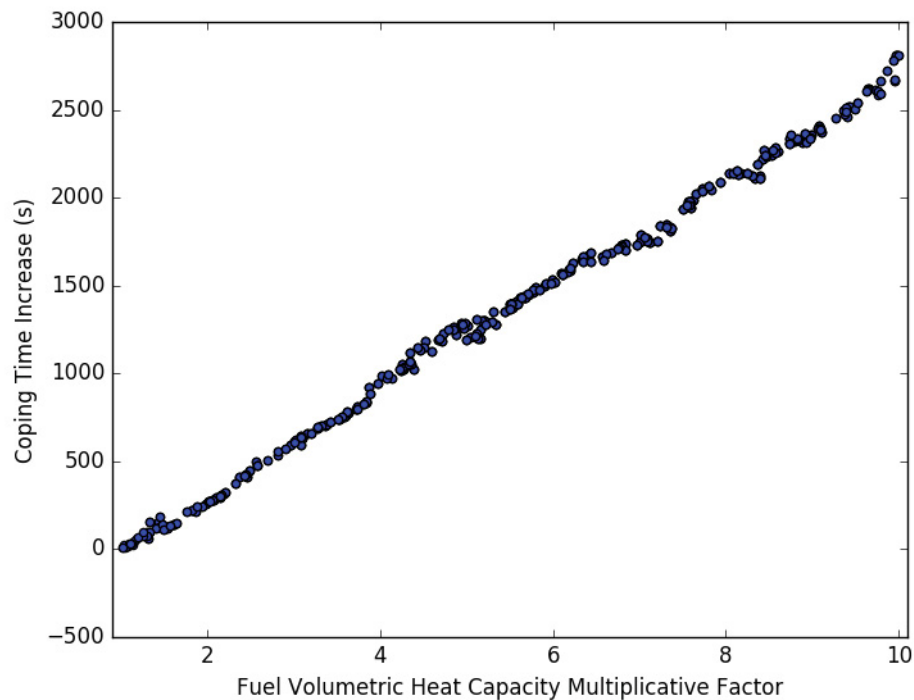


**Figure 7-3. Copping Time versus Fuel Volumetric Heat Capacity.**

Figure 7-2 indicates an asymptotic relation between coping time and fuel thermal conductivity ( $k_{fuel}$ ). This confirms intuition that initial increases in  $k_{fuel}$  help to reduce thermal resistance between clad and the interior of the fuel. However, after a factor of 5 increase in  $k_{fuel}$ , the fuel begins to approach a lumped capacitance thermal behavior with further increases in  $k_{fuel}$  producing diminishing returns.

The magnitude of coping time in Figure 7-2 of approximately two minutes indicate that no significant gains in coping time will result from increases in  $k_{fuel}$ . This is further evinced by the previously stated asymptotic relation, indicating that even a hypothetical  $k_{fuel}$  of infinity would still yield insignificant coping time gains.

Fuel volumetric heat capacity ( $\rho c_{p_{fuel}}$ ) is the most impactful input on coping time as clearly shown in Figure 7-3. The relation is highly linear, indicating that even greater gains could be obtained with still higher  $\rho c_{p_{fuel}}$ . Essentially the fuel acts as a heat sink allowing increased storage of decay heat thereby delaying rises in cladding temperature. While the coping time gain of approximately 45 minutes is the most significant increase of this analysis, it is still of small benefit from a plant operator's perspectives.

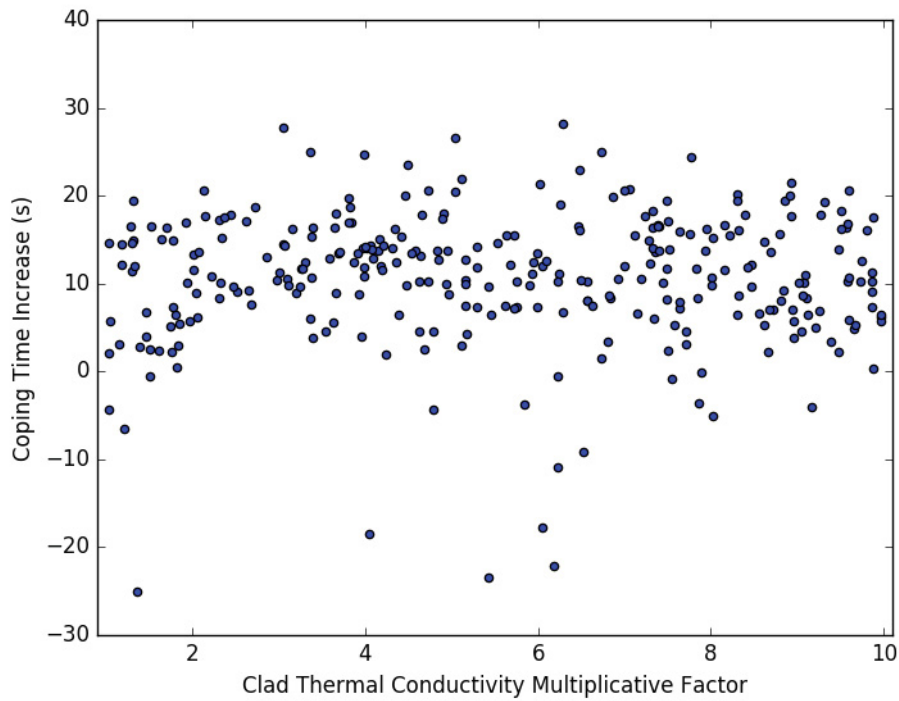
Table 7-2 contains approximate values for  $k_{fuel}$  and  $\rho c_{p_{fuel}}$  for both traditional oxide fuel as well as the ATF fuel materials of uranium silicide and metallic fuel. It should be noted that while both properties are strong functions of temperature and burnup, for the sake of simplicity only the unirradiated values at 600 K are reported here.

While the  $k_{fuel}$  of ATF designs may have over a fivefold increase,  $\rho c_{p_{fuel}}$  shows no improvement. Barring a radically different fuel design involving a deliberate chemical or phase transition, it is highly unlikely that any ATF fuel candidate will ever exhibit an order of magnitude increase in  $\rho c_{p_{fuel}}$ . Thus from a coping time perspective, this analysis confirms previous work (EPRI, 2018) in stating that no significant improvements can be obtained from alternative fuel materials.

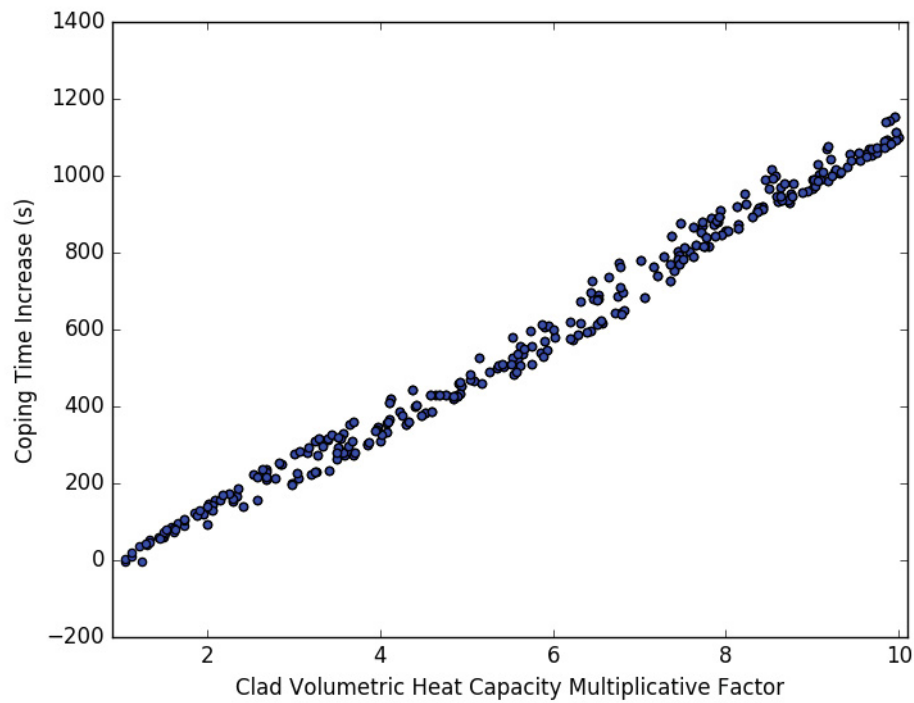
**Table 7-2. Approximate Material Properties for Traditional and ATF Fuel**

<b>Fuel Type</b>	<b>Thermal Conductivity(<math>W/m \cdot K</math>)</b>	<b>Volumetric Heat Capacity(<math>J/cm^3 \cdot K</math>)</b>
Traditional Ceramic Fuel	4 <sup>(1)</sup>	3.0 <sup>(2)</sup>
Uranium Silicide	20 <sup>(3)</sup>	2.6 <sup>(4)</sup>
Metallic Fuel	27 <sup>(5)</sup>	2.6 <sup>(6)</sup>

Note: the data in this table are obtained from (IAEA, 1966) for (1), (Popov, Carbajo, Ivanov, & Yoder, 2000) for (2), (Nelson, et al., 2014) for (3), (Matos & Snelgrove, 1992) for (4), (Takahashi, Yamawaki, & Yamamoto, Thermophysical properties of uranium-zirconium alloys, 1988) for (5), and (Takahashi, et al., 1989) for (6).



**Figure 7-4. Copping Time versus Clad Thermal Conductivity.**



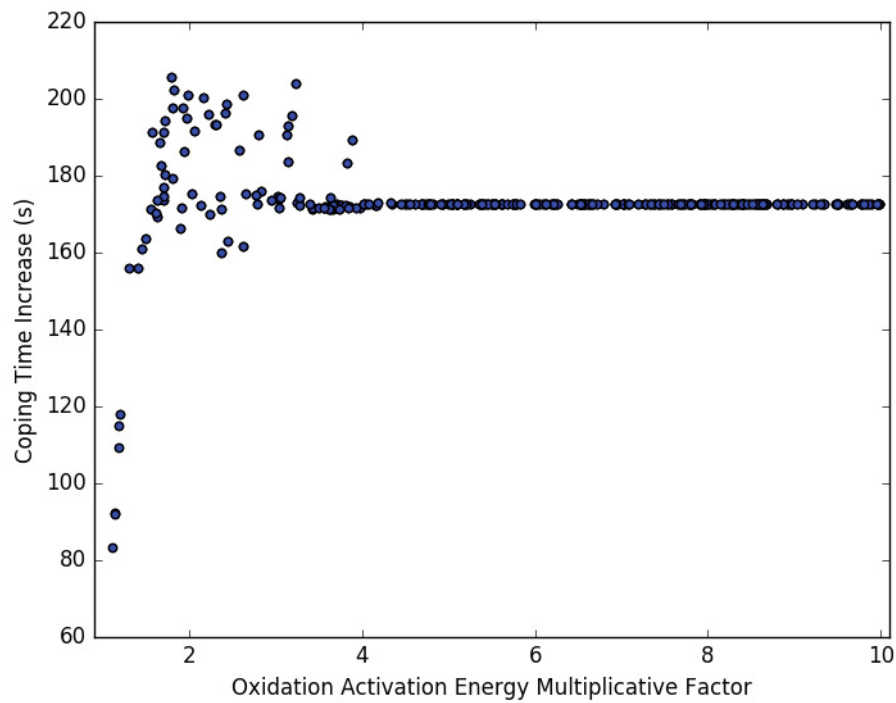
**Figure 7-5. Copping Time versus Clad Volumetric Heat Capacity.**

Figure 7-4 and Figure 7-5 mirror Figure 7-2 and Figure 7-3 though to a lesser magnitude due to the relatively thin clad contributing less thermal resistance and thermal capacitance than fuel. Figure 7-4 shows small serendipitous behavior between  $k_{clad}$  and coping time (i.e. numerical noise), indicating no discernible gains from  $k_{clad}$ . Figure 7-5 indicates a 20 minute gain with the same linear behavior between  $\rho c_{p_{clad}}$  and coping time as seen in Figure 7-3. However as previously stated, these gains are of little benefit to plant operators. Furthermore, the reported material properties for ATF clad candidates shown in Table 7-3 indicate that while an order of magnitude increase in  $k_{clad}$  is feasible, such drastic improvements are not possible for  $\rho c_{p_{clad}}$ .

**Table 7-3. Approximate Material Properties for Traditional and ATF Fuel**

Fuel Type	Thermal Conductivity( $W/m \cdot K$ )	Volumetric Heat Capacity( $J/cm^3 \cdot K$ )
Traditional Zircaloy	12.6 <sup>(1)</sup>	2.1 <sup>(1)</sup>
FeCrAl	15.7 <sup>(2)</sup>	4.5 <sup>(2)</sup>
Silicon Carbide	126.0 <sup>(3)</sup>	3.4 <sup>(3)</sup>

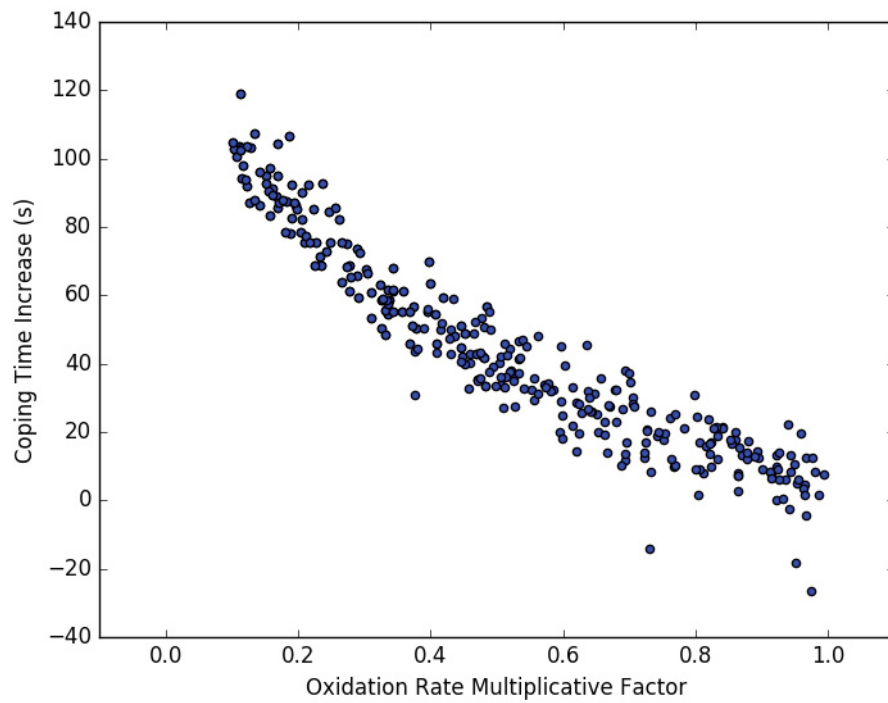
Note: the data in this table are obtained from (Murabayashi, Tanaka, & Takahashi, 1975) for (1), (Field, Snead, Yamamoto, & Terrani, 2017) for (2), and (Nilsson, et al., 1997) for (3).



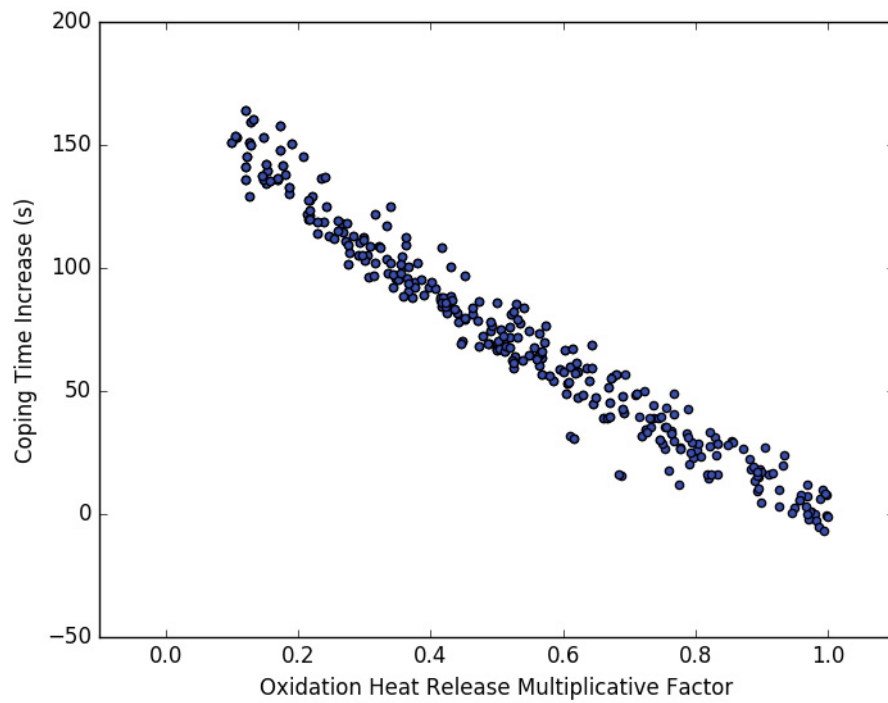
**Figure 7-6. Copping Time versus Clad Oxidation Activation Energy.**

Figure 7-6 reveals that for a hypothetical material immune to oxidation, there is a mere three minute increase in coping time. The coping time relation with oxidation activation energy is asymptotic. This hints that after a threshold of a factor 4 increase in activation energy is reached, effectively no oxidation is formed, resulting in further increases of activation energy having no effect. Investigation of cases with high activation energy confirmed that negligible oxidation forms in said cases. Thus it seems like that all potential advancements in cladding oxidation might not significantly increase coping time.





**Figure 7-7. Copping Time versus Clad Oxidation Rate.**



**Figure 7-8. Copping Time versus Clad Oxidation Heat Release.**

Figure 7-7 shows a negative correlation between coping time and oxidation rate. The trend is somewhat nonlinear most likely due to the exponential nature of the Arrhenius equation governing oxidation. Similarly,

Figure 7-8 shows increases in coping time resulting from decreases in oxidation heat release. Figure 7-8 also establishes that despite the complex phenomena of boil off and run away oxidation, the relation between heat release and coping time is predominantly linear. However the coping time increases resulting from improvements in either oxidation rate or heat release never exceed three minutes. Thus the conclusions from Figure 7-7 and Figure 7-8 mirror those of Figure 7-6, i.e., it seems no significant gains in coping time could be achieved through cladding oxidation reduction.

In conclusion, it seems like that no meaningful increases in coping time during a station blackout could be achieved through improvements in thermal conductivity or volumetric heat capacity of clad or fuel, and no significant gains could be acquired through improvements in cladding oxidation. However, this should not be misinterpreted as ATF being devoid of benefits in an accident scenario. Other figures of merit, such as the total core hydrogen production, are likely more significantly affected by ATF designs. Nevertheless, if an extension in coping time is desired, research and development must focus primarily on advancements at the systems level.

## 8. FUEL PERFORMANCE ANALYSIS

This section presents the fuel performance analysis for the ATF design with the BISON code. ATF fuel rods are designed to have similar or improved behavior in normal operation and provide increased coping time during design-basis accidents. BISON has been developing the capability to model ATF fuel rods, including FeCrAl cladding, Cr-coated cladding and  $U_3Si_2$  fuel. Currently, Cr-coated cladding model is under development by the BISON team. In this report on the ATF fuel modeling and simulations with the BISON code, the focus is on the FeCrAl cladding. In fact, BISON's capability for the FeCrAl cladding includes models for thermophysical properties as a function of temperature, volumetric swelling, and oxidation. Thermophysical properties include the thermal conductivity, specific heat, Young's modulus, Poisson's ratio, yield stress, ultimate tensile strength (UTS), and coefficient of linear thermal expansion. These empirical models are based upon the existing data for the either C35M or APMT<sup>TM</sup> alloy (Gamble & et al., 2017).

During an accident situation of SBO or LOCA, the combination effect of the outward creep deformation of the cladding tube leading to cladding ballooning and the overstress under the effect of internal pressurization and high temperature may eventually drive failure due to burst. Thus, a failure criterion for FeCrAl during transient conditions is required for performance analyses under accident conditions. In order to reliably predict the thermo-mechanical behavior and integrity (deformation and burst) of the full-length nuclear fuel rods during accidents, a more realistic cladding failure criterion model was developed at INL (Gamble & et al., 2017) for BISON. Correspondingly, this novel model will be utilized to study the thermo-mechanical behavior of full-length fuel rods with the FeCrAl cladding.

The traditional cladding of fuel rods is zirconium-based alloys. Models included in BISON are temperature dependent thermal conductivity, specific heat, and young's modulus, thermal and irradiation creep, plasticity, irradiation growth, phase transformation, oxidation, and failure (burst) of Zircaloy-4 (Williamson & et al., 2012). Compared to model thermo-mechanical behavior of fuel rod under normal, steady-state reactor operating conditions, it is significantly more difficult to model accurately thermo-mechanical behaviors of fuel rod under accident scenarios of SBO or LOCA. Such difficulty is due to the increased complexity in the thermo-mechanical response of both the fuel and cladding brought about by transient phenomena involved with high temperature and pressure. In order to capture the complex material response during accident situations, dedicated material models have been incorporated in the thermo-mechanics analysis framework of BISON. These models cover the main physical processes involved and make realistic simulations of SBO or LOCA tests possible. BISON's capability enhancements for accident analysis include models for high-temperature steam oxidation of Zircaloy cladding, crystallographic phase transformation of Zircaloy, high-temperature cladding creep and cladding failure due to cladding burst. In addition, BISON's model of fission gas swelling and release in  $UO_2$  was extended to include a specific treatment of the burst release effect during transients (Pastore & et al., 2017).

With the capability to model thermo-mechanical behaviors of the full-length nuclear fuel rod during accidents for both Zircaloy and FeCrAl claddings, the coping time difference between the FeCrAl-coated fuel cladding ATF design and the conventional fuel cladding design will be obtained through carrying out the BISON code. In this study, to facilitate comparisons between traditional cladding and the proposed accident tolerant FeCrAl cladding, simulations are carried out using FeCrAl and Zircaloy-4 claddings.

In order to analyze the fuel rod base irradiation, all of phenomena involved in  $UO_2$  fuel with FeCrAl and Zircaloy-4 claddings behavior during normal reactor operations need to be modeled first. The final outputs from these simulations will serve as the initial conditions for the followed SBO simulations. In addition, specific models for the complex high-temperature, transient phenomena involved under accident are needed, which are briefed above.

In order to perform a realistic fuel rod analysis for the SBO case, five boundary conditions (BCs) specified as user inputs to control the BISON simulations are the outputs from RELAP5-3D results. The first BC is the power, which is associated with an LWR fuel rod and is typically given as rod averaged linear power (or linear heat rate) in units of W/m given as a function of time. During the SBO, the power is switched into the decay

heat. The power should vary in time and space which leads to the second BC, the axial variation in power. It is given as a scaling factor as a function of distance from the bottom of the rod and time, and it is fixed in the BISON simulations during both normal reactor operation and SBO. Fast neutron flux is the third BC and it is reset to zero during SBO condition. The last two BCs are coolant temperature and pressure, which are as a function of distance from the bottom of the rod and time.

Several preparatory BISON simulations were completed to investigate fuel rod behaviors under normal, steady-state reactor operating conditions and SBO accident conditions. The evolution of the full-length fuel rod behavior during the normal reactor operation is a prerequisite to investigate the SBO and determine the coping time. Figure 8-1 shows the evolution of the full-length fuel rod behavior of a 3-loop operation (~4.5 years) during normal reactor operation of UO<sub>2</sub> fuel with FeCrAl and Zircaloy-4 claddings. As one can see, it seems that under normal operation, fuel behaviors are very similar between the FeCrAl-coated fuel cladding ATF design and the conventional fuel cladding. Meanwhile, the cladding temperature is about same for 17x17 and 15x15 designs. However, the fuel temperature is higher for the 15x15 design; better retention of fission gas with the 17x17 design is observed, probably due to the lower fuel temperature.

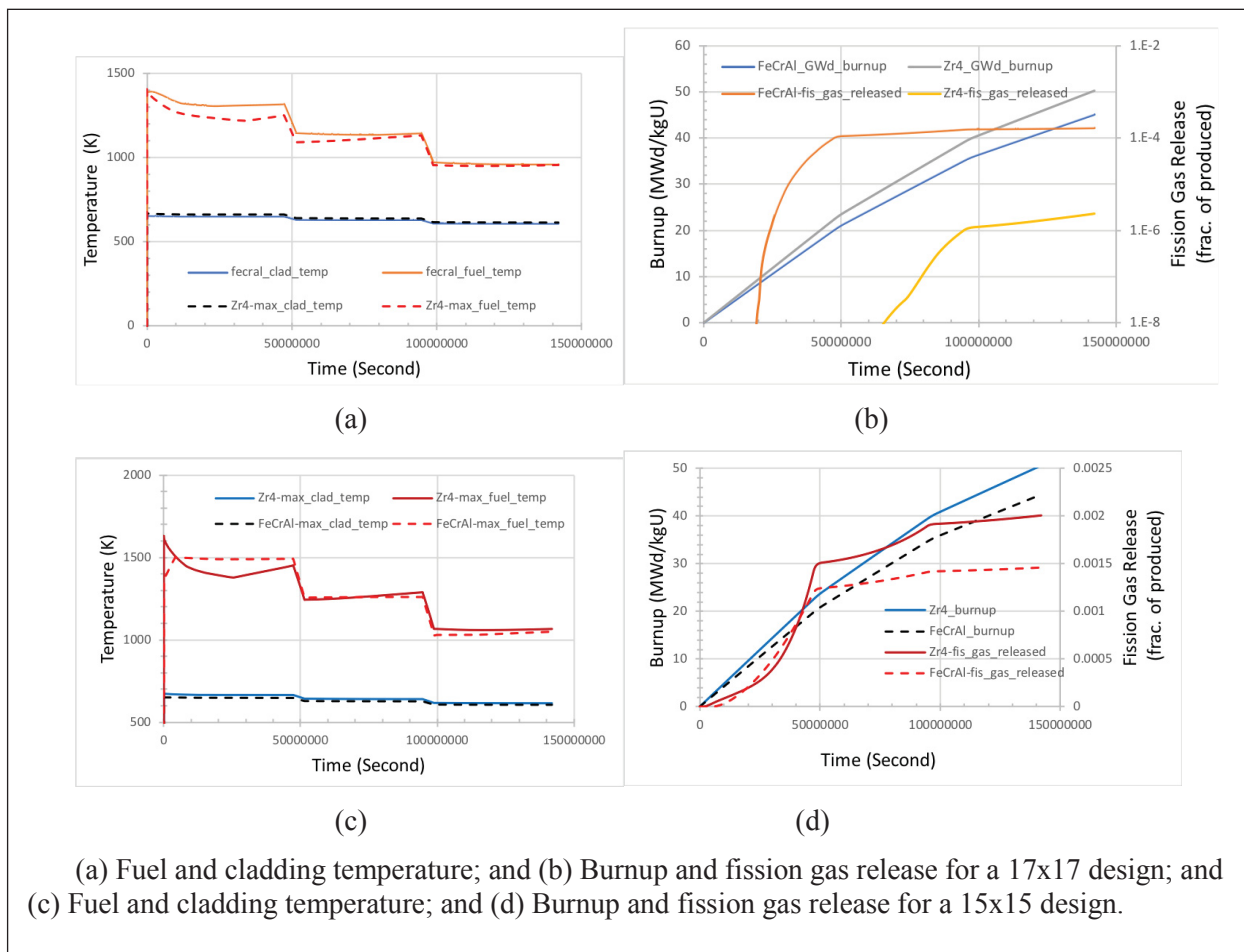
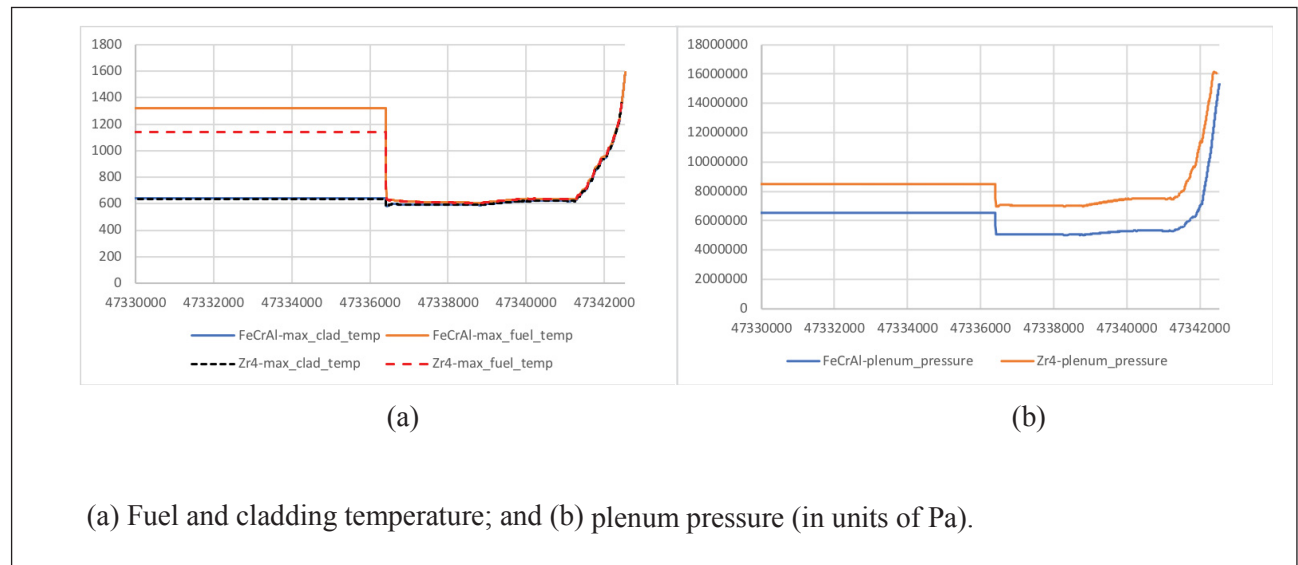


**Figure 8-1. Evolution of the Full-Length Fuel Rod Behavior of a 3-loop Operation (~4.5 years) during Normal Reactor Operation of UO<sub>2</sub> Fuel with FeCrAl and Zircaloy-4 Claddings.**

Figure 8-2 shows the evolution of the full-length fuel rod behavior for the postulated SBO accident scenario after 1st-loop normal operation (~1.5 years) for the 17x17 design. Our BISON simulation results indicate that it is unlikely able to reach the cladding melting temperature before the cladding failure. Meanwhile the fuel temperature drops rapidly as SBO starts. As shown in Figure 8-2(a), cladding and fuel temperatures are about same during SBO. The coping time is purely determined by the time when the cladding is melted, and the

cladding temperature is directly controlled by the coolant temperature as the user input from REALP-5 boundary conditions. With the identical coolant temperature as a function of time, and a higher melting temperature of Zircaloy-4 cladding (~1850 C) than that of FeCrAl cladding (~1500 C), it is expected that FeCrAl cladding will have shorter coping time. Alternately, as shown in Figure 8-2(b), the plenum pressure is higher with the Zircaloy-4 cladding, thus it may be taken as an indicator of failure. Qualitatively, the coping gain from FeCrAl cladding is about 200 seconds, through the estimation the time difference between two claddings when the plenum pressures reach 12, 14, and 16 MPa. A more realistic cladding failure criterion model due to the burst developed at INL is being utilized in this study. The detail will be reported in the near



future.

**Figure 8-2. Evolution of the Full-Length Fuel Rod Behavior from Normal Reactor Operation to SBO after the First-Loop Operation (~1.5 years) during Normal Reactor Operation of UO<sub>2</sub> fuel with FeCrAl and Zircaloy-4 Claddings for a 17x17 design.**

The above preliminary BISON analysis results show that the evolution of the full-length fuel rod behavior is mainly determined in terms of cladding/coolant temperatures under the postulated SBO accident scenario. It is probably more realistic to use cladding failure criterion due to the cladding burst to determine the coping time, rather than the clad melting temperature. Ultimately predict the time to cladding burst failure is closely related to the coping time during an SBO accident.

## 9. RESILIENCE ANALYSIS FOR LONG-TERM SBO SCENARIOS

### 9.1 Overview of This Section

Analyses presented in earlier sections of this report have discussed the benefit of ATF in delaying the onset of core damage when core cooling is lost. Those analyses show that the benefit of specific ATF types in long-term blackout is modest, in the sense that neither of the ATF forms analyzed extend the time available for AC recovery by very much: the additional time interval made available by ATF is small compared to the time scales on which recovery is likely in the scenarios of interest here (long-term station blackout). In the present section, the plant resilience discussion therefore focuses on accomplishing the core cooling function despite the blackout, rather than on the ability of ATF to survive without core cooling.

The following discussion is based on two reports:

1. “State-of-the-Art Reactor Consequence Analyses Project / Volume 2: Surry Integrated Analysis” (NRC, 2012), hereafter “the SOARCA report,” and
2. “Diverse and Flexible Coping Strategies (FLEX) Implementation Guide” (NEI, 2016).

The SOARCA report analyzed a few variants of long-term station blackout scenarios including credit for FLEX equipment. As suggested by the full name of that project, quoted above, the purpose of that report was to present representative Consequence analyses, not to analyze specific designs in detail, or present justifiable accident frequency assessments, and the analyses were done for a specific plant (Surry). The NEI document presents generic FLEX “implementation guidance,” including pointers to where plant-specific analysis will be necessary. Both reports make interesting points about coping ability under blackout conditions.

### 9.2 Comparison of Success Strategies

#### 9.2.1 The SOARCA Analysis for Long-Term SBO

Excerpt from the SOARCA report:

In summary, the following actions are credited in the mitigated scenario calculations:

- Provide vessel injection using a portable, high-pressure, diesel driven (Kerr) pump through three drain lines on the low head safety injection (LHSI) piping
- Use portable air bottles to operate the steam generator power operated relief valves, which allows for depressurization and cooldown of the RCS
- A portable power supply is used to restore SG and RCS level indication
- Manual operation of the TDAFW pump without DC power is credited
- A portable, diesel driven, low-pressure (Godwin) pump is used to supply water to the fire header. The firewater can then be supplied via fire hose to the AFW pumps.

While not used in the mitigated scenario calculations, the following additional mitigative measures were identified as additional options for consideration.

- Use firewater or pumper truck for cooling the charging pump oil cooler
- Use an alternative power source for high-head safety injection pump RCS makeup.

Observations:

1. In its analysis of long-term blackout scenarios, the SOARCA report considers RCS heat removal through the secondary, using either the turbine-driven AFW pump or a portable pump.
2. If RCS leakage is not zero, then it will eventually become necessary to furnish RCS makeup in order to maintain core cooling. However, the time scale on which makeup is required depends on the leakage

rate, which depends on the effective leak size and on the degree to which the plant is cooled down by heat removal through the secondary.

- If RCS leakage is very small, then power recovery within some hours is soon enough to provide makeup with normal plant systems.
- If leakage is somewhat greater, and power is not recovered, it is necessary to furnish makeup from a portable pump (in the SOARCA report, which mentioned, but did not analyze, providing alternate power to an existing high-pressure system). In order to inject with the portable pump discussed in the SOARCA report (the “Kerr” pump), it is additionally necessary to depressurize the primary to a pressure at which that pump can inject. This is done by depressurizing the secondary, taking care to maintain secondary pressure above the pressure needed to maintain steam pressure for the turbine of the TDP (said to be 150 psi). MELCOR analyses done for the SOARCA report show that if the plant is cooled down in this way, the seal leakage itself reduces significantly, and the Kerr pump easily maintains RCS coolant level.

In short: analyses done for the SOARCA report addressed a range of possible RCP seal leak rates. The results indicate that if:

- Secondary cooling is maintained by
  - Injecting to the steam generators using the TDAFW

**OR**

  - Injecting to the steam generators using a portable (“Godwin”) pump

**AND**
- Primary inventory is maintained by minimizing leakage, and/or
  - Recovering AC and injecting to the RCS with CVCS or HPI

**OR**

  - Absent AC, providing makeup from some other source (e.g., the diesel-driven “Kerr” pump), depending on magnitude of RCP Seal leakage
    - If the leak is small, then (*especially if the plant is cooled and depressurized*) the initial inventory is adequate for a long time without makeup
    - Injecting to primary with Kerr pump to make up for RCS leakage
      - Need to depressurize the primary to where Kerr pump can inject; this is done by cooling down the primary by depressurizing the secondary

then the core is protected for a long time. The SOARCA report stresses the benefit of reduced RCP seal leakage that results from the depressurization.

These findings are summarized notionally in the figure below.



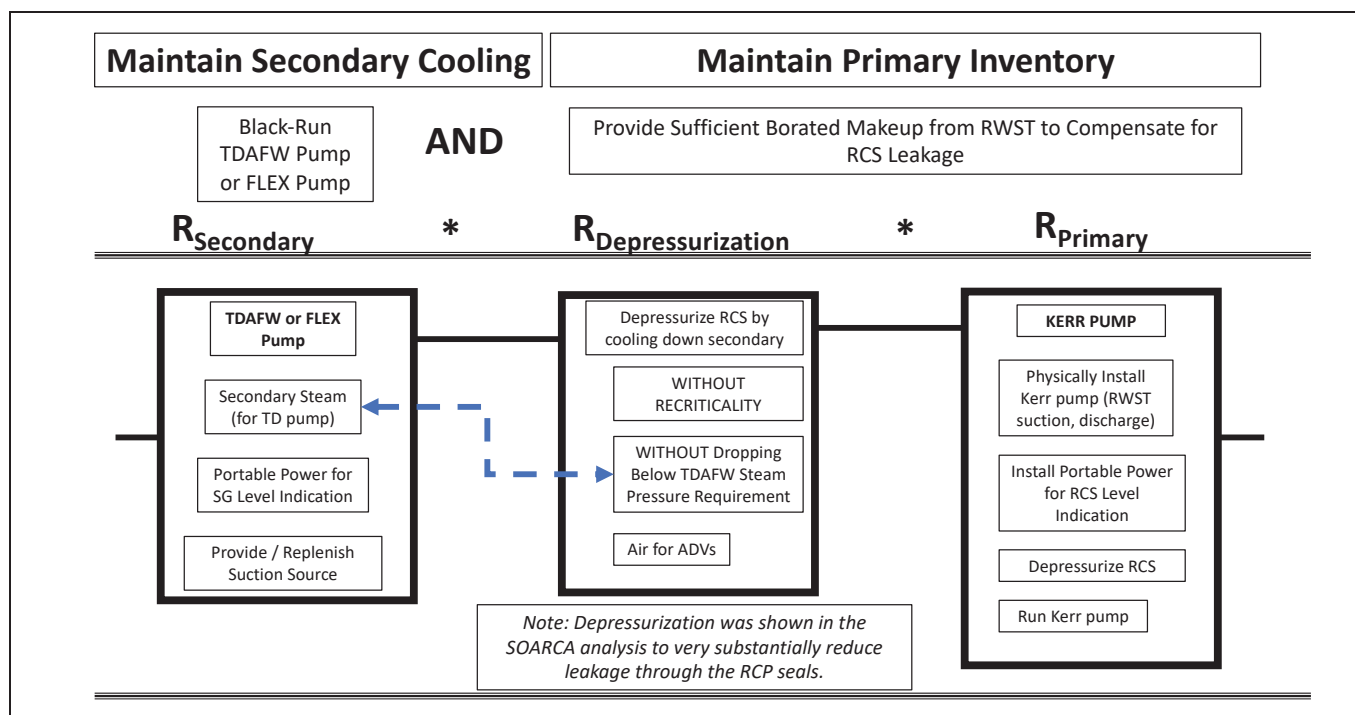


**Figure 9-1. The SOARCA Report Success Path(s), Viewed in Reliability Block Diagram Format.**

Limiting the leakage rate could be done by any of several means. Unlike the NEI guidance document, discussed further below, the SOARCA report does not stress inherently low-leakage seals (although it analyzes a range of seal leak rates); but it does stress the leakage-reduction benefits of the depressurization that is needed anyway, in order for the Kerr pump to operate (it cannot inject against normal RCS pressure). This relationship is noted in the above figure. There is also a two-way arrow connecting “Secondary Steam” under the TDAFW block to “Depressurize” in the Leak Rate block; excessive depressurization would affect the operability of the TDAFW.

This two-way arrows means that the blocks are not strictly independent of each other, even if there were no other relationships; but there ARE other relationships. This makes overall reliability considerations slightly more complicated than they would be if the blocks were all independent. For example, all three blocks depend heavily on operator action, which is in turn affected by operators’ ability to access the places where they need to carry out the implied actions.

Although the SOARCA report does not stress the need to borate, the RCS injection modeled in the SOARCA report is from the RWST, and is therefore borated. However, the FLEX pump modeled (the Kerr pump) cannot inject against normal RCS pressure, so RWST water is only injected after a very significant plant cooldown has taken place in order to depressurize the RCS. Depressurizing the RCS has the further benefit of bringing accumulator inventory into play.

Before the accumulators inject, does this cooldown induce recriticality? Would this matter, even if it occurred? The SOARCA report does not discuss this. We have not established whether considering boration explicitly would change anything in the SOARCA analysis for Surry; and, as remarked in the NEI report, the need for boration is potentially quite plant-specific.



## 9.2.2 NEI Guidance for Long-Term SBO

The NEI document, being generic, does not analyze specific FLEX pump types, but otherwise paints a somewhat similar picture: it addresses heat removal and the need to maintain RCS inventory. Interesting differences from the SOARCA report are that the NEI document (a) places more stress on trying to minimize RCS leakage through seal technology, and (b) repeatedly cites a need to think about boration in the long term (while noting that the issue is plant-specific).<sup>3</sup> [A PWR would normally borate as part of its cooldown.]

The picture from the NEI guidance in Table D-1 of their report can be summarized as follows:

- Secondary cooling is maintained by
  - Injecting to the steam generators using the TDAFW

**OR**

  - Injecting to the steam generators using a portable pump

**AND**
- Primary inventory is maintained by
  - Reducing or eliminating RCS leakage (avoid RCP seal LOCA and other leakage paths)

**AND/OR**

  - Getting portable AC power to CVCS in order to make up for inventory loss

**AND/OR**

  - If CVCS is not restored, providing makeup from some other source if necessary, depending on magnitude of RCP Seal leakage

**AND**
- Maintain appropriate boration
  - ...

---

<sup>3</sup> “RCS makeup capability is assumed to be required at some point in the extended loss of ac power condition for inventory **and reactivity control**.” [emphasis added]

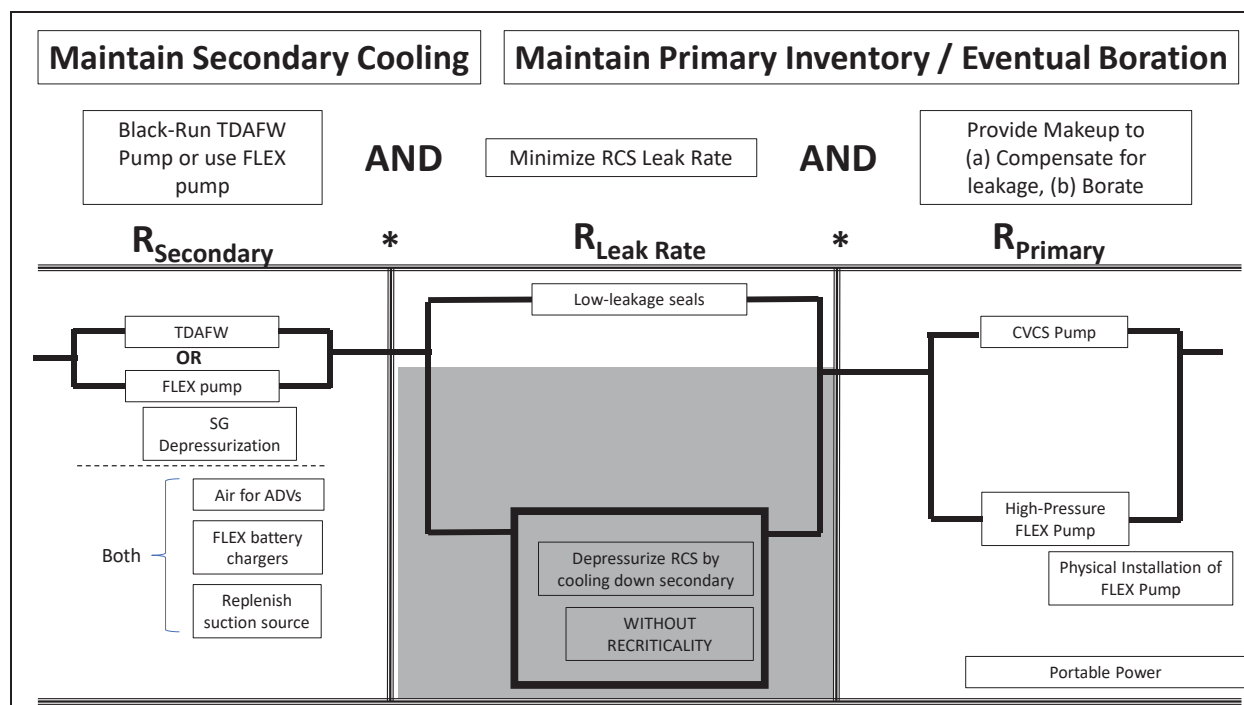


**Figure 9-2. A notional description of the NEI Table D-1 guidance, viewed in Reliability Block Diagram format.** The dark shading under  $R_{\text{Leak Rate}}$  corresponds to items that are not discussed in the NEI report, but are shown here for comparison purposes

For RCS makeup, the NEI report does not discuss use of a *low*-pressure FLEX pump, which would require RCS depressurization; but it does mention use of a *high*-pressure FLEX pump for RCS makeup, and in fact contemplates allowing for both pumps (plant high-pressure pump AND FLEX pump).

## 9.3 Comparison

For present purposes, we will limit the discussion to reliability considerations, although other considerations (such as cost) surely bear on the decision process.

Given two precisely specified success paths, and the needed reliability parameters, we can quantify their success probabilities, and simply compare them. However, a slightly better perspective is afforded by considering the overall benefits of combinations of success paths. A useful way to think about this uses the concept of “Prevention Worth” (PW). PW is introduced briefly below, after which the benefits of various approaches are discussed.

### 9.3.1 Prevention Worth

In order to think semiquantitatively about the capability afforded by combinations of different strategies, it is useful to consider the concept of Prevention Worth (PW). The PW of a collection of success paths is the success probability of the union of those paths: that is, the probability that at least one of them will succeed in a given challenge. For some purposes, it may be useful to consider the PW of a particular component (say, component  $i$ ). Then

$$PW^i = P(\cup_j MPS_j^i) \quad (10)$$

where

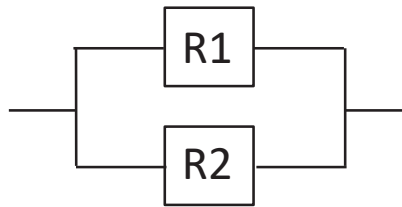
$MPS_j^i$  is the  $j$ th minimal path set containing component  $i$ .

Since success probabilities tend to be of order unity, it is useful to revert to a tradition within the reliability community, and think in terms of the number of “nines” of reliability provided by a particular collection of success paths:

$$NINES(PW) = -\log_{10}(1 - PW) \quad (11)$$

For example, a success path having success probability 0.9990 has a “NINES” index of 3: it provides 3 nines of reliability.

If we have two success paths, and we wish to compare the reliability of just those two paths, we do not need a concept like PW: we can just calculate the two path reliabilities and compare them. But PW is useful if we consider having functional redundancy (multiple success paths) within a plant, and we wish to consider the worth of being able to credit *combinations* of success paths. For example, consider

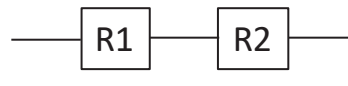


This configuration succeeds if either block (either path) succeeds. Denoting the success probability of block  $i$  by  $R_i$ , applying the usual formula for probability of an “OR”, and assuming independence between the two blocks, we have that the success probability (the reliability) of the configuration is

$$R_1 + R_2 - R_1 * R_2.$$

Taking for example  $R_1 = 0.9 = R_2$ , we have that the probability of the configuration is 0.99, having a NINES index of 2. This illustrates that when the blocks are independent, the NINES index is additive.

The reliability of a path comprising two blocks in series,



is given by  $R_1 * R_2$ , where  $R_i$  is the reliability of block  $i$ , and it is assumed that the two blocks are completely independent. Path reliability is reduced by addition of things that need to work in order for the path to succeed.

### 9.3.2 Comparison

Above, mention was made of different methods of injecting to the secondary, different methods of injecting to the RCS, and different methods for limiting RCS leakage. Where do we get the greatest reliability benefit?

Answering such a question definitively would call for access to highly plant-specific details that are not available to this project.

However, assuming that the hardware involved is within its usual operating envelope, and that there is no conceptual flaw in the design of the strategies (wrong hardware provided to install pumps, ...), it is likely that the dominant influences on success path reliability will be related to the success probability of the human actions needed to align the necessary pumps, support systems, instrumentation, and so on. These are actions that

- are not commonly performed;

- (if needed) may be required to be executed under unusual time constraints;
- (if needed) are performed under the stress associated with being in an extended station blackout scenario, performing an ad hoc installation of what may be the plant's last hope.

The “SPAR-H” model is a widely-used framework for scoping analyses of human reliability, partly because it is simple enough to apply that it lends itself to parametric analysis of failure probability as a function of various performance shaping factors.

As a scoping exercise, let us apply SPAR-H to the action of installing a FLEX pump. To “do” SPAR-H, one specifies “diagnosis,” “action,” or both, and decides on the performance shaping factors. For this purpose, we assume that no “diagnosis” is necessary, only “action;” the action analyzed is to install the pump and get it running. SPAR-H assumes a failure probability of 1E-3 for a generic “action,” and modifies that probability with multipliers that are associated with assessed performance-shaping factors.

This is illustrated below for an “action” with conservative extremes assigned for several performance shaping factors. One sees that the result is a failure probability of 0.6.

**Table 9-1. SPAR-H for a Conservatively-Assessed “Action”**

<u>DESCRIPTION/ SHAPING FACTOR</u>	<u>DISTRIB. TYPE/ PSF</u>	<u>PROBABILITY/ %</u>	<u>MULTIPLI ER</u>
<b>INSTALL FLEX PUMP (CONSERVATIVE ASSUMPTIONS)</b>	<b>Point Value</b>	<b>6.000E-1</b>	
Diagnosis is not Modeled			
Action is Modeled		Nominal Value	1.000E-3
Available Time	Just enough time	100%	1.000E+1
Stress/Stressors	High	100%	2.000E+0
Complexity	Moderately complex	100%	2.000E+0
Experience/Training	Low	100%	3.000E+0
Procedures	Available, but poor	100%	5.000E+0
Ergonomics/HMI	Nominal	100%	1.000E+0
Fitness for Duty	Nominal	100%	1.000E+0
Work Processes	Nominal	100%	1.000E+0
Negative factor adjustment		PSF Total	6.000E+2

Compare the above with a less-conservatively assessed action illustrated below in Table 9-2. The result is then a failure probability of 4E-3, worse than the “nominal” value of 1E-3, but much improved relative to the 0.6 value obtained above. One of the key differences is the “available time” factor. In a given scenario, the time actually *available* is determined by the phenomenology; but the time that the action will actually *need* is a function of how well the needed action has been designed. If it is convenient to install the FLEX pump, this will

have an enormous effect on the assessed error probability relative to a pump-installation task that is barely possible (or worse) in the available time. Another important difference between the two tables is the “experience / training” factor. Competent people who have not had a chance to practice an unusual *ad hoc* installation cannot be expected to succeed at the same rate as competent people who have practiced the installation.

Given the complexity of the human actions that are needed in all strategies discussed, the benefits of crediting redundant success paths for coping would need to be analyzed carefully. Even though the hardware involved might be distinct, some of the same factors would operate on all of the actions.

A performance-shaping factor not included in this model is operator “reluctance.”<sup>4</sup> This refers to a situation in which the procedures clearly mandate a particular action, but the operators are aware that the action has a significant downside, and there are real or imagined reasons for the operators to hope that the action will turn out not to have been necessary in the specific event. A famous case of this is the decision not to initiate feed-and-bleed cooling during the 1985 loss-of-feedwater event at Davis-Besse. In that event, secondary feed was eventually re-established, but the plant procedures had called for feed-and-bleed before secondary cooling was restored. It is not obvious why there would be this sort of reluctance to install a needed pump; but if the drastic cooldown needed for the FLEX action discussed in SOARCA will have adverse downstream consequences for plant operation, it may be worth asking whether reluctance might affect the success probability of that action.

**Table 9-2. SPAR-H for a Less Conservatively Assessed “Action”**

<u>DESCRIPTION/ SHAPING FACTOR</u>	<u>DISTRIB. TYPE/ PSF</u>	<u>PROBABILITY / %</u>	<u>MULTIPLIER</u>
<b>INSTALL FLEX PUMP (ARGUABLY OPTIMISTIC ASSUMPTIONS)</b>	<b>Point Value</b>	<b>4.000E-3</b>	
Diagnosis is not Modeled			
Action is Modeled		Nominal Value	1.000E-3
Available Time	Nominal time	100%	1.000E+0
Stress/Stressors	High	100%	2.000E+0
Complexity	Moderately complex	100%	2.000E+0
Experience/Training	Nominal	100%	1.000E+0
Procedures	Nominal	100%	1.000E+0
Ergonomics/HMI	Nominal	100%	1.000E+0
Fitness for Duty	Nominal	100%	1.000E+0
Work Processes	Nominal	100%	1.000E+0
Dependency is not Modeled			

<sup>4</sup> See, for example, “Good Practices for Implementing Human Reliability Analysis (HRA) / Final Report,” NUREG-1792 (USNRC, 2005).

## 9.4 Summary

According to the SOARCA report and the NEI document, the capability exists to provide core cooling even in extended SBO.

However, the actual reliability of this capability remains to be demonstrated. Very significant operator actions are needed in order to assure adequate cooling and (barring zero-leakage seals) adequate boric acid inventory. Assuming that the design of the equipment configuration to be used during blackout is sound, and that the hardware, once connected, is reasonably reliable, conventional human reliability analysis will conclude that the failure probability of the strategy, taken as a whole, is dominated by human performance under difficult conditions, barring very significant prior preparations to make the needed actions straightforward, adequately rehearsed, and so on. Even then, the time available will be set by the plant and the initial conditions.

### Secondary Cooling

In SBO, secondary cooling is needed, and there seems to be little variation in the consideration of methods for performing that function. If it is practical to make the needed arrangements to operate the TDAFW, this is apparently simpler than installing a FLEX pump, but all success paths discussed in this section need one or the other, and significant operator action is required either way.

### Minimizing RCS Leakage

Unless RCS leakage is effectively zero, makeup to the RCS will eventually be needed, and it is not trivial to do this in a blackout. Therefore, there are significant benefits to reducing RCS leakage as much as possible. RCP seals are not necessarily the only source of leakage, but in an SBO, they may be an important source. The NEI document strongly recommends looking for ways to reduce RCP seal leakage (Table D-1):

Extended coping without RCS makeup is not possible without minimal RCS leakage. Plants must evaluate use of low leak RCP seals and/or providing a high pressure RCS makeup pump.

The first sentence is not insisting that RCS leakage is necessary; it is presumably saying that the leakage must be minimal if coping is to succeed without makeup. From the point of view of the analyses discussed in this report, “low leak RCP seals” would qualify as a very significant enhancement, where they do not already exist. Over the years, different seal package characteristics have been discussed in this context.

The SOARCA analysis actually showed that leakage is reduced very considerably if the pressure in the RCS is significantly reduced. Others have reached a similar conclusion.<sup>5</sup> This is discussed further in Table 9-3.

Since human performance probably limits the PW of any SBO coping strategies formulated so far, reducing the demands placed on the operators during the SBO seems like a good tactic. Of the strategies listed above, the low-leakage seals do the best job of that.

Once the necessary steps are taken to assure secondary cooling, and ADV operation, RCS depressurization at least does not require much more hookup; but the consequences of such rapid cooling for subsequent plant operation were not discussed in the report consulted.

---

<sup>5</sup> For example, see [Andrej Prošek](#) and [Leon Cizelj](#), “Long-Term Station Blackout Accident Analyses of a PWR with RELAP5/MOD3.3,” Science and Technology of Nuclear Installations Volume 2013, Article ID 851987.

**Table 9-3. Methods for Reduction of RCP Seal Leakage**

<b>Characteristics of RCP Seal Leakage Rate Reduction Strategies</b> <i>Note: Reducing Leakage Rate Reduces Demand for Makeup (but not necessarily for boration...)</i>	
<b>Leak Rate Reduction Strategy</b>	<b>Characteristics / Comments</b>
RCP Seals that leak only minimally, even without injection or cooling	Not yet deployed universally
Depressurization (substantially reducing pressure on secondary side in order to reduce pressure on primary side)	<ul style="list-style-type: none"> <li>• Requires secondary cooling</li> <li>• Requires supports for SG pressure indication, and for operating the ADVs</li> <li>• Has to be done in a certain time window</li> <li>• Could increase demand for boration</li> <li>• Should avoid interfering with steam supply to TDAFW</li> <li>• In the SOARCA study, depressurization has significant benefits in reduction of leakage rate</li> <li>• Plant implications of rapid cooldown not addressed</li> </ul>
Seal injection	Normally provided by CVCS, which is not available in SBO unless steps are taken to make it so (portable power, ...). If we are going to use CVCS for inventory maintenance, can we use it for seal injection as well?

#### RCS Makeup and Boration

As noted above, RCS makeup will be needed on a time scale determined by the leakage rate. If leakage is very small, there may be enough time available to recover offsite power, but if the leakage rate is higher, makeup will be needed during blackout conditions. There are significant constraints on supplying RCS makeup in a blackout:

1. the RCS is at high pressure, so either the injection must be at high pressure, or the RCS has to be depressurized, or some combination of both; and
2. the water injected needs to be borated.

The SOARCA document, which focused on Surry, contemplates a mode of RCS makeup that uses a pump that operates at a discharge pressure much lower than normal RCS pressure; this is enabled by depressurizing the secondary very significantly.

Table D-1 of the NEI document contemplates high-pressure makeup, and stresses the point that it needs to be borated. Late in Table D-1, mention is made of depressurization to access the inventory available in the accumulators, but there is no discussion in the NEI document of low-pressure-pump RCS makeup enabled by depressurization.

**Table 9-4. Different Strategies for RCS Makeup**

<b>Possible Discriminators Affecting Reliability of Different Strategies for RCS Makeup</b>	
<b>Kerr Pump Strategy</b>	<b>CVCS Pump Strategy</b>
Pump is diesel-powered, needs fuel	Needs Portable AC Power Hookup
Pump needs to be installed: both suction and discharge	Pump is already installed
Needs level indication	Needs level indication



## 10. SUMMARY AND FUTURE WORK

This report documents the activities that investigate integrated evaluation approaches that combine the plant PRA models with multi-physics best estimate analyses and perform detailed risk and benefit assessments of introducing ATF and FLEX into current nuclear power plants to achieve both safety and operational performance enhancements. Risk analysis was conducted for the FeCrAl and Cr-coated cladding design impact on a generic Westinghouse 3-loop PWR for postulated SBO and LBLOCA accident scenarios using SAPHIRE, RELAP5-3D, and RAVEN codes.

For SBO, the RELAP5-3D simulations estimate only marginal increase of the coping time with FeCrAl and Cr-coated in most SBO scenarios, from about several minutes in short term SBO to about twenty minutes in long term SBO with a battery life of 4 hours. The maximum increase of the coping time is 1 hour in long term SBO with a battery life of 8 hours for FeCrAl. The timing to core damage is dictated by the timing of the core uncover, the decay power level and the oxidation kinetics. FeCrAl is showing here some slight advantage on Cr-coated.

With only marginal increase of the time to core damage with the FeCrAl and Cr-coated designs, the risk benefit on behalf of the CDF as the risk metrics would be very small. A simplified approach using a multiplication factor is developed in this report to estimate the risk impact of the ATF design with the small increase of the coping time, which show that the marginal coping time increase would lead to about 4% and 2% CDF reductions for the FeCrAl and Cr-coated designs, respectively. However, this should not be misinterpreted as that ATF brings no risk benefits. Actually the hydrogen production with ATF is one or two order of magnitude lower than the Zircaloy clad. And the timing to release significant hydrogen production (0.5 Kg) with ATF is about 0.5 hour to 1.5 hours later than that with Zircaloy.

Coupled calculations of RELAP5-3D and RAVEN were conducted for evaluating the effects of aleatory uncertainties on the SBO accident. RAVEN was used to perturb selected parameters of RELAP5-3D input deck and to derive Limit Surfaces (LS) for different cases. The LS calculations provided a qualitative and quantitative assessment of the change of CDF and they highlighted the slight improvements derived from the ATF introduction for the PWR SBO accident.

For LBLOCA, a dynamic PRA analysis was performed by coupling RELAP5-3D and RAVEN with the scope of identifying the safety impact of ATF from a PRA perspective. We were able to identify few accident sequences where ATF was able to withstand the loss of cooling without reaching code damage condition.

An investigation of other analysis approaches for the ERP was performed for the project. For example, risk-informed plant enhancement analysis uses a risk informed approach to analyze potential design changes that could enhance the plant operation safety with minimum economy burdens due to the changes. SBO model was used as a case study for the analysis.

Risk-informed sensitivity analysis used one at a time methods to obtain a qualitative understanding of the relations between coping time increases and various fuel cladding material properties. The selected inputs include thermal conductivity and volumetric heat capacity for both fuel and cladding, as well as the cladding side oxidation parameters of activation energy, rate, and heat release. The analysis concludes that it seems like that no meaningful increases in coping time during a station blackout could be achieved through improvements in thermal conductivity or volumetric heat capacity of clad or fuel, and no significant gains could be acquired through improvements in cladding oxidation. Other figures of merit, such as the total core hydrogen production, are likely more significantly affected by ATF designs.

Fuel performance analysis using the BISON fuel performance code was conducted for SBO scenario. It is suggested that the evolution of the full-length fuel rod behavior is mainly determined in terms of cladding or coolant temperatures. Though the clad melting temperature may be a direct indicator of the failure of fuel rods, our results from BISON modeling and simulations strongly suggest that it is probably more realistic to use cladding failure criterion due to the cladding burst to determine the coping time. In the future, it is desirable to carry out more extensive investigations of thermo-mechanical behavior of fuel rod under accident scenarios, including the effect of high burnup with different fuel rod designs, and cladding failure due to the cladding



burst. Compared to fresh or lightly irradiated fuel rods, further complexities are arisen at the time of the accident with high burnup. These, for example, include the degraded fuel thermal conductivity such as related to the highly porous rim structure in the edge of high burnup pellets and the presence of released low-conductivity fission gas in the rod plenum and fuel-cladding gap, which both will eventually exacerbate cladding heat-up during an accidental transient. In addition, a pre-oxidized cladding will also increase the cladding temperature due to the additional thermal resistance and affect the cladding's mechanical properties as well.

For the future work, we plan to

**FY 2019:**

- Perform ERP risk analyses for selected PWR accident scenarios such as loss of feedwater, steam generator rupture
- Develop LERF model for the existing generic PWR SAPHIRE model and perform ERP LERF analyses for selected PWR accident scenarios
- Perform human reliability analysis for FLEX and develop FLEX risk models
- Continue the investigation of the risk-informed plant enhancement analysis
- Continue the fuel performance analysis for ATF
- Benchmark the ATF TH and risk impact analysis results

**FY 2020 and beyond:**

- Develop generic BWR SAPHIRE Level 1 model and perform ERP risk analyses for selected BWR accident scenarios such as SBO, LOCA, loss of feedwater, steam generator rupture
- Develop LERF model for the generic BWR SAPHIRE model and perform ERP LERF analyses for selected BWR accident scenarios
- Develop enhanced resilient plant systems analysis framework for long-term ATF concepts

## 11. REFERENCES

- Aldemir, T. (2013). A Survey of Dynamic Methodologies for Probabilistic Safety Assessment of Nuclear Power Plants. *Annals of Nuclear Energy*, 52, 113-124.
- Aldemir, T., & et al. (2010). Probabilistic Risk Assessment Modeling of Digital Instrumentation and Control Systems using Two Dynamic Methodologies. *Reliability Engineering and System Safety*, 95, 1011–1039.
- Alfonsi, A., Rabiti, C., Mandelli, D., Cogliati, J., Wang, C., Talbot, P. W., . . . Smith, C. L. (2017). *RAVEN Theory Manual and User Guide*. Idaho National Laboratory. Idaho Falls: Idaho National Laboratory.
- Altman, N. S. (1992). An Introduction to Kernel and Nearest-Neighbor Nonparametric Regression. *The American Statistician*, 46:3, 175-185.
- ASME and ANS. (2013). *Addenda to ASME/ANS RA-S-2008 Standard for Level 1/Large Early Release Frequency Probabilistic Risk Assessment for Nuclear Power Plant Applications*. ASME and ANS.
- Bayless, P. D. (1987). *Natural Circulation during a Severe Accident: Surry Station Blackout*. EG&G. Idaho Falls: EG&G.
- Bragg-Sitton, S. (2014). Development of Advanced Accident Tolerant Fuels for Commercial LWRs. *Nuclear News*(83).
- Cathcart, J. V., & et al. (1977). *Reaction Rate Studies, IV, Zirconium Metal-Water Oxidation Kinetics*.
- Dominion. (2007). *Surry Power Station Units 1 and 2. Updated Final Safety Analysis Report. Rev. 39*. Virginia Electric and Power Company (Dominion). Washington, DC: US NRC.
- Eide, S., Gentillon, C., Wierman, T., & Rasmuson, D. (2005). *Reevaluation of Station Blackout Risk at Nuclear Power Plants - Analysis of Loss of Offsite Power Events: 1986-2004*. Nuclear Regulatory Commission.
- EPRI. (2012, April 16). *Modular Accident Analysis Program: A Software Toll for Analyzing Nuclear Plant Accident Scenarios*. Electric Power Research Institute. Retrieved April 16, 2018, from <https://www.epri.com/#/pages/product/000000000001025795>
- EPRI. (2018). *Accident Tolerant Fuel Technical Update*. Electric Power Research Institute.
- Federal Register. (1995). *Use of Probabilistic Risk Assessment Methods in Nuclear Activities: Final Policy Statement*. Washington, DC: Federal Register.
- Field, K. G., Snead, M. A., Yamamoto, Y., & Terrani, K. A. (2017). *Handbook on the Material Properties of FeCrAl Alloys for Nuclear Power Production Applications*. Oak Ridge National Laboratory, Nuclear Technology R&D.
- Gamble, K. A., & et al. (2017). An investigation of FeCrAl cladding behavior under normal operating and loss of coolant conditions. *Journal of Nuclear Materials*, 491, 55-66.
- Gaston, D., Hansen, G., & Newman, C. (2009). MOOSE: A Parallel Computational Framework for Coupled Systems for Nonlinear Equations. *International Conference on Mathematics, Computational Methods, and Reactor Physics*. Saratoga Springs, NY: American Nuclear Society.
- Gauntt, R. O., Cash, J., Cole, R. K., Erickson, C. M., Humphries, L., Rodriguez, S. B., & Young, M. F. (2005). *MELCOR Computer Code Manuals*. Nuclear Regulatory Commission.
- George, N. M., Terrani, K., Powers, J., Worrall, A., & Maldonado, I. (2015). Neutronic analysis of candidate accident-tolerant cladding concepts in pressurized water reactors. *Annals of Nuclear Energy*, 75, 703-712.

- Hales, J. D., & al., e. (2015). *BISON Theory Manual, The Equations behind Nuclear Fuel Analysis*. Idaho National Laboratory.
- Holzwarth, U., & Stamm, H. (2002). Mechanical and thermomechanical properties of commercially pure chromium and chromium alloys. *Journal of Nuclear Materials*, 300, 161-177.
- IAEA. (1966). *Thermal Conductivity of Uranium Dioxide*. International Atomic Energy Agency.
- INL. (2018). *Light Water Reactor Sustainability Program Integrated Program Plan*. Idaho National Laboratory.
- Larson, F. R., & Miller, J. (1952). A Time-Temperature Relationship for Rupture and Creep Stress. *Transactions of the ASME*, (pp. 765-775).
- Ma, Z., & et al. (2017). A Simulation-based Dynamic Approach for External Flooding Analysis in Nuclear Power Plants. *Proceedings of the 20th Pacific Basin Nuclear Conference*. Springer.
- Matev, A. (2006). Analysis of Operator Response to Station Blackout. *International RELAP5-3D User Group Meeting*. West Yellowstone: Idaho National Laboratory.
- Matos, J. E., & Snelgrove, J. L. (1992). *Research Reactor Core Conversion Guidebook*. International Atomic Energy Agency.
- Murabayashi, M., Tanaka, S., & Takahashi, Y. (1975). Thermal Conductivity and Heat Capacity of Zircaloy-2, -4 and Unalloyed Zirconium. *Journal of Nuclear Science and Technology*, 12(10), 661-2.
- NEI. (2016). *Diverse and Flexible Coping Strategies (FLEX) Implementation Guide*.
- Nelson, A., White, J., Byler, D., Dunwoody, J., Valdez, J., & McClellan, K. (2014). Overview of properties and performance of uranium-silicide compounds for light water reactor applications. *Transactions of the American Nuclear Society*. 110, pp. 987-9. American Nuclear Society.
- Nilsson, O., Mehling, H., Horn, R., Fricke, J., Hofmann, R., Müller, S. G., & al., e. (1997). Determination of the thermal diffusivity and conductivity of monocrystalline silicon carbide (300-2300 K). *High Temperatures High Pressures*, 29(1), 73-9.
- NRC. (2012). *State-of-the-Art Reactor Consequence Analyses Project / Volume 2: Surry Integrated Analysis*. Nuclear Regulatory Commission.
- NRC. (2012). *TRACE V5.0 Theory Manual: Field Equations, Solution Methods, and Physical Models*. (N. R. Commission, Producer) Retrieved April 16, 2018, from <https://www.nrc.gov/docs/ML0710/ML071000097.pdf>
- NRC. (2017). *Loss of Offsite Power*. Retrieved 07 28, 2017, from US NRC: <http://nrcoe.inel.gov/resultsdb/publicdocs/LOSP/loop-glossary.pdf>
- Parisi, C., Prescott, S. R., Szilard, R. H., Coleman, J. L., Spears, R. E., & Gupta, A. (2016). *Demonstration of External Hazards Analysis*. Idaho National Laboratory. Idaho Falls: Idaho National Laboratory.
- Pastore, G., & et al. (2017). *LOCA Demonstration with Experimental Assessment (IFA-650.10)*.
- Popov, S., Carbajo, J., Ivanov, V., & Yoder, G. (2000). *Thermophysical properties of MOX and UO<sub>2</sub> fuels including the effects of irradiation*. ORNL, Fissile Materials Disposition Program.
- Prosek, A., & Cizelj, L. (2013, April). Long-Term Station Blackout Accident Analyses of a PWR with RELAP5/MOD3.3. *Science and Technology of Nuclear Installations*, 2013.
- RELAP5-3D Code Development Team. (2003). *SCDAP/RELAP5-3D Code Manual. Volume 2: Modeling of Reactor Core and Vessel Behavior During Severe Accidents*. Idaho Falls: INEEL.
- RELAP5-3D Code Development Team. (2018). *RELAP5-3D Code Manual Volume I*. Idaho National Laboratory. Idaho Falls: Idaho National Laboratory.

- Robb, K. R., Howell, M., & Ott, L. J. (2017). *Parametric and Experimentally Informed BWR Severe Accident Analysis Using FeCrAl*. Oak Ridge National Laboratory, Nuclear Technology R & D.
- Schultz, R. R. (2015). *RELAP5-3D(c) Code Manual Volume V: User's Guidelines*. Idaho National Laboratory. Idaho Falls: Idaho National Laboratory.
- Scikit-Learn*. (2017). Retrieved 07 28, 2017, from Scikit-Learn: <http://scikit-learn.org/stable/>
- Siu, N. (1994). Risk Assessment for Dynamic Systems: an Overview. *Reliability Engineering and System Safety*, 41, 43–73.
- Smith, C. L., & Wood, S. T. (2011). *Systems Analysis Programs for Hands-on Integrated Reliability Evaluations (SAPHIRE)*. Idaho National Laboratory. Idaho Falls: US NRC.
- Szilard, R. H., Coleman, J. L., Prescott, S. R., Parisi, C., & Smith, C. L. (2016). *RISMC Toolkit and Methodology Research and Development Plan for External Hazards Analysis*. Idaho National Laboratory. Idaho Falls: Idaho National Laboratory.
- Takahashi, Y., Yamamoto, K., Ohsato, T., Shimada, H., Terai, T., & Yamawaki, M. (1989). Heat capacities of uranium-zirconium alloys from 300 to 1100 K. *Journal of Nuclear Materials*, 167, 147-51.
- Takahashi, Y., Yamawaki, M., & Yamamoto, K. (1988). Thermophysical properties of uranium-zirconium alloys. *Journal of Nuclear Materials*, 154(1), 141-4.
- Virginia Electric and Power Company. (2010). *Measurement Uncertainty Recapture Power Uprate*. Richmond.
- Williamson, R. L., & et al. (2012). Multidimensional multiphysics simulation of nuclear fuel behavior. *Journal of Nuclear Materials*, 423(1), 149-163.
- Zhang, H., Szilard, R., & Hess, S. (2018). *R&D Roadmap for Enhanced Resilient Plant Systems, Metrics, Scenarios, Risk Analysis, and Modeling and Simulation*.

# APPENDIX A SBO EVENT TREE MODEL

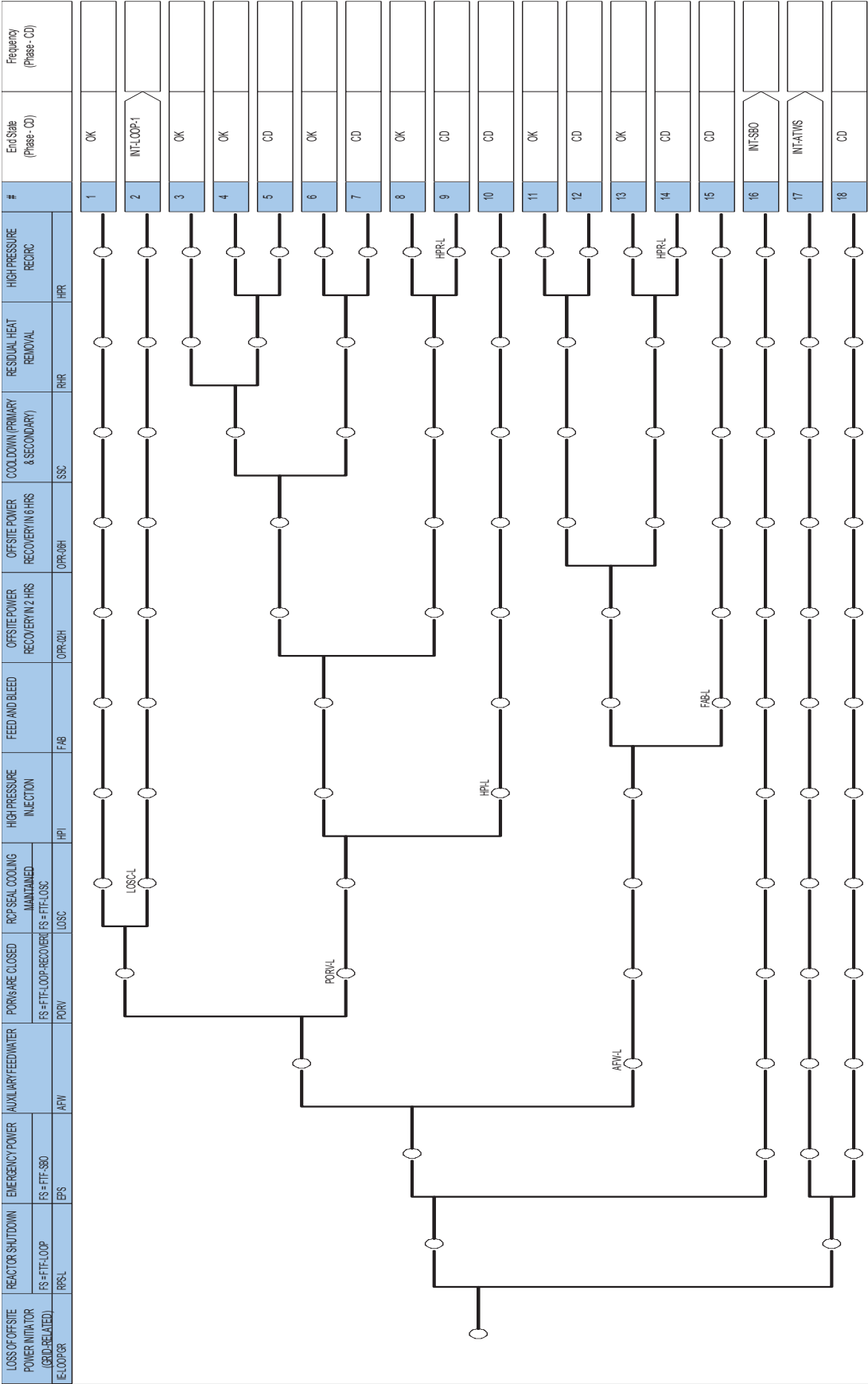


Figure A-1. LOOPGR Event Tree.

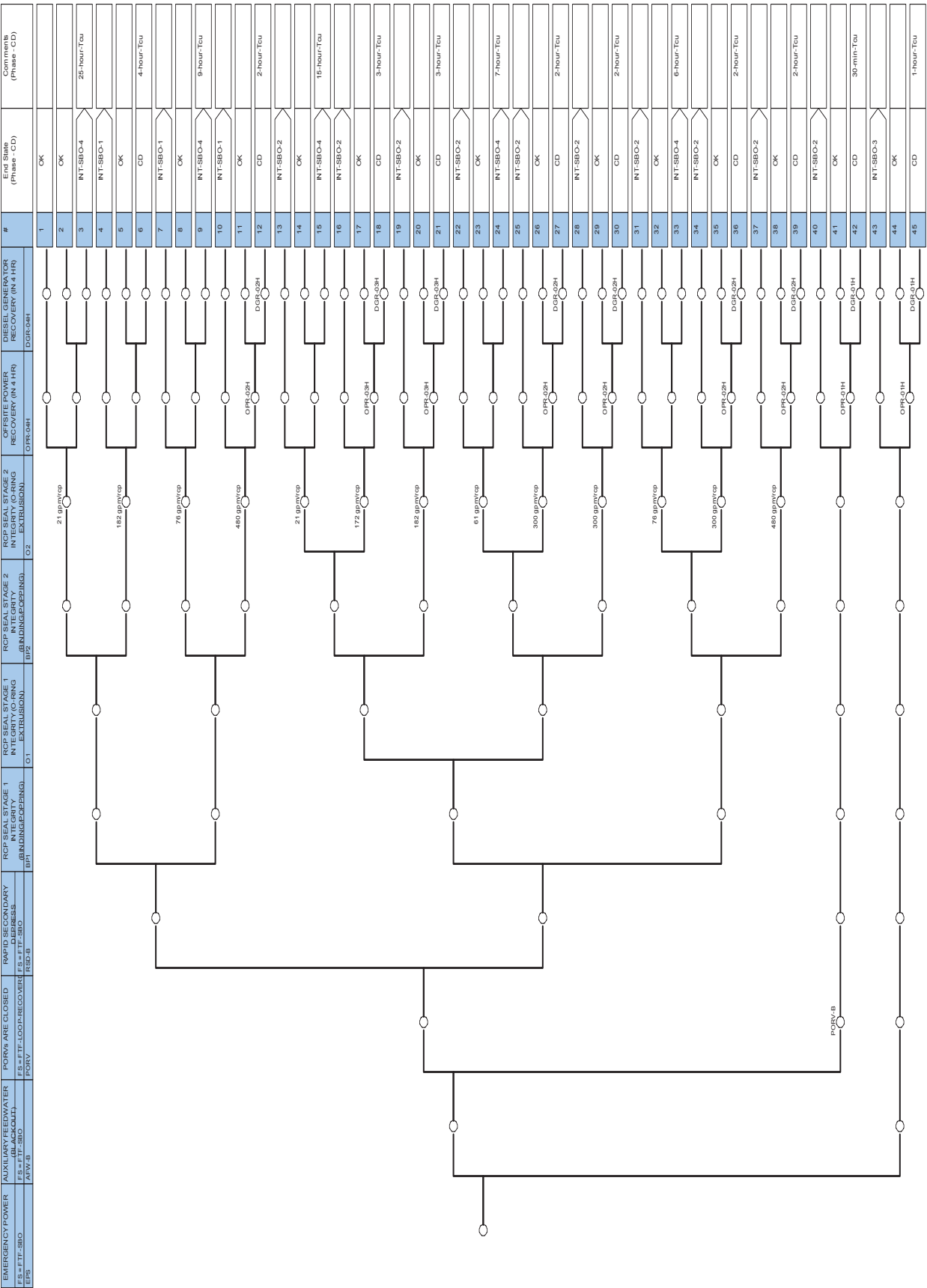


Figure A-2. SBO Main Event Tree.

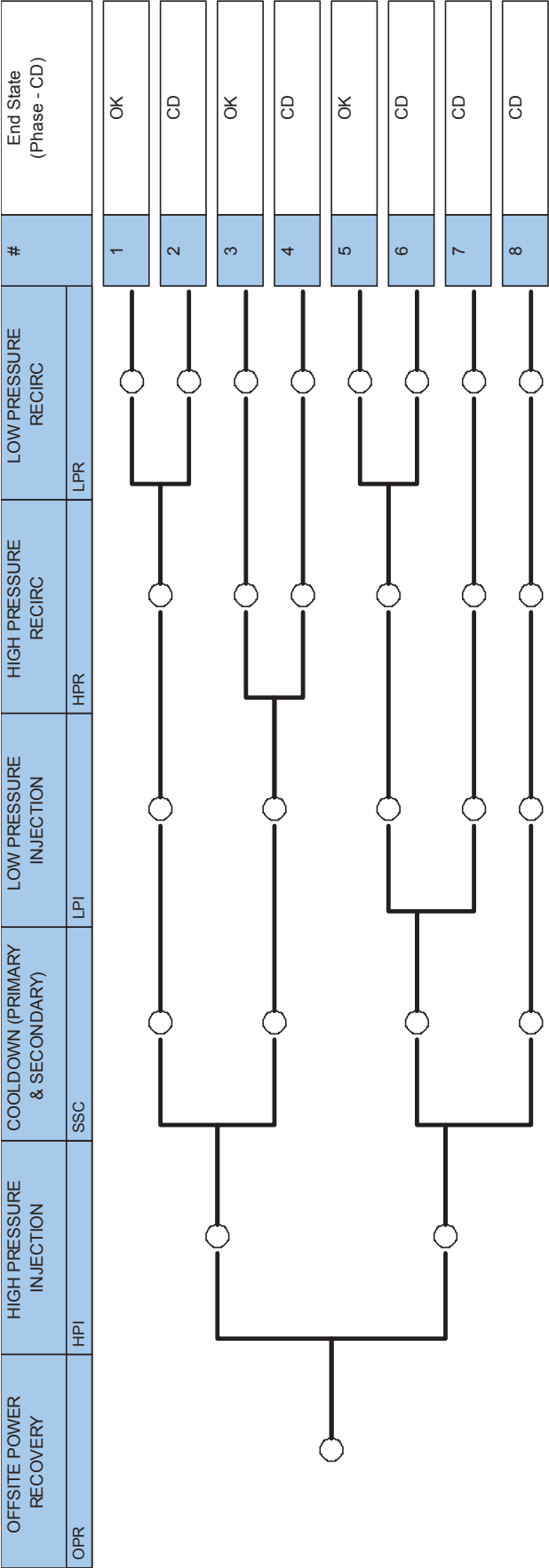


Figure A-3. SBO-1 Sub-Event Tree.

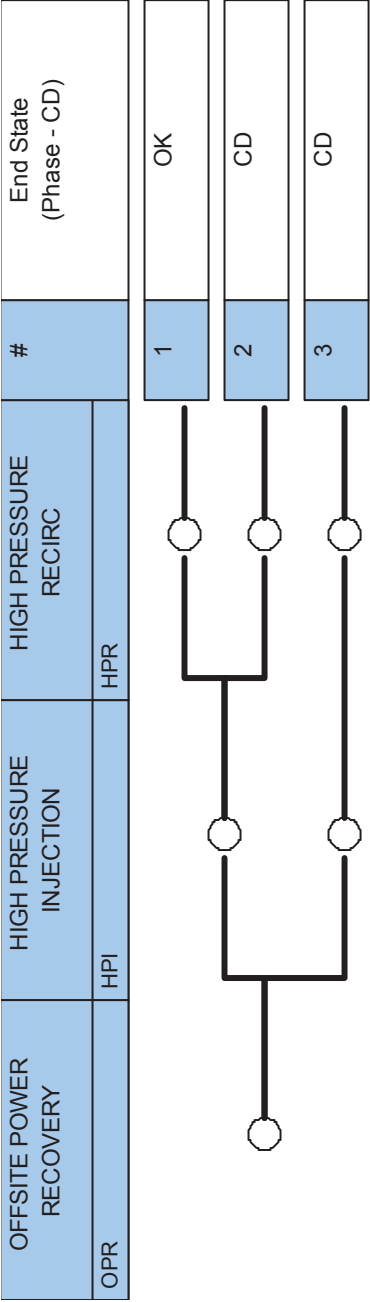


Figure A-4. SBO-2 Sub-Event Tree.

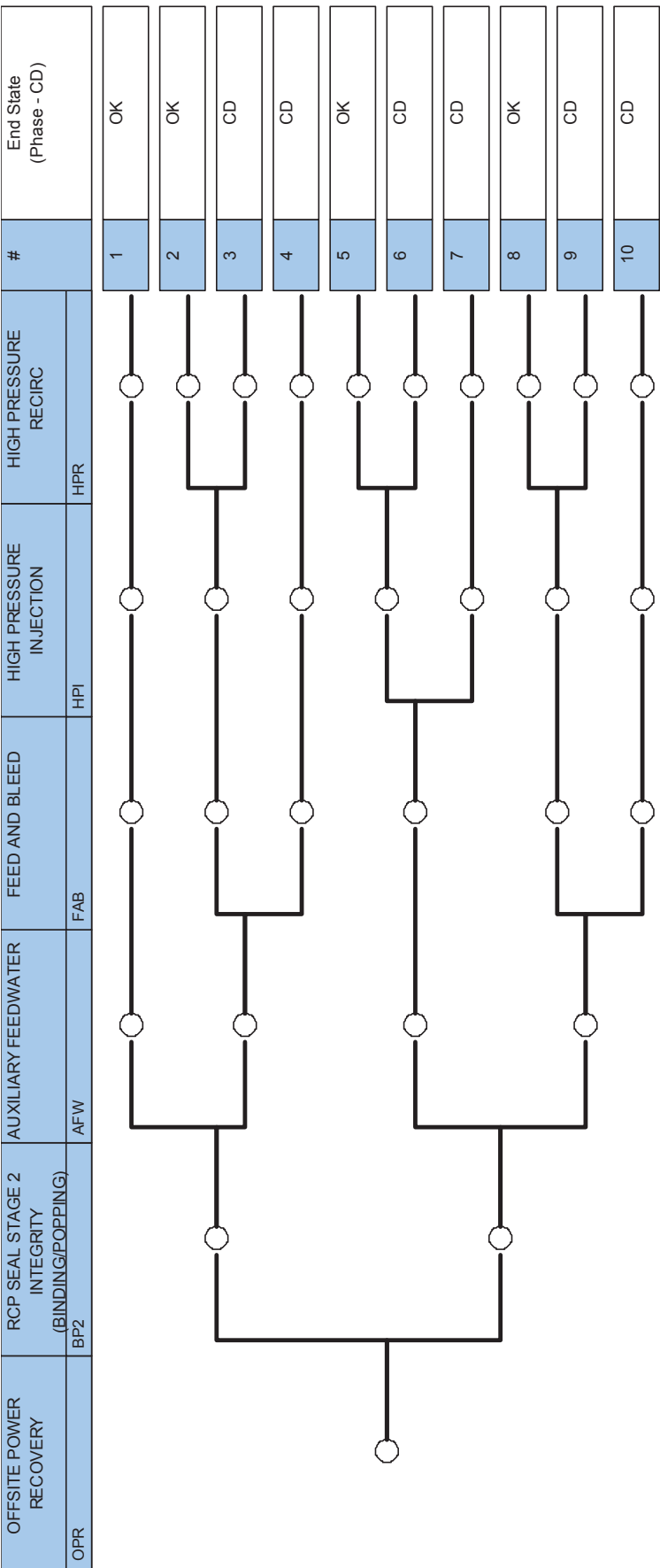


Figure A-5. SBO-3 Sub-Event Tree.





## APPENDIX B

### RELAP5-3D SBO RESULTS

This appendix presents the charts of the main parameters calculated by the RELAP5-3D code for selected postulated SBO accident scenarios of Section 错误！未找到引用源。.

**SBO-2.0, SBO (LOOP occurs, both EDG fail, TDAFP success, No PORV remained opened, 76 gpm/RCP leakage, Rapid Secondary Depressurization success, No offsite power recovery and TDAFP stops after DC battery depletes @ t=4 hours)**

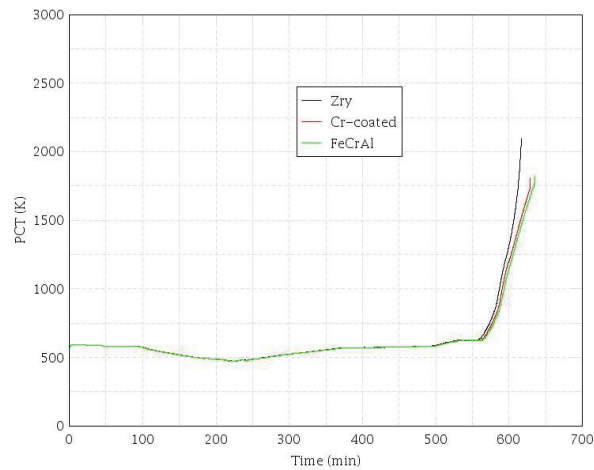


**Figure B-1. SBO-2.0 - PCT.**

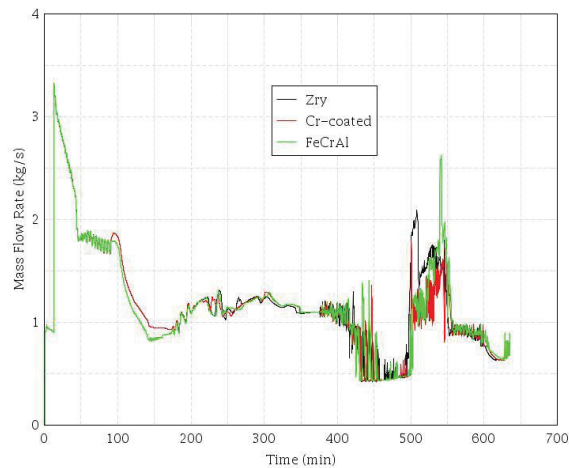


**Figure B-2. SBO-2.0 – MCP Seal Leakage.**

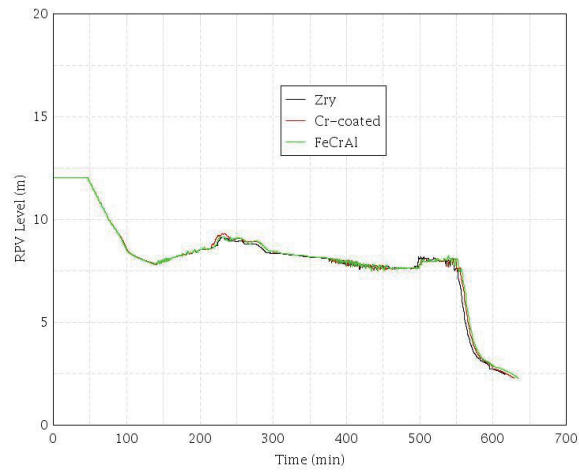


**Figure B-3. SBO-2.0 - RPV Liquid Level.**

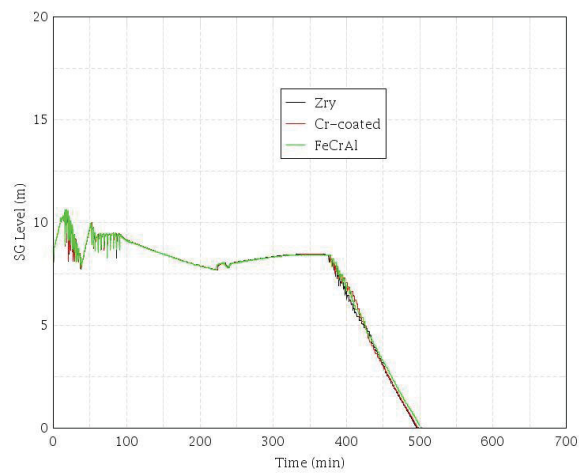


**Figure B-4. SBO-2.0 - SG Liquid Level.**

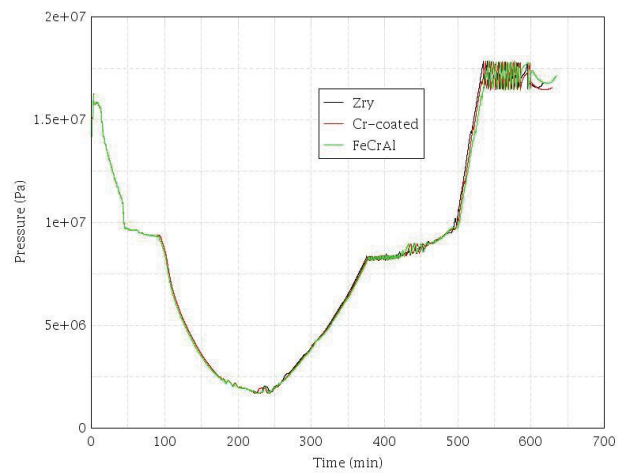


**Figure B-5. SBO-2.0 - Primary Side Pressure.**

**SBO-3.0, (LOOP occurs, both EDG fail, TDAFP success, No PORV remained opened, 182 gpm/RCP leakage, Rapid Secondary Depressurization success, No offsite power recovery and TDAFP stops after DC battery depletes @ t=4 hours)**

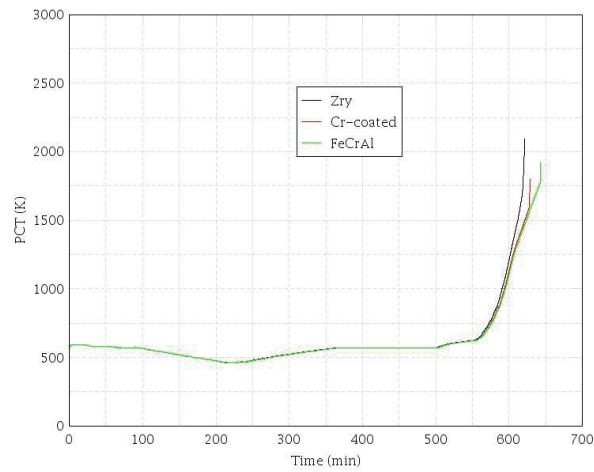


**Figure B-6. SBO-3.0 - PCT.**

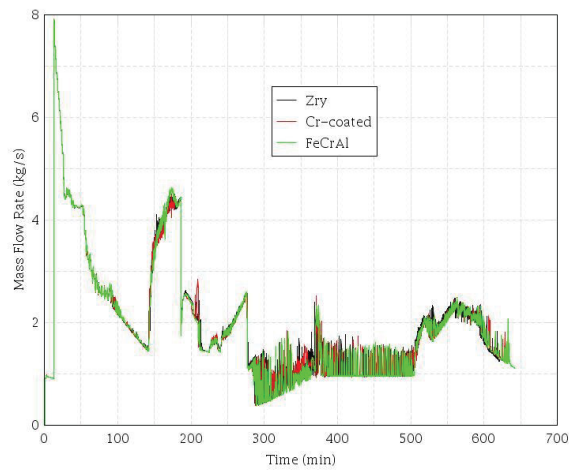


**Figure B-7. SBO-3.0 – MCP Seal Leakage.**

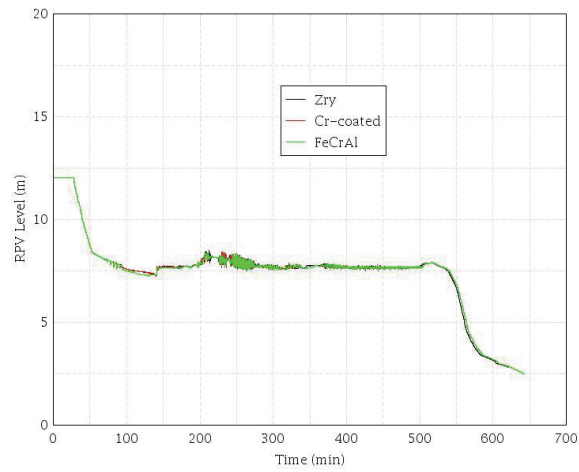


**Figure B-8. SBO-3.0 - RPV Liquid Level.**

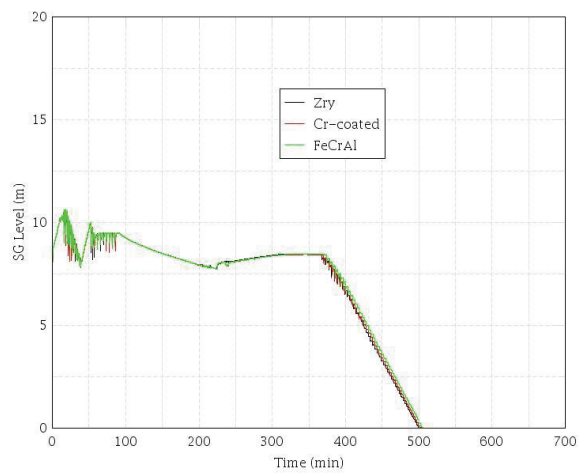


**Figure B-9. SBO-3.0 - SG Liquid Level.**

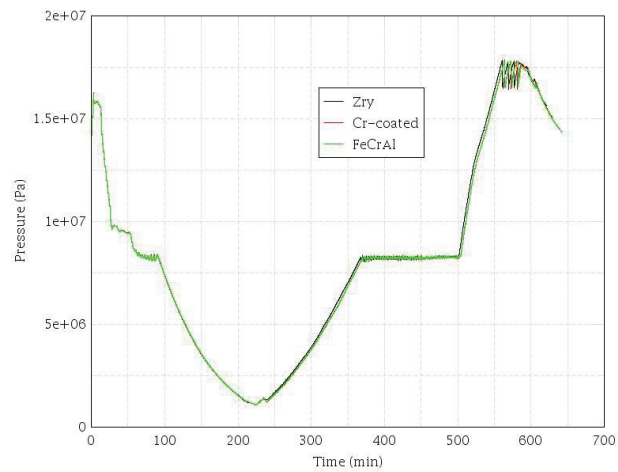


**Figure B-10. SBO-3.0 - Primary side pressure.**

**SBO-3.1, LOOP occurs, both EDG fail, TDAFP success, No PORV remained opened, 182 gpm/RCP leakage, Rapid Secondary Depressurization fails, No offsite power recovery and TDAFP stops after DC battery depletes @ t=4 hours**

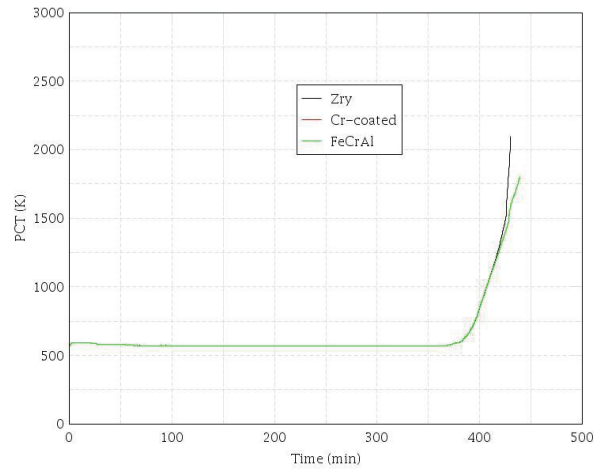


**Figure B-11. SBO-3.1 - PCT.**

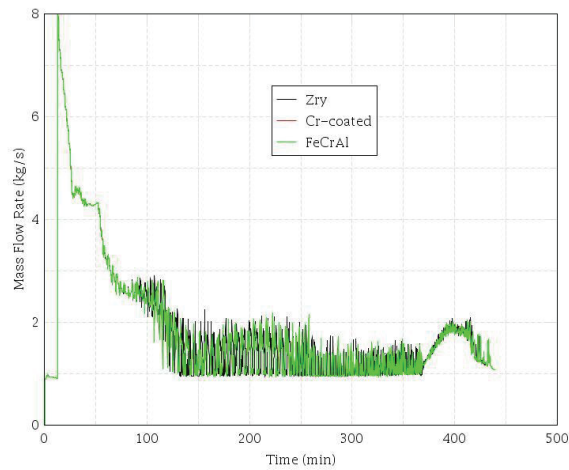


**Figure B-12. SBO-3.1 – MCP Seal Leakage.**

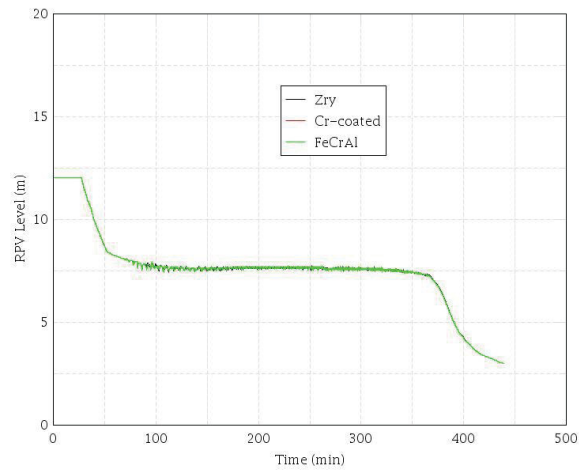


**Figure B-13. SBO-3.1 - RPV Liquid Level.**

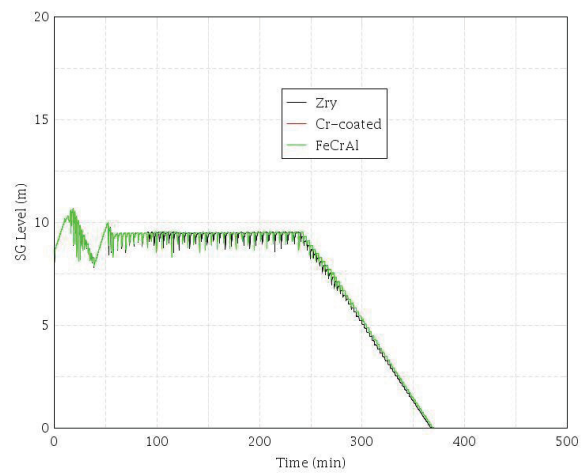


**Figure B-14. SBO-3.1 - SG Liquid Level.**

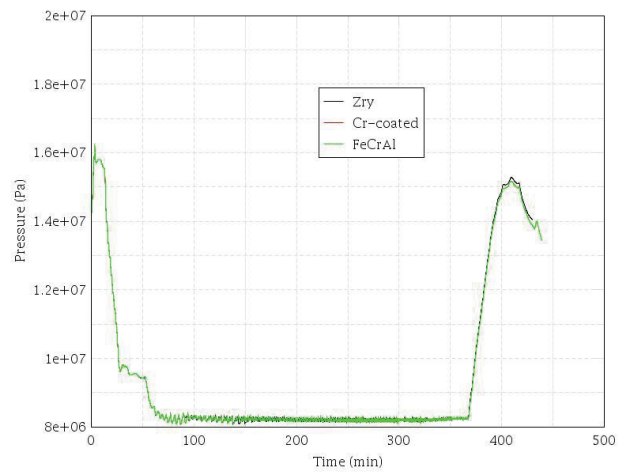


**Figure B-15. SBO-3.1 - Primary Side Pressure.**

**SBO-4.0, (LOOP occurs, both EDG fail, TDAFP success, No PORV remained opened, 480 gpm/RCP leakage, Rapid Secondary Depressurization success, No offsite power recovery and TDAFP stops after DC battery depletes @ t=4 hours)**

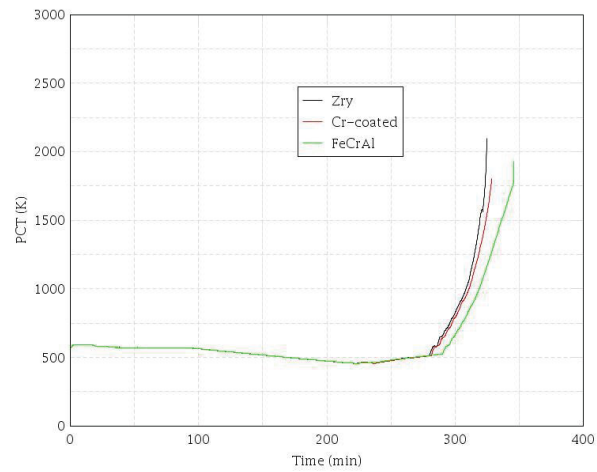


**Figure B-16. SBO-4.0 - PCT.**

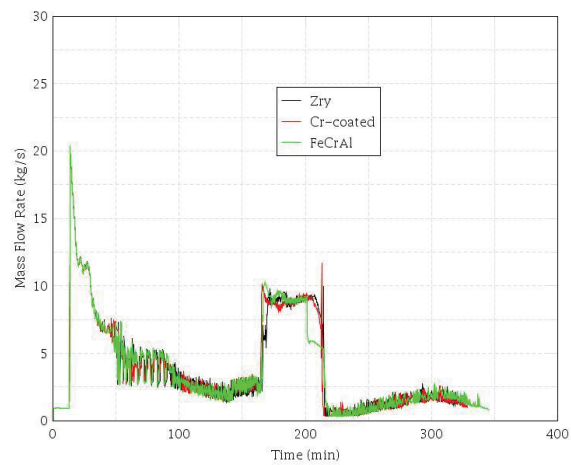


**Figure B-17. SBO-4.0 – MCP Seal Leakage.**



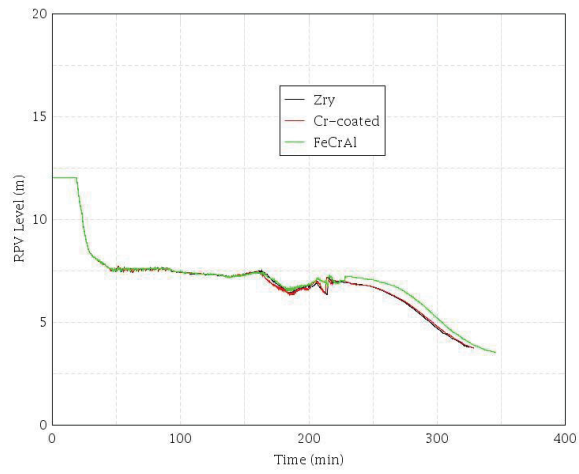


**Figure B-18. SBO-4.0 - RPV Liquid Level.**

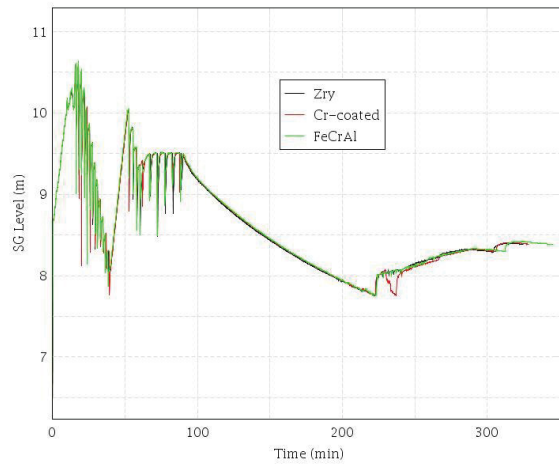


**Figure B-19. SBO-4.0 - SG Liquid Level.**

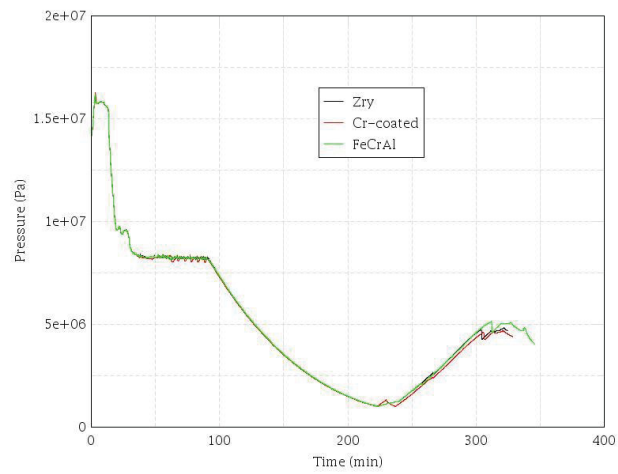


**Figure B-20. SBO-4.0 - Primary Side Pressure.**

**SBO-5.1 – (LOOP occurs, both EDG fail, TDAFP success, No PORV remained opened, 300 gpm/RCP leakage, Rapid Secondary Depressurization fails, No offsite power recovery and TDAFP stops after DC battery depletes @ t=4 hours)**

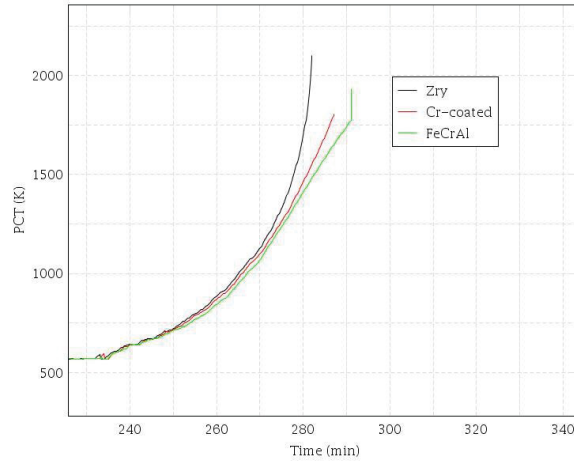


**Figure B-21. SBO-5.1 - PCT.**

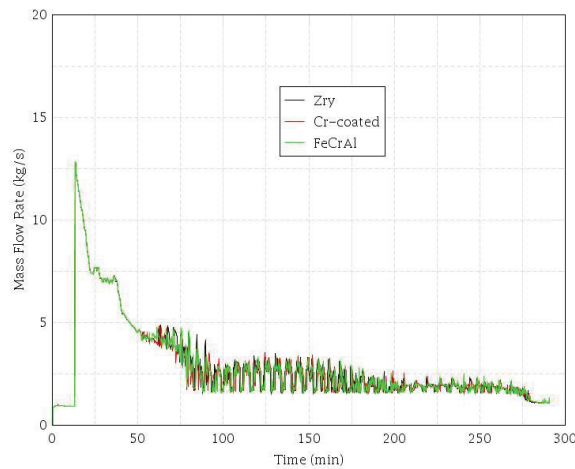


**Figure B-22. SBO-5.1 – MCP Seal Leakage.**

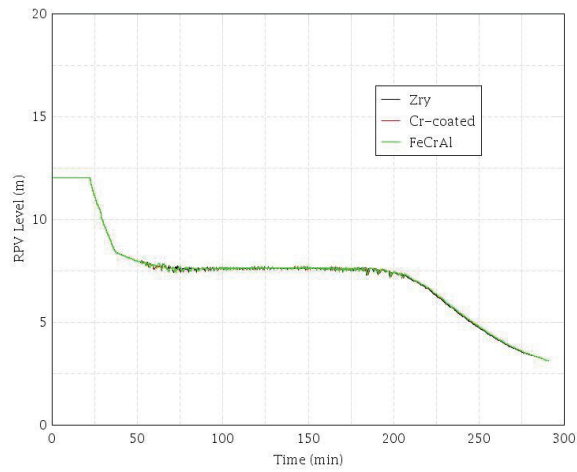


**Figure B-23. SBO-5.1 - RPV Liquid Level.**

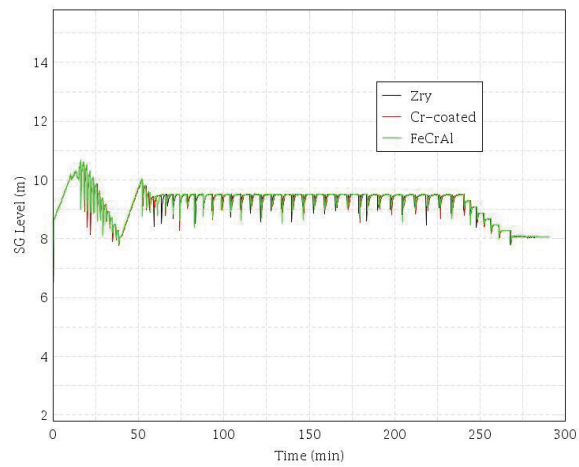


**Figure B-24. SBO-5.1 - SG Liquid Level.**

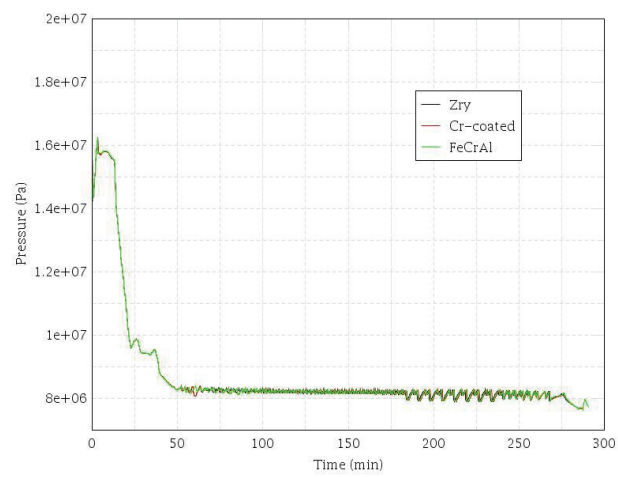


**Figure B-25. SBO-5.1 - Primary Side Pressure.**

**SBO-6.0 – SBO (LOOP occurs, both EDG fail, TDAFP success, PORV remained opened, No offsite power recovery and TDAFP stops after DC battery depletes @ 4 hours)**

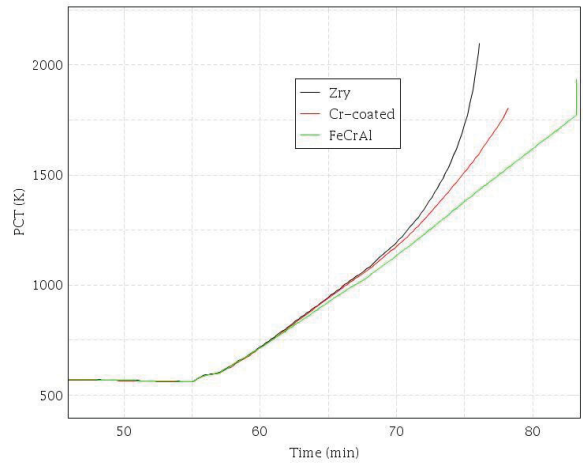


**Figure B-26. SBO-6.0 - PCT.**

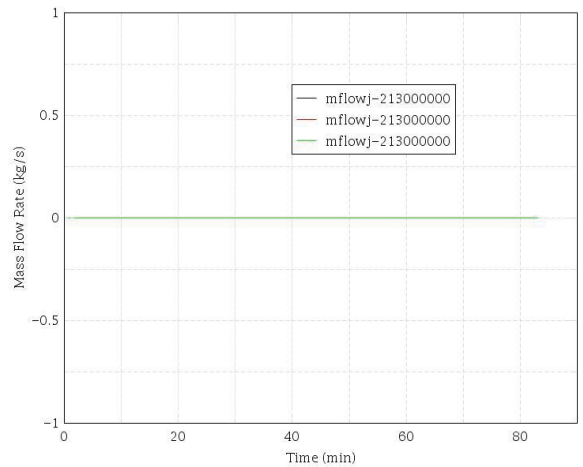


**Figure B-27. SBO-6.0 – MCP Seal Leakage.**

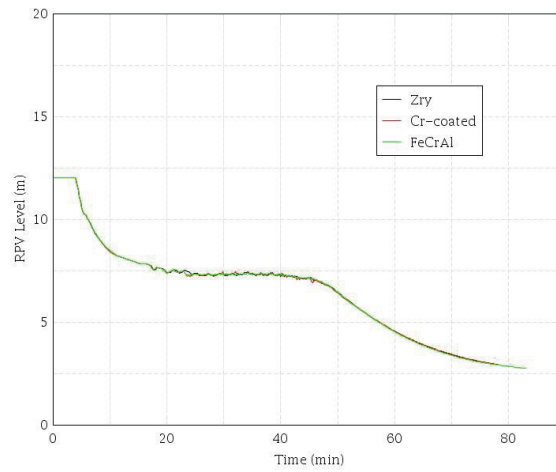


**Figure B-28. SBO-6.0 - RPV Liquid Level.**

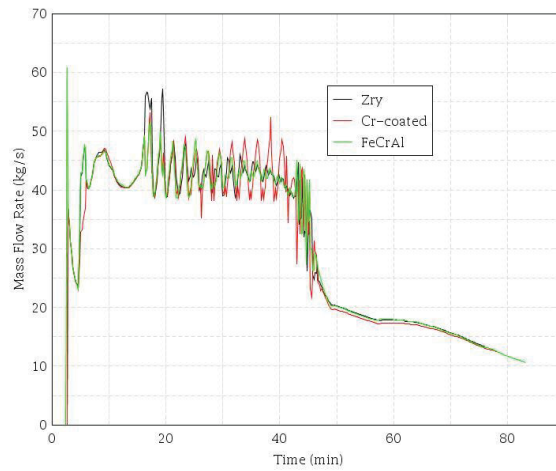


**Figure B-29. SBO-6.0 - PRZ PORV Mass Flow.**

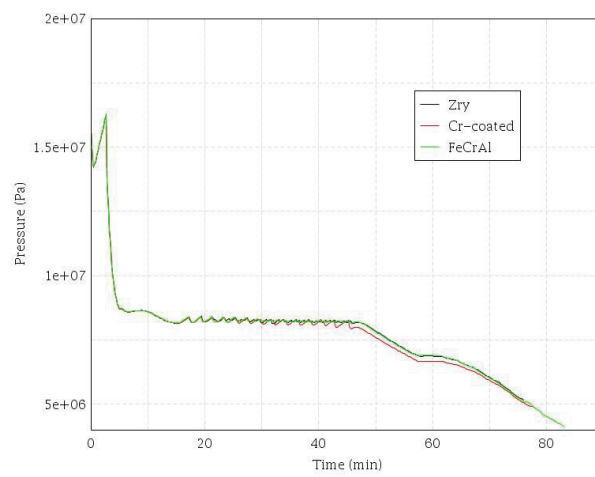


**Figure B-30. SBO-6.0 - Primary Side Pressure.**

**SBO-6.1 – SBO (LOOP occurs, both EDG fail, TDAFP success, PORV remained opened, SG depressurization at t=30 min, No offsite power recovery and TDAFP stops after DC battery depletes @ 4 hours).**

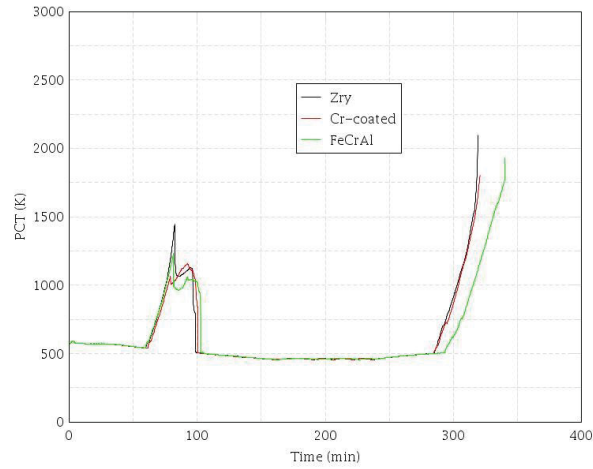


**Figure B-31. SBO-6.1 - PCT.**

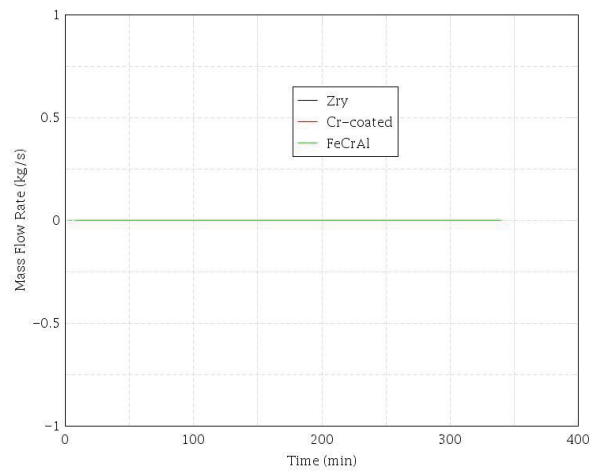


**Figure B-32. SBO-6.1 – MCP Seal Leakage.**

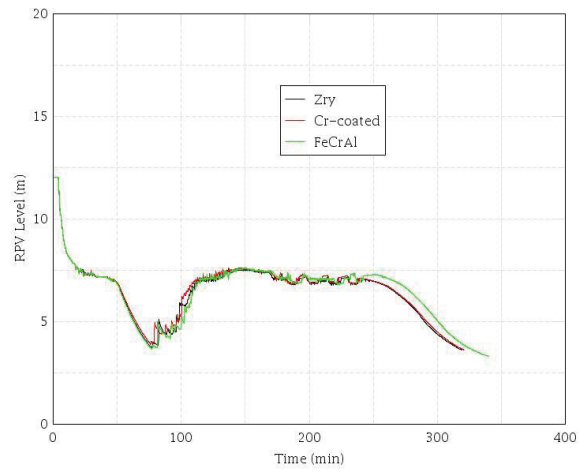


**Figure B-33. SBO-6.1 - RPV Liquid Level.**

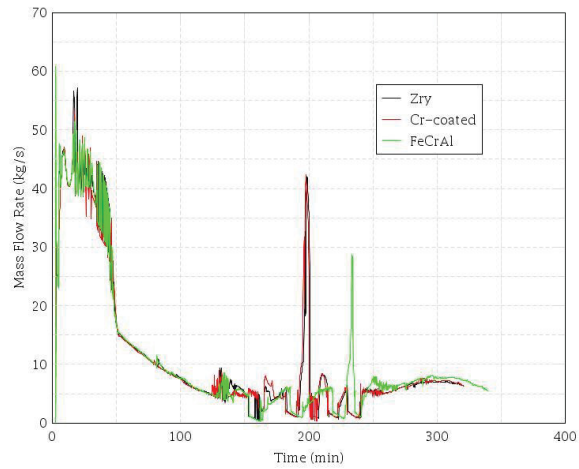


**Figure B-34. SBO-6.1 - PRZ PORV Mass Flow.**

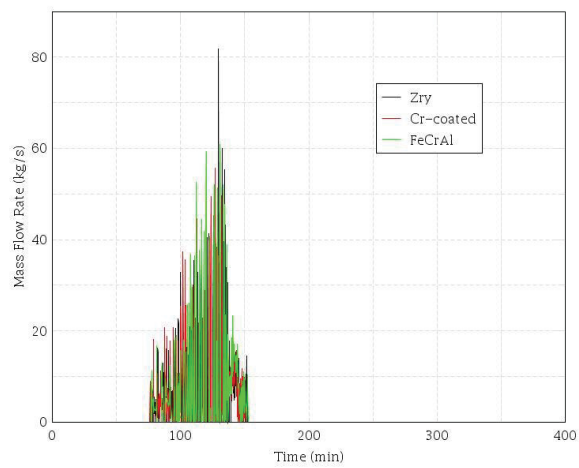


**Figure B-35. SBO-6.1 - Accumulators Mass Flow.**

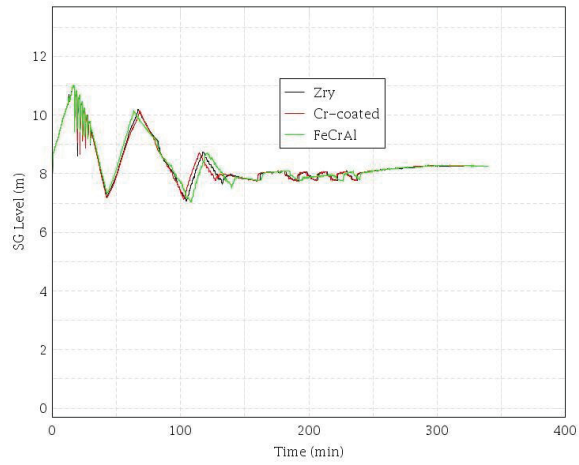


**Figure B-36. SBO-6.1 - SG Liquid Level.**

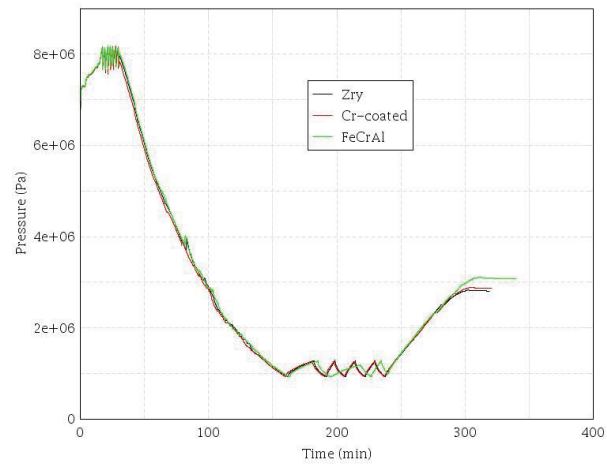


**Figure B-37. SBO-6.1 – Secondary Side Pressure.**

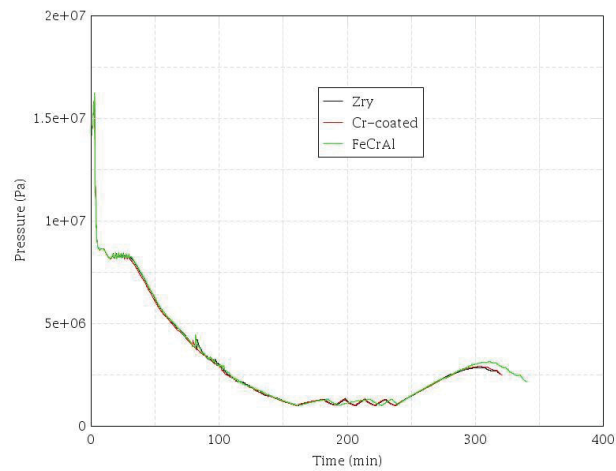


**Figure B-38. SBO-6.1- Primary Side Pressure.**



**SBO-7.0 –ST-SBO (LOOP occurs, both EDG fail, TDAFP fails, 21 gpm/RCP leakage, No offsite power recovery)**

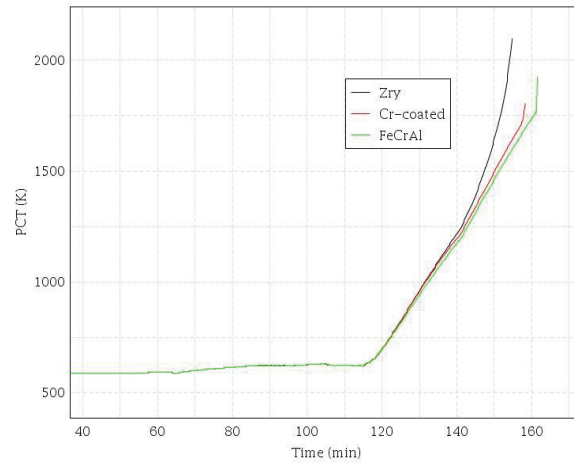


**Figure B-39. SBO-7.0 - PCT.**

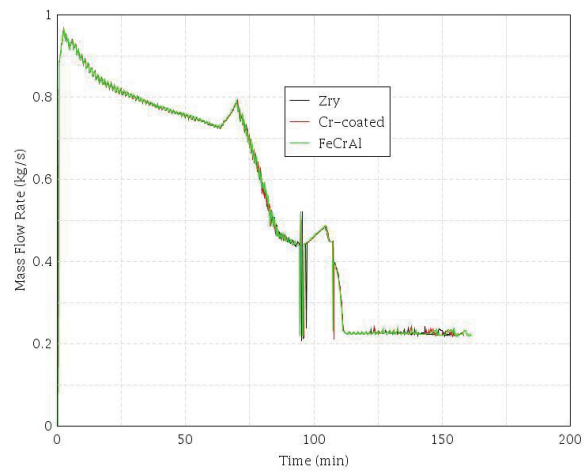


**Figure B-40. SBO-7.0 – MCP Seal Leakage.**

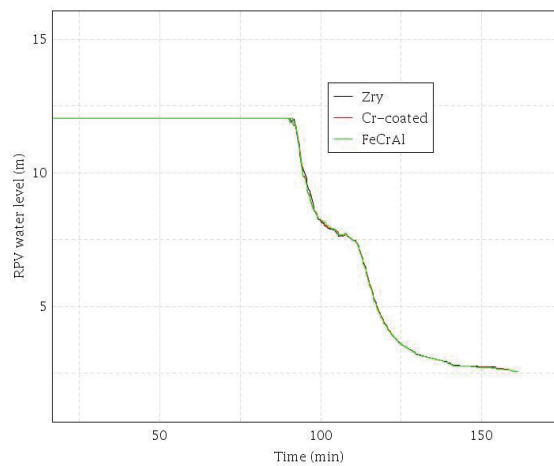


**Figure B-41. SBO-7.0 - RPV Liquid Level.**

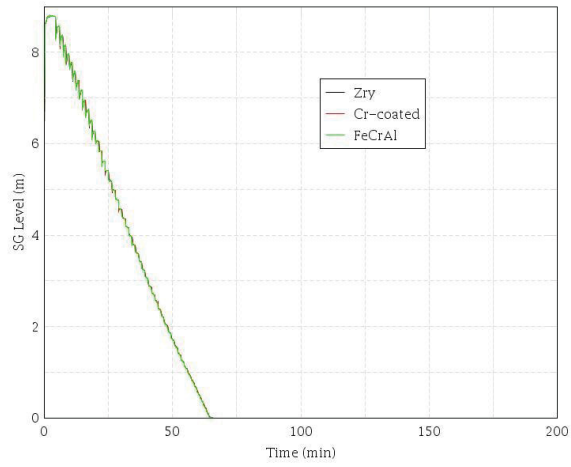


**Figure B-42. SBO-7.0 - SG Liquid Level.**

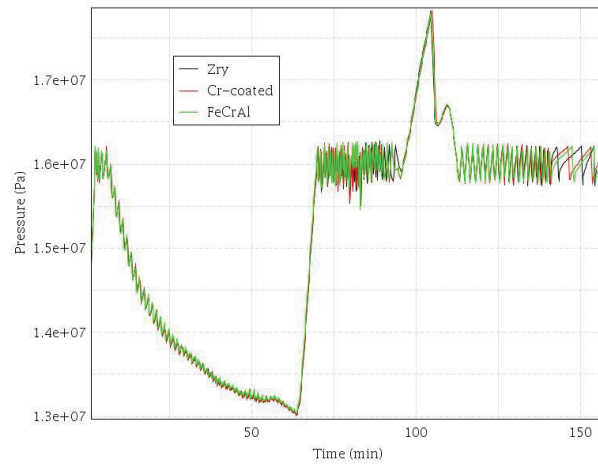


**Figure B-43. SBO-7.0 - Primary Side Pressure.**